

THE UNIVERSITY OF SYDNEY

DEPARTMENT OF ARCHITECTURAL SCIENCE

AND

DEPARTMENT OF CIVIL ENGINEERING

// "A STUDY OF CRACKING IN REINFORCED
CONCRETE PRESSURE VESSELS USING
MICRO-CONCRETE MODELS" //

FOR A

MASTER OF BUILDING SCIENCE THESIS

SUBMITTED BY

APOLLO E.W.K. MUSOKE (B.Sc. Eng. (Hons), M.U.K.)

SYDNEY, JULY 1976

University of NAIROBI Library



0356032 3

SYNOPSIS

Reinforced Concrete Pressure Vessels (and Reactor Vessels) are increasingly being built because of the great advantage provided by their massive walls for shielding.

Cracking of these vessels may lead to the leakage of their containments - a situation that is very much undesirable, especially for safe environmental requirements.

New methods of analysis and design of these vessels, as well as experimental investigation using 'micro-concrete' models, are necessary to prevent any excessive cracking leading to leakage.

This thesis has been prepared for this purpose.

A.E.W.M.

INTRODUCTION

The 'Study of Cracking in Reinforced Concrete Pressure Vessels (RCPV's) Using Micro-Concrete Models' presented in this thesis, is largely a review of literature and theories of analysis and design for these vessels, given with practical applications.

In Chapters 1 and 2, problems associated with building 'direct' models with micro-concrete are discussed, and solutions sought - for RCPV's. The importance of a preliminary analytical mathematical model is emphasized, the results of which must be used during testing. Also instrumentation is given thorough investigation during the planning and design of the small scale model.

Chapter 3 outlines in detail the stages followed in constructing the micro-concrete model at the Hydraulics Laboratory, Sydney University (1975-1976). The prototype reactor vessel on which the model is based is typical of the containment structures constructed for small scale experimental reactor vessels.

I spent some time planning and designing this model, for which 2 construction stages out of 6 were completed by the time of writing.

Chapter 4 discusses methods used to date, of analysing pressure vessels of reactor vessel complexity. The Finite Element Method (FEM) analysis has proven most suitable and its application to RCPV's is discussed at some length.

In Chapter 5, I have presented ideas on how the model should be tested, and what results to expect based on previous work done in the field. One of the main purposes of the model is to simulate the 'structural integrity' and 'leakage rate' tests, outlined for the prototype in Chapter 6.

(Due to shortage of time and funds, it was not possible to construct completely and test the model for experimental conclusions. This will be done at some future date).

NOTATION

a: acceleration
Subscript a: for accident (as in P_a = accident pressure)
A: area
c: specific heat
Subscript c: for concrete
(d: displacement)
D: thermal diffusivity
DBA: Design Basis Accident
E: Modulus of Elasticity
(f: stress)
f', F': compressive strength
h: co-efficient of heat transfer
Subscript i: for modelled quantity
k: thermal conductivity
l: linear dimension
Subscript m: for model
M: moment
N: Nusselt's number
P, p: pressure
PCPV: Prestressed Concrete Pressure Vessel
PCRv: Prestressed Concrete Reactor Vessel
(q: pressure)
Q: concentrated load
Subscript r: for reinforcement
/ RCPV: Reinforced Concrete Pressure Vessel
RCRV: Reinforced Concrete Reactor Vessel
Subscript s: for steel, or shear
SBA: Small Break Accident
SSE: Safe Shutdown Earthquake
t: time
Subscript t: for concrete cover
T: temperature
Subscript u: for ultimate
U: bond strength per unit length
v: velocity

w: crack width
W: line load

α : co-efficient of thermal expansion
 β : angular displacement
 δ : displacement
 Δ : displacement
 ϵ : strain
 λ_i : scaling factor for quantity i ; $\lambda_i = i_p / i_m$
 θ : temperature dimension; temperature
 ρ : specific mass; (mass density)
 σ : stress
 γ : Poisson's Ratio

KEYWORDS

bond, concrete, cracking, creep, direct models, Finite Element Method (FEM), leakage, loading, mathematical models, micro-concrete, pressure vessels, similitude, shrinkage, strain-gauges, structural integrity, testing, thin shell, thick shell, thermal effects, thermocouples, through-cracks, yield lines.

SYNOPSIS

INTRODUCTION

NOTATION

CHAPTER 1	MODELLING WITH 'MICRO-CONCRETE'	
1.1	The Structural Model and its History -----	1
1.2	Types of Models -----	3
1.3	Scales of Models -----	6
1.4	Micro-Concrete -----	7
1.5	Reinforcement in Micro-Concrete Models -----	8
1.6	Similitude Requirements -----	9
1.7	Special Considerations -----	14
CHAPTER 2	MODELS FOR CONCRETE REACTOR VESSELS AND CONTAINMENTS	
2.1	Introduction (General) -----	20
2.2	Loading Considerations in Design -----	20
2.3	Model Design -----	22
2.4	Model Loading Analysis -----	24
2.5	Loading Systems -----	28
2.6	Instrumentation -----	32
2.7	The FEM Analysis -----	38
CHAPTER 3	CONSTRUCTION OF THE REINFORCED CONCRETE REACTOR VESSEL MODEL	
3.1	Planning and Design -----	40
3.2	Construction and Construction Stages of the Model ----	51
CHAPTER 4	THE ANALYSIS OF CONCRETE REACTOR VESSELS (PRESSURE VESSELS)	
4.1	Introduction -----	69
4.2	Two and Three-Dimensional FEM Analyses -----	69
4.3	The General Analytical Scheme for Cracking -----	76
4.4	Elastic Analysis of the Entire RC Structure -----	78
4.5	Local Cracked - Concrete Analysis -----	80
4.6	The Analysis for a Specific Vessel -----	83
4.7	Results of the Three-Dimensional FEM Analysis -----	91
CHAPTER 5	TESTING OF MODEL, AND EXPECTED RESULTS	
5.1	Introduction -----	95
5.2	Internal Pressure Tests -----	96
5.3	Creating Internal Heat -----	99
5.4	The Thermal Test -----	99
5.5	A Simultaneous Thermal and Pressure Test -----	100

5.6	Testing To Failure -----	102
5.7	Expected Results of the Internal Pressure Tests ---	102
5.8	Expected Results of the Thermal Test -----	105

CHAPTER 6	TESTING OF REACTOR VESSELS (PRESSURE VESSELS)	
6.1	Introduction -----	111
6.2	General Preparations for the Tests -----	111
6.3	The Equipment and Facilities -----	112
6.4	The Tests -----	113
6.5	The Structural Integrity Test -----	113
6.6	The Leakage Rate Test -----	114

CHAPTER 7	DISCUSSIONS AND CONCLUSIONS	
7.1	Introduction -----	116
7.2	Cracking in Reinforced Concrete Pressure Vessels (RCPV's) -	117
7.3	Models -----	120
7.4	Construction and Testing of Micro-Concrete Models -	122

ACKNOWLEDGEMENTS -----	125
------------------------	-----

REFERENCES -----	126
------------------	-----

MODELLING WITH 'MICRO-CONCRETE'

1.1. The Structural Model and its History

A suggested definition of a structural model is as follows:

- (Ref. 1.1)

"A structural model is any structural element or assembly of structural elements built to a reduced scale (compared to the full size structure) which is tested, and for which laws of similitude must be employed to interpret test results."

A structural model can be used as an aid in design, a check on theoretical analysis, a feasibility study tool, or as a guide to the actual behaviour of the structure which is otherwise unpredictable by theory.

As early as the 13th century, Domenico Fontana used lead to model the obelisk outside St. Peter's in Rome. Even before then, ancient Egyptian, Greek, Persian and Roman builders made models to assist themselves in planning structures and cities. Michelangelo, Leonardo da Vinci, and Galileo used models for architectural ideas and structural clarity.

However, it wasn't until the 18th to 19th centuries that structural modelling became an aid to analysis from the structural engineer's viewpoint. At this time, advances were made in the more accurate measurement of deformation.

The Howard Strain gauge of 1888, measuring to an accuracy of 0.0001 inches, was being used. The 'miniature compound-lever tensometer', developed by Huggenberger in the 1920's, was next in expanding the use of small scale models.

"Indirect" model techniques, also used to measure deflection and deformations, were developed by Begg, Goltshalk, Eney

and others using the Muller-Breslau's theorem. These techniques are however restricted to linear elastic problems where the principle of super position is directly applicable.

Three-dimensional model analysis made real progress only after the invention of bonded electric-resistance strain-gauges in the late 1930's. Photo-elastic techniques in modelling (for stress analysis) developed by such men as Mesnager, Coker and Filon, were first applied to 3 dimensional structures between 1938 and 1945 by Drucker, Mindlin, Hetenyi and others.

More recently, electric and mechanical analogues have been introduced in model techniques, the most recent being the computer.

1.2 Types of Model

Four broad types of model can be identified. These are:

- (a) Qualitative Models.
- (b) Indirect Models.
- (c) Direct Models.
- (d) Mathematical Models.

(a) Qualitative Models.

These are models with scales usually smaller than 1/10; normally ranging from scales of 1/20, 1/100 through to 1/500. (Beyond the 1/500 limit, most of the detail of the prototype is lost, hence the model can hardly be representative of the real structure.)

Such models are made normally to give the designer a 'feel' of how the structure is going to behave.

Also they are very useful in modelling multi-storey buildings of great height - where detail of each storey is not as important as the overall behaviour of the large structure.

Small scale models are normally made of plastic materials (e.g. perspex), or thin pieces of steel or aluminium. The investigation is limited to linear elastic systems.

Sometimes these models are used to give a visual impression of stress distribution of bridges; or give an idea of deformed shapes of complex shells, domes, vaults, etc.; without direct analysis of results.

(b) Indirect Models

These apply the principle of Müller-Breslau, mentioned in Section 1.1. The principle of super-position is applied to a linear elastic system. This creates an influence line characteristic of the model. The investigation is normally two-dimensional.

Often severely distorted models are used to determine distribution of moments and forces. The technique is obviously 'indirect'.

Begg's 'deformeter' at Princeton University in 1922 pioneered the use of these models.

The use of this type of elastic model is being phased out due to the ease of computer results.

Indirect models tend to be 'qualitative'. They cannot be used for investigations dealing with 'micro-concrete'.

(c) Direct Models

These models are built with the aim to simulate a complete structural elastic and post-elastic (inelastic) behaviour through to failure. In the case of concrete, a 'micro-concrete' that will reveal information on phenomena like cracking, creep, bond, shrinkage, thermal capacity and gradient, etc., is required for such models. The results are then got directly from measurements on the three-dimensional scaled-down structure.

In order to get appreciable, quantitative measurements, scales are seldom less than 1/10 (1/20 is normally the lower limit). Full scale models are sometimes used.

Direct models used to analyse columns, beams or similar concrete structural elements, tend to be restricted to a 1/8 scale. With larger structures like dams, reactor vessels, or large complex hyperbolic domes or similar shapes, the scale is extended to 1/10 or 1/12. It must be born in mind that cracking similitude is worsened by use of a smaller model.

Sometimes direct models are used for feasibility studies of complex structures (cf. Le Corbusier's prestressed concrete Phillip's Pavillion at Brussels, 1958).

Direct measurements of strain, temperature, force, acceleration, etc., may be made on these models.

These are the models employed in modelling with 'micro-concrete'.

(d) Mathematical Models

An idealisation of material properties and topology of structure creates a 'deterministic model' of that structure. If that idealisation can be analysed mathematically (e.g. by solution of compatibility or flexibility equations), then a 'mathematical model' of that structure has been identified.

Such an analysis is normally carried out by computer. Computer programs for this purpose have been developed - some general, some specific to particular structures.

The Finite Difference or Finite Element Methods have been developed to analyse structural systems as mathematical models.

Results from the other types of models (previously discussed) are normally compared with those of the mathematical model. This helps to confirm theory, or otherwise point out weak areas in the theoretical analysis.

Now that the Finite Element Method (FEM) of analysis is very widely used, models are being built in Japan, USA and Europe to determine the adequacy and relative accuracy of this method - amongst other aims.

The future sees the use of 'probabilistic' models as an aid in design. Such models, unlike the 'deterministic' ones, create a mathematical idealisation based on probability laws for material properties and topology of structures.

1.3 Scales of Models

Purpose of model dictates choice of its scale. Other factors that are considered with purpose are: cost, space requirements, ease of fabrication, materials available, importance of detail, minimum thicknesses, time of construction, etc. Whenever practicable, the full scale should be considered, since the best scale is the full scale.

In modelling with 'micro-concrete', for instance, direct models of relatively 'larger' scales must be used if phenomena like cracking, shrinkage, creep, bonding, etc. are to be investigated. Furthermore, reinforcing bars of a diameter less than 1 mm are not practical. Scales of 1/10, 1/8, 1/6, 1/2 or full scale, are best suited for this type of modelling. Only in rare circumstances is one forced to limiting scales of 1/12, say (see Chapter 3).

On the other hand, when modelling a 200 m multi-storey building, a scale should be chosen such that the model can be housed in a laboratory for testing and instrumentation. A scale of 1/50 to 1/100 would have to be chosen, for 2 m to 4 m is a suitable height to work on.

1.4 Micro-Concrete

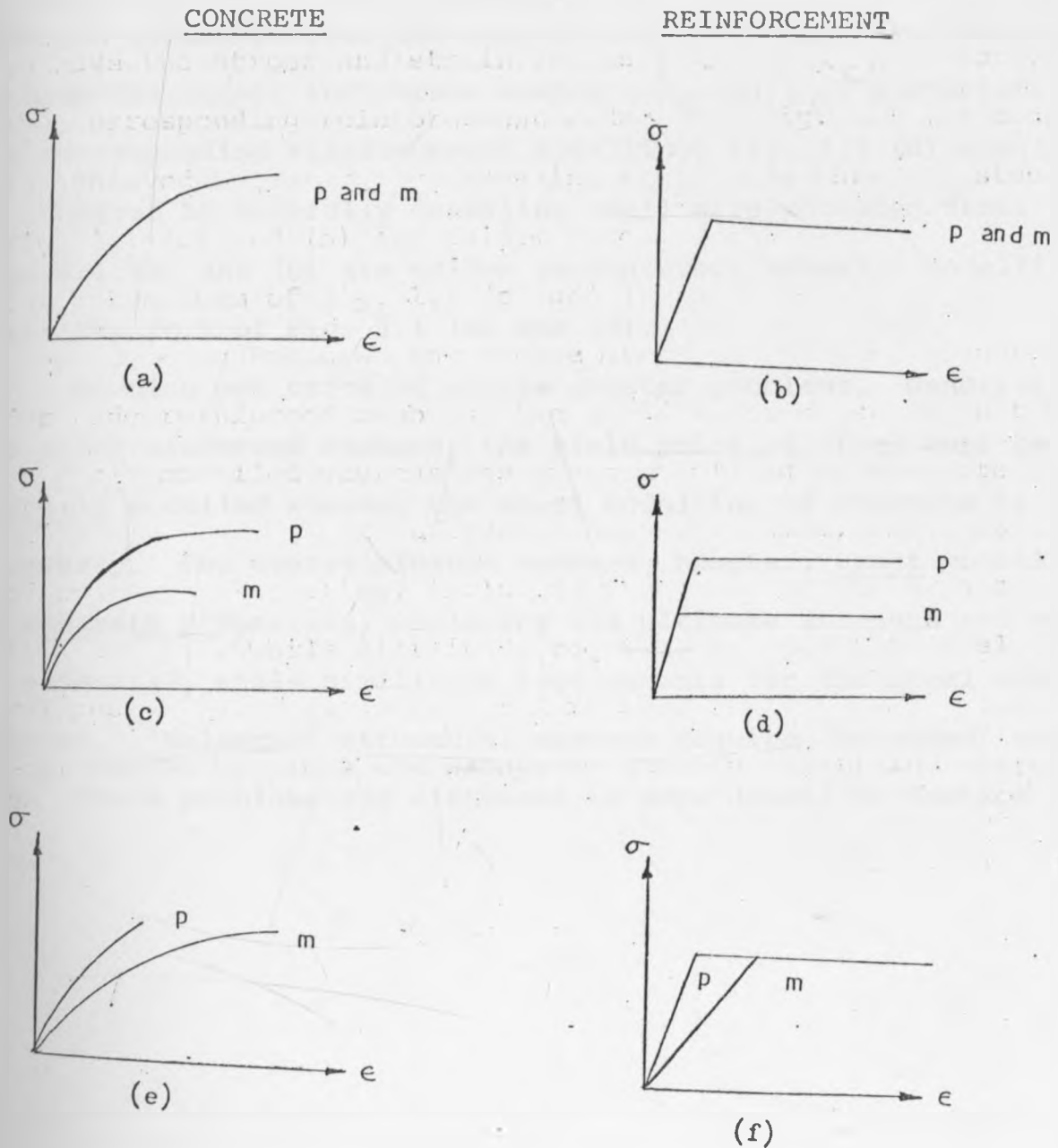
Concrete, shows not only non-linear deformation under load, it also has well-known marked differences in tensile and compressive strength. Creep, shrinkage, cracking complicate the picture further. Bonding with steel bars is also essential for strength. In order to investigate these phenomena, a concrete with aggregate particle size, sand particle size and reinforcing bars size (or area), all scaled down, is required. Such a material is called micro-concrete. The laws of similitude must be followed for meaningful results.

Micro-concrete is sometimes referred to as mortar (since it is normally made of water, sand and cement).

Successful attempts to simulate concrete with high strength gypsum plaster have also been advanced (ref. 1.2). In this case the 'micro-concrete' takes such a form.

1.5 Reinforcement in Micro-Concrete Models

Small size steel wires are used for this purpose. Sometimes, annealed small size threaded steel rods are needed to satisfy special requirements. Stress-strain relationships are shown below for concrete and reinforcing steel.



p - prototype

m - model

Fig. 1.1 Stress-strain relationships for micro-concrete and reinforcement

Fig. 1.1 (a) and (b) show a 'micro-concrete' reinforced with small size steel wires, with similitude laws strictly observed (i.e. no 'distortion'). This is done by careful mortar design, and choice of suitable steel wires.

The mortars shown in Fig. 1.1 (c) and (e) are made of high strength gypsum plaster and sand mixes, where the requirement is to have the stress and strain scales (λ_σ and λ_ϵ) distorted. The corresponding reinforcement modelling, Fig. 1.1 (d) and (f) is achieved by carefully annealing small size threaded steel rods. Fig. 1.1 (a) and (b) are seldom encountered; normally modelling takes the form of Fig. 1.1 (e) and (f).

Bonding and cracking create greater problems. Generally, for underreinforced members, the yield point of steel must be properly modelled whereas the exact modelling of concrete is not necessary. For overreinforced members, however, exact modelling of concrete properties, including its ultimate strength and strain is essential, while similitude requirements for the steel can be relaxed. 'Balanced' structural members require 'balanced' modelling. These problems are discussed in more detail in Section 1.7.

1.6 Similitude Requirements (for Direct Models)

For a model to represent the prototype, similitude 'laws' or requirements must be applied during model design. These requirements are summarised in Table 1.1, below. (for RC models). The scale factor ' λ_i ' is defined (in this thesis) as the multiplier required to convert the model quantity ' i_m ' to the corresponding prototype quantity ' i_p ' or:-

$$i_p = \lambda_i * i_m .$$

In the context of modelling with micro-concrete, these requirements have been restricted to 'direct' models (see Section 1.2 (c)).

QUANTITY	SYMBOL	DIMENSION	TRUE MODEL	DISTORTED MODEL		
				$E_{rp}/E_{rm} \neq \lambda\sigma/\lambda\epsilon$	$E_{rp}/E_{rm} = \lambda\sigma/\lambda\epsilon$	$E_{rp}/E_{rm} = 1$
Concrete Stress	σ_c	FL^{-2}	$\lambda\sigma$	$\lambda\sigma$	$\lambda\sigma$	$\lambda\sigma$
Concrete Strain	ϵ_c	-	1	$\lambda\epsilon$	$\lambda\epsilon$	$\lambda\epsilon$
Modulus of Concrete	E_c	FL^{-2}	$\lambda\sigma$	$\lambda\sigma/\lambda\epsilon$	$\lambda\sigma/\lambda\epsilon$	$\lambda\sigma/\lambda\epsilon$
Poisson's Ratio	ν_c	-	1	1	1	1
Concrete Mass Density	ρ_c	FL^{-3}	$\lambda\sigma/\lambda\epsilon$	$\lambda\sigma/\lambda\epsilon$	$\lambda\sigma/\lambda\epsilon$	$\lambda\sigma/\lambda\epsilon$
Reinforcement Stress	σ_r	FL^{-2}	$\lambda\sigma$	$\lambda\epsilon E_{rp}/E_{rm}$	$\lambda\sigma$	$\lambda\epsilon$
Reinforcement Strain	ϵ_r	-	1	$\lambda\epsilon$	$\lambda\epsilon$	$\lambda\epsilon$
Linear Dimension	l	L	λl	λl	λl	λl
Displacement	δ	L	λl	$\lambda\epsilon \lambda l$	$\lambda\epsilon \lambda l$	$\lambda\epsilon \lambda l$
Angular Displacement	β	-	1	$\lambda\epsilon$	$\lambda\epsilon$	$\lambda\epsilon$
Area of Reinf't.	A_r	L^2	λl^2	$\lambda\sigma \lambda l^2 E_{rm} / \lambda\epsilon E_{rp}$	λl^2	$\lambda\sigma \lambda l^2 / \lambda\epsilon$
Concentrated Load	Q	F	$\lambda\sigma \lambda l^2$	$\lambda\sigma \lambda l^2$	$\lambda\sigma \lambda l^2$	$\lambda\sigma \lambda l^2$
Line Load	W	FL^{-1}	$\lambda\sigma \lambda l$	$\lambda\sigma \lambda l$	$\lambda\sigma \lambda l$	$\lambda\sigma \lambda l$
Pressure	q	FL^{-2}	$\lambda\sigma$	$\lambda\sigma$	$\lambda\sigma$	$\lambda\sigma$
Moment	M	FL	$\lambda\sigma \lambda l^3$	$\lambda\sigma \lambda l^3$	$\lambda\sigma \lambda l^3$	$\lambda\sigma \lambda l^3$

TABLE 1.1. SCALE FACTORS FOR REINFORCED CONCRETE MODELS

1.6.1 Materials Similitude

In order to model the behaviour of concrete structure, the stress-strain curve of the model material must be geometrically similar to that of concrete. λ_σ and λ_ϵ must be constant for all levels of stress and strain. Fig. 1.1(a) - (f) shows such curves for reinforced micro-concrete. In some cases, the moduli of elasticity for the reinforcement are related thus:

$$E_{rp}/E_{rm} = 1; \text{ in others}$$

$$E_{rp}/E_{rm} \neq \lambda_\sigma / \lambda_\epsilon .$$

In the former, the stress scale for steel must equal the strain scale for concrete ($\lambda_{\sigma_r} = \lambda_{\epsilon_c}$), if the model is to properly simulate the prototype yield condition (see Fig. 1.1(c) and (d)). In the latter, the steel and concrete stresses must be modelled by different factors - (Fig. 1.1(e) and (f)). This of course affects the area of reinforcement in the model.

The required λ of unity for Poisson's ratio tends to be restrictive. It is fully satisfied only if the model and prototype materials are identical. Fortunately, for one-dimensional analysis where flexural and axial stiffness predominates, this is not so important. However, for two and three-dimensional structural elements, where shear and torsion are important, serious errors may result if this condition is not met. The solution would be to pick out a 'critical' element, and build and test it at full scale.

Mass density scaling (λ_{ρ_c}) is only important if the dead load stresses are important. From Table 1.1, λ_{ρ_c} depends on λ_σ and λ_ℓ and if $\lambda_\sigma = 1$, then $\lambda_{\rho_{cm}} = \lambda_\ell * \rho_{cp}$. This is usually practically impossible, and if it is important it is obviated by additional, artificial distributed loads. However, if $\lambda_\sigma = \lambda_\ell$ by design, then $\lambda_{\rho_c} = 1$, solving the problem.

1.6.2 Geometry Similitude

Geometric similarity demands that all linear dimensions of the model be scaled down from the corresponding prototype ones by a constant ratio. Practical limitations exclude certain structural details. Also the scaling down of fine aggregates, cement particles and steel deformation is impossible. Fortunately, such minute details do not cause serious problems provided the material properties similitude is adhered to.

The effect of specimen size on strength is well known. The strength and the mode of failure vary as the size of test specimen varies. However, this factor is of importance with scales much less than 1/10; and these are seldom with micro-concrete models.

Displacement and deformation are of linear scaling and are accurately simulated until large deformations that cause change in geometry occur. As seen in the Table 1.1, $\lambda_s = \lambda_l \lambda_e$; now λ_e is normally unity so that $\lambda_s = \lambda_l$; but when there is serious change in geometry, λ_e is no longer unity. The solution is to design a distorted model with λ_e slightly less than unity.

1.6.3 Loading Similitude

To simulate an applied force satisfactorily, not only the magnitude, but the distribution must be properly scaled. Concentrated loads are easy to apply, but distributed loads may need vacuum or hydrostatic pressure to set up.

From the Table 1.6 we note that loading similitude (λ_Q) is independent of λ_e . Moreover, if $\lambda_l \gg 1$ and $\lambda_\sigma > 1$, the model load would be very much reduced (since $\lambda_Q = \lambda_\sigma \lambda_l^2$). This is why small scale models have rather simplified loading systems.

1.7 Special Considerations

1.7.1 Bond

Certain aspects of behaviour of reinforced concrete is attributed wholly or very strongly to the bond between reinforcement and concrete.

These are :

- (i) Complete bond failure due to fatigue loading;
- (ii) Progressive destruction of bond caused by loading;
- (iii) Combined failure modes that include bond failure;
- (iv) Transfer of prestress in pretensioned concrete;
- (v) Cracking behaviour in size, extent and growth of cracks.

The basic similitude requirement for bond is that bond stresses developed by model reinforcement be identical to those of the prototype reinforcement. Also the ultimate bond strength of model and prototype should be identical; this implies that $\lambda\sigma = 1$. Scale of model is important here. For smaller models, one is forced to use rusted, deformed or threaded wires or stranded cables (for prestressed models).

Knowledge of the bond mechanism in concrete is limited. The ACI Code (1970) gives the ultimate bond strength per inch of bar length as :

$$U_u = 30 \sqrt{f_c'} < 25000 \quad (\text{psi units})$$

(standard notation).

This expression is derived from tests on prototype concrete observations. It would be in error if used for modelling. However, the difficulty may be obviated by providing model steel which will duplicate the local bond behaviour of the prototype. Alternatively, if knowledge of model reinforcement bond behaviour is available, then the required bond strength can be modelled by proper choice of number and size of bars. This provides the

required total bond strength. This alternative should be preferred if the bond behaviour of both prototype and model are available.

'Pull out' experimental tests on reinforced micro-concrete specimens are used to indicate the best type of reinforcement to be used.

1.7.2 Cracking Similitude

"Modelling of cracking behaviour is just as difficult as the modelling of bond; the two are intimately related phenomena" (Ref. 1.1). The inelastic load deflection response of an RC structure depends on the degree of cracking. Similitude is insured only if crack width and spacing are scaled linearly by λ_l . This simple requirement is far from easy to achieve. Not only does it require that $\lambda_e = 1$, it also requires that the model steel bond properties are exactly adequate. Higher tensile strength of model concrete initiates cracking at a high load levels, this affecting the deflection response. If bond properties are inadequate, relatively wider cracks, less in number, will result. Furthermore, Broms and Lutz (1965) showed that crack spacing is almost directly proportional to effective side cover of concrete. It hasn't been shown whether this is true in models, with small covers.

The best one can get to modelling cracking adequately is by using as large a model as possible. In 'direct' modelling where this factor is important, cracking similitude may dictate the scale.

1.7.3 Thermal Modelling

Here, both temperature and thermal properties must be mutually considered. The common thermal properties are coefficient of Thermal Expansion α , Specific Heat c , Thermal Conductivity k and Coefficient of heat transfer h . When modelling, these properties are best treated collectively, combining some or all at once. Examples are treating the Thermal Diffusivity,

$D = k/c\rho$ (ρ - mass density) for massive dams; or application of the Nusselt's number for surface heat considerations,

$$N = hl/k \quad (l - \text{linear length}).$$

These quantities should be the same for both model and prototype.

The four principal dimensions involved here are : F , L , T and θ . Table 1.2 shows the significant quantities required, unique to thermal modelling. A problem that requires more than these four dimensions demands distortion.

When the Poisson's ratio, ν , are unequal in model and prototype, special similitude relationships for a general stress state or a state of plane strain; and for a state of plane stress, are used (Hovanesian and Kowalski, 1967). The strain scale, then depends on θ and α ; and λ_t is proportional to $(\lambda_\alpha)^2$. This means that long term thermal effects can be modelled for greatly reduced time.

In choosing a material for thermal modelling, it is important to ensure that thermal and elastic properties do not change with temperature. Mortars should therefore have a higher preference to plastics and metals, in that regard.

PROPERTIES		SCALE FACTOR		
Quantity	Dimension	Different Materials in model and prototype with $\nu_p = \nu_m$	Different Materials in model and prototype with $\nu_p \neq \nu_m$	Same Materials in model and prototype and same temperature
Stress, σ	FL^{-2}	$\lambda_\alpha \lambda_\theta \lambda_E$	$C_2 \lambda_\alpha \lambda_\theta \lambda_E$	1
Strain, ϵ	-	$\lambda_\alpha \lambda_\theta$	$C_1 \lambda_\alpha \lambda_\theta$	1
Elastic Modulus, E	FL^{-2}	λ_E	λ_E	1
Poisson's ratio, ν	-	1	λ_ν	1
Coefficient α	θ^{-1}	λ_α	λ_α	1
Thermal Diffusivity, D	$L^2 T^{-1}$	λ_D	λ_D	1
Linear dimension, l	L	λ_l	λ_l	λ_l
Displacement, δ	L	$\lambda_\alpha \lambda_\theta \lambda_l$	$C_1 \lambda_\alpha \lambda_\theta \lambda_l$	λ_l
Temperature, θ	θ	λ_θ	λ_θ	1
Time, t	T	λ_l^2 / λ_D	λ_l^2 / λ_D	λ_l^2

For: General stress state, or plane strain

For Plane stress

$$C_1 = \frac{(1+\nu_p)(1-\nu_m)}{(1-\nu_p)(1+\nu_m)} ; C_2 = \frac{1-\nu_m}{1+\nu_p} \quad \parallel \quad C_1 = \frac{1+\nu_p}{1+\nu_m} ; C_2 = 1$$

TABLE 1.2 : SCALE FACTORS FOR THERMAL MODELLING.

1.7.4 Dynamic Modelling

In this regard, modelling time is an important factor. The common time dependant effects in concrete structures are creep, shrinkage, relaxation of prestress and vibration loading. However, these are no where near as important as ground motion due to earthquake or dynamic loadings.

Similitude requirements for earthquake response of structures are listed in Table 1.3; F, L and T are the fundamental dimensions. Again, when more than these three are needed for a particular case, distortion is inevitable.

Simulation of random displacements creates a major problem here. Sine wave vibrations and impacts have been used to approximate the effects, but these are still inadequate.

Furthermore, material properties vary under dynamic loading. Strain-rate affects ultimate strength, yield point, modulus of elasticity, etc. Structural damping affects structural behaviour. These phenomena are to date not clearly investigated.

Quantity	Dimension	Scale Factor
		(No distortion)
Geometry, l	L	λ_l
Spec. mass, ρ	$FL^{-4}T^2$	λ_ρ
Modulus, E	FL^{-2}	λ_E
Acceleration, a	LT^{-2}	$\lambda_E / \lambda_\rho \lambda_l$
Velocity, v	LT^{-1}	$\sqrt{\lambda_E / \lambda_\rho}$
Force, Q	F	$\lambda_E \lambda_l^2$
Time, t	T	$\lambda_l \sqrt{\lambda_\rho / \lambda_E}$
Stress, σ ; pressure, q	FL^{-2}	λ_E
Strain, ϵ	-	1
Displacement, δ	L	λ_l
Frequency, f	T^{-1}	$(\sqrt{\lambda_E / \lambda_\rho}) / \lambda_l$
Poisson's ratio, ν	-	1

TABLE 1.3 : SCALE FACTORS FOR DYNAMIC (EARTHQUAKE)
STRUCTURAL RESPONSE

CHAPTER 2

MODELS FOR CONCRETE REACTOR VESSELS AND CONTAINMENTS

2.1 Introduction (General)

In this chapter, two main types of reactor vessel models will be discussed: models for prestressed concrete reactor vessels (PCRVR) and those for reinforced concrete reactor vessels (RCRV). In this context these vessels may be referred to as "pressure" vessels from time to time. (The abbreviations then become PCRV and RCPV).

Typical PCRVR's are prestressed with thousands of hoop, head and longitudinal post tensioning elements to resist internal pressure. Mild steel deformed bars are used. Sometimes vessel cavities are lined with thin, leak tight steel plates. Interior temperatures for a reactor vessel may reach 95°C under normal operating conditions. A large number of penetrations for refuelling are made through the thick, heavy walls. (Fig. 2.1 shows such penetrations). The combination of prestressing, reinforcement and penetration hardware makes some areas of the vessel very congested; this forces use of concrete with aggregate size no more than 25mm, normally.

2.2 Loading Considerations in Design

Loading conditions that are considered in analysis and design include:-

- (a) Dead load; induced strains and stresses during construction.
- (b) Prestress
- (c) Isothermal pressurisation, cycling, creep and shrinkage under mechanical loading.
- (d) Overpressure leading to extensive vessel cracking.
- (e) Overpressure leading to ultimate loading.
- (f) Combined thermal and pressurising cycling.

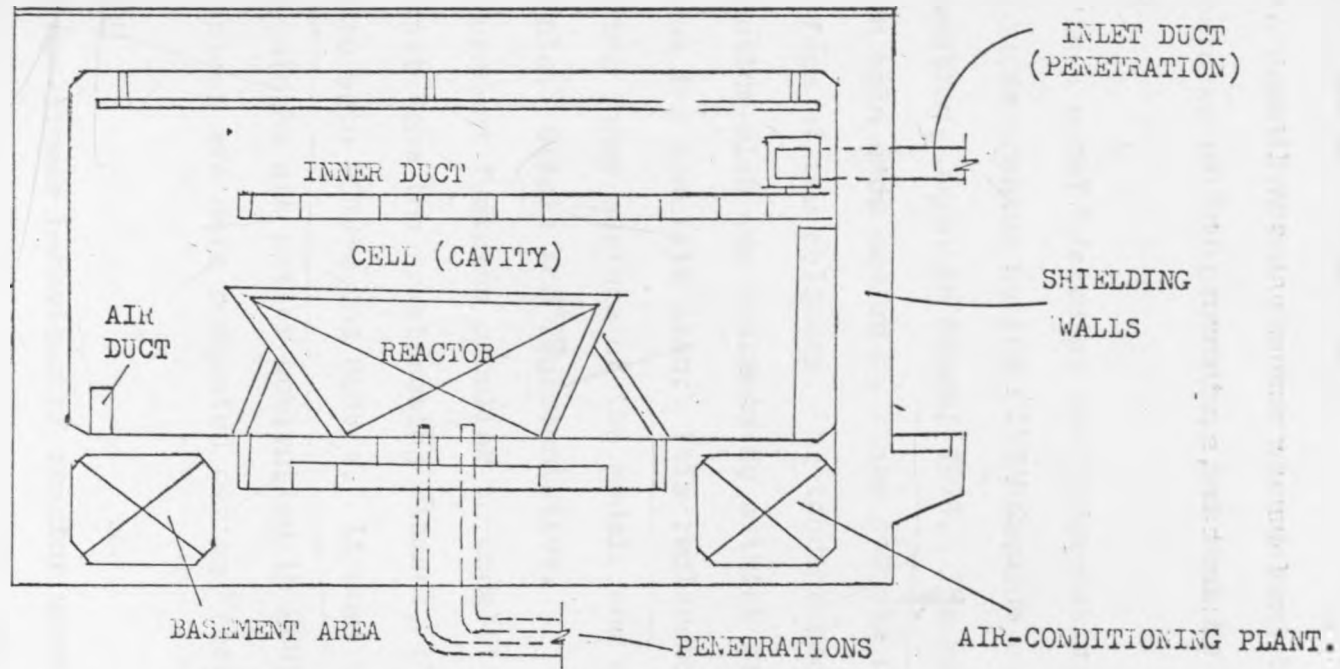


Fig 2.0 Layout of a Typical Reactor Vessel

- (g) Thermal creep and shrinkage.
- (h) Earthquake (Ground motion).
- (i) Combinations of above loads.

Basically, a model for any reactor vessel must be representative of the principal features of the prototype, and must be as simple as possible.

An example is a model tested at Oak Ridge National Laboratory in the United States, later adopted by the PCPV Research and Development Group, Kajima Corporation, Japan in March, 1973. The model was a hollow cylinder with both ends sealed by slabs and six pilasters located along the outer surface of the cylinder. 57 tendons prestressed the model. Here, the bottom slab was replaced by a thick steel plate with the same stiffness as the concrete slab. This replacement enabled instrumentation on the inner surface of the model, and observation of cracks became possible. Simple and representative.

I will now present features peculiar to modelling of a 'typical' reactor vessel. Apart from the prestressing element, the features are equally applicable to both PCRV's and RCRV's. It must be born in mind, however, that crack widths are better controlled in PCRV's than in RCRV's. Also the former are more congested during fabrication.

2.3.1 Model Design

Due to the non-linear behaviour of reactor vessels, direct models, utilising materials similar to the prototype ones, must be used. This facilitates the full investigation of such behaviour.

Model design begins with choice of the scale factor, λ_l . This is normally done by guidelines laid out in Chapter 1, namely type and purpose of model. Since a direct model is used for investigation of non-elastic phenomena, λ_l is normally between 10 and 20. This then is a 'large' scale model, with typical model heights ranging from 2m to 10m.

-62-

Most of the model characteristics are assessed here by similitude laws, once λ_l is established. The scale factor discussed hitherto refers to linear dimensions of length. However, other quantities must be considered. Cracking and general non-linear response depend highly on material properties. Hence, every effort should be made to obtain a model prestressing and reinforcement with $E_p/E_m = 1$. This model will of course be distorted. Additional similitude requirements are given in Table 1.1 (Chapter 1.)

Prototype steel areas are reduced by a factor of λ_l^2 . In order to simplify model construction, the total number of prestressing elements may be reduced by a factor (of 2 or 3, say). Similarly, for the same reason, the reinforcing bars may be changed by use of a uniform diameter bar throughout construction.

Other features of the vessel such as liners and penetrations are scaled geometrically. Finally, all linear materials must meet the requirements of $\lambda_\sigma = \lambda_\epsilon = 1$.

2.3.2 Further Design Considerations

(a) Design Procedure

The preliminary stage of design, normally based on the theory of simple thin shell analysis, determines the proportions of top slab to wall thickness. Three dimensional finite element analysis is then applied to model load cases, individually and combined. The results of this analysis gives the choice of prestressing, and prestressing forces.

(b) Design Pressure

The maximum expected incident pressure (as well as the normal operation pressure) are used in this regard.

(c) Prestressing Forces

These are determined by three criteria:-

(i) Results based on the finite element analysis.

(ii) For internal pressure up to design level, prestress should remain on the compression sides at the various parts of the vessel. For internal pressure up to 1.5 times design level, the stress should be less than the concrete tensile strength.

(iii) For vertical prestressing, the vessel wall should be securely fixed to the base plate (say, a steel plate), to prevent slipping under circumferential prestressing and internal pressurising.

2.4 MODEL LOADING ANALYSIS

2.4.1 Construction and Dead Loads

If $\lambda_\sigma = 1$, then the required mass density of the model materials is λ_ρ times that of the prototype materials. This cannot be achieved normally. The model dead load stresses will then be only 5%-10% of the prototype ones; the distortion so produced must be assessed. As pointed out in Table 1.1, externally applied prototype line loads, concentrated loads, and moments will be scaled by factors λ_ρ , λ_ρ^2 and λ_ρ^3 , respectively.

2.4.2 Pressurisation and Cycling

When $\lambda_\sigma = 1$, the pressure scale factor is unity. The model should be designed to respond elastically to the prototype design maximum operation pressure; this giving very good predictions of the prototype response. As with the prestress load, stresses and strains of model should be the expected prototype ones; while the displacements are scaled by λ_ρ .

2.4.3 Steady State Thermal Gradient and Pressure

This condition necessitates similitude laws shown in Table 1.2. If λ_D and λ_ρ are essentially unity for micro-concrete, then all model properties correspond to the prototype; except for displacement and time, which are scaled by λ_ρ and $(\lambda_\rho)^2$ respectively. This advantage will yield undistorted thermal stresses, strains, and displacements which can be

measured directly in combination with other stresses, since $\lambda_\sigma = \lambda_\epsilon = 1$.

If this is not the case, then once λ_E is set to unity, model temperatures can be adjusted by λ_θ to yield $\lambda_\alpha * \lambda_\theta = 1$. This gives undistorted stresses, strains and displacement. Where this adjustment is impracticable (or impossible), separate results of internal pressure and thermal action are taken and superimposed.

Boundary heat transfer is modelled by Nusselt's number,

$$N = hl/k \quad (\text{see section 1.7.3})$$

2.4.4 Creep and Shrinkage (under normal temperatures)

"Modelling creep and shrinkage places severe demands on model concrete properties" (Ref. 1.1). It becomes impossible to model for creep if the aggregate size of the micro-concrete is too small. Again with a large λ_l , the model thicknesses are too small to model moisture conditions.

Careful measurements on the model will give a reasonable indication of the prototype creep and shrinkage. In most cases this would be only qualitative.

2.4.5 Creep and Shrinkage from Temperature Effects

Under operating conditions, creep in a reactor vessel will be accelerated by elevated temperatures. The time scale for creep is given by $(\lambda_t)^2$ (for the case $\lambda_D = 1$, Table 1.2). For large values of λ_l , this creates creep and thermal strains occurring at an incompatible time scaling. For any meaning, then, creep and shrinkage modelling should be done on the largest possible model (λ_l small); the best being the full scale model ($\lambda_l = 1$).

2.4.6 Severe Vessel Cracking from Overpressure

Tensile strength of concrete, and bond between concrete and reinforcement are of importance here. The condition $\lambda_\sigma = 1$, necessitates that the tensile strengths of model and prototype be identical. For

true cracking similitude, the above condition must be met for all combined stress states, and for uniaxial stresses.

2.4.7 Overpressure Leading to Ultimate Load

Similitude requirements beyond the elastic range become operative at this stage. Obviously, $\nu_p \neq \nu_m$ (Table 1.2). Bending produces high compressive stresses, concrete cracks more, the steel yields, and excessive cracking leads to the gushing out of the pressurising fluid (water or oil) which leads to loss of pressure.

With a carefully built model, this behaviour should indicate the ultimate failure of a reactor vessel; which, one hopes, should never occur!

2.4.8 Dynamic Loading (Earthquakes)

Table 1.3 gives an outline of the similitude laws to be followed. Earthquake loads are idealised to three components of soil acceleration (two horizontal, one vertical). An average duration of ground motion of 30 seconds is normally taken.

Similitude laws are based on D'Alembert's law of dynamic equilibrium. This leads to the limiting cases of Cauchy and Froude.

$$\begin{array}{l} \text{Cauchy:} \quad \frac{(\text{Inertia Force})}{(\text{Elastic Force})} = \text{Constant} \\ \text{Froude:} \quad \frac{(\text{Inertia Force})}{(\text{Gravity Force})} = \text{Constant} \end{array} \quad \begin{array}{l}) \\) \end{array} \quad \begin{array}{l} \text{For model and} \\ \text{Prototype} \end{array}$$

Depending on the purpose of test, one of these conditions is adopted.

2.4.9 Load Combination

Work done by R. McGeorge and L. F. Swec Jnr (Ref. 4.1), indicates the most severe load combinations and sequences. These should be designed for, and investigated fully. Dead load + shrinkage + operational temperature + earthquake + pressure was found most severe, creating 25%

crack penetration on both inside and outside surfaces of vessel wall. The same combination, but with 'accident' pressure and maximum operational temperature added, created 80% horizontal and 80% vertical crack penetration on the outside surface of model. Other less severe combinations created 10% crack penetrations, that sealed up with release of load.

o

2.5 Loading Systems

Systems that create internal pressure, and thermal effects on models will now be discussed. Carefully planned loading systems, coupled with sound instrumentation have been shown to yield excellent results in modelling PCPV's and RCPV's.

2.5.1 Internal Pressure

To create this pressure, air, a gas, water, or oil can be used.

(a) Air Pressure

Nitrogen is normally used in this regard. Since no less than 70% in a volume of air is taken up by nitrogen, it is considered to be representative of air. Also it is less inflammable and less active than ordinary air - and hence safer.

The pressure is created by connecting compressed nitrogen cylinders to the model through a leak-proof tube, fitted with control valves and pressure gauges. As the compressed nitrogen is released, to the interior of the model, a measurable internal pressure is created, which can be controlled during testing.

The disadvantage of air is its danger at high pressure. A leakage crack could create a sudden pressure drop, resulting in an explosive action. For this reason, air-pressurising is used only in moderation, with pressures seldom exceeding 80kPa. Due to this, only the elastic behaviour of the direct model can be investigated using air pressure. Early leakage cracks can be detected using the 'soap-film-bubble' method, (Ref 6.2, Section 4.5), during this test.

(b) Water Pressure

Water is basically incompressible, and therefore high pressures can be suddenly released without danger of explosion.

The pressure is achieved by filling the central cavity of the model with water. Referring to Bernoulli's equation:-

$$\frac{v^2}{2g} + h + \frac{p}{\rho g} = H \dots \dots 2.1$$

the pressure is exerted by one or all of the three component 'heads' of the total 'head', H. The elevation head 'h' depends on how high the water level is of the feeding water tank. If this is insufficient, the velocity head ' $v^2/2g$ ' can be added by controlling the velocity of the water entering the model. An additional pressure head ' $p/\rho g$ ' (p-external pressure), can be added if required.

Water pressure can be used to investigate elastic and post-elastic phenomena of the model, up to severe cracking and probably failure. The pressure should be applied in quarterly (loading and unloading) instalments of the design value. At every stage, readings must be taken and compared to theoretically analysed results, before proceeding further. At failure, cracks widen, a sudden pressure drop results, then water gushes out of the model.

If air-pressure is used before water pressure, arrangements must be made to remove all the air from the model cavity, and replace it with water. In Chapter 5, this aspect is discussed in more detail.

(c) Oil Pressure

Pressurising oil (a petroleum based hydraulic fluid) is filled in the cavities of the model and an external pressure is applied.

The amount of pressure and its rate (e.g. 10Pa/min) should be carefully controlled. This way the pressure can be increased, decreased or left constant uniformly throughout the model cavities during the test.

After severe cracking, the pressure drops; any further increase in external pressure widens cracks and makes the oil to gush out, which leads to the ultimate failure of the vessel.

2.5.2 Heating Systems (for Thermal Tests)

A suggested system is shown in Fig 2.1. This was used by the

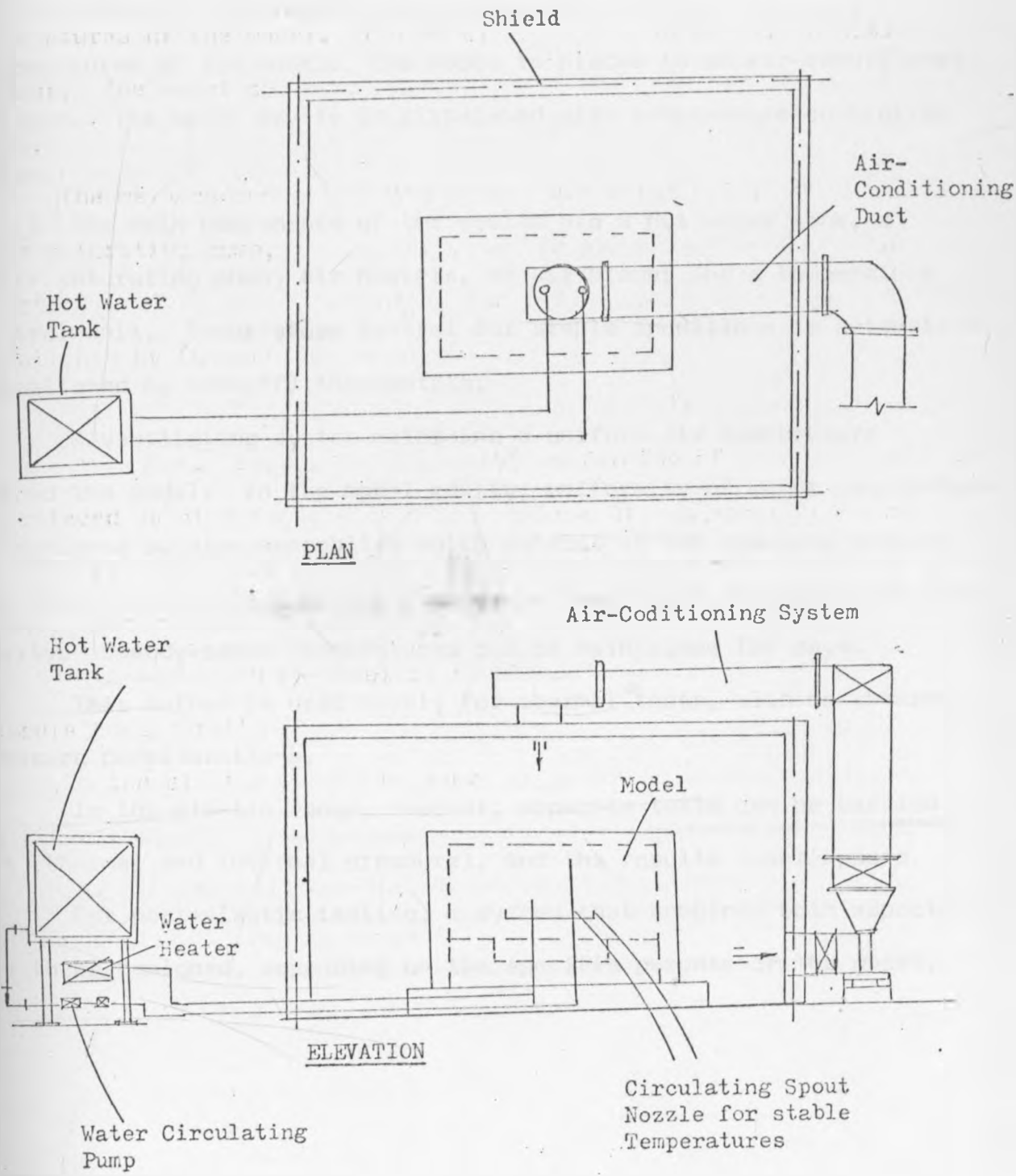


Fig. 2.1 Proposed Heating System for the Thermal Test

Kajima Corporation, PCPV Research and Development Group in April, 1973, (Ref. 2.2).

The setup is essentially to control the inner and outer temperatures of the model. The model is placed in an air-conditioned chamber. The model cavity is circulated with temperature controlled water.

The main components of the system are a hot water tank, a water saturating pump, air heaters, an air blower and a temperature control unit. Temperature control for stable conditions is automatically established by (on-off) thermostats.

A ventilating system maintains a uniform air temperature around the model. In the model cavity, uniformity of water temperature is achieved by pipe assemblies which consist of two spouting nozzles and four drawing pipes arranged in a way to produce whirlpools in the cavity. Steady-state temperatures can be maintained for days.

This method is used solely for thermal tests, with no internal pressure considerations.

In the elastic range, however, separate tests can be carried out (thermal and internal pressure), and the results superimposed.

For post-elastic testing, a system that combines both aspects has to be designed, depending on the specific purpose of the model.

2.6 INSTRUMENTATION

A well planned layout of instrumentation, together with a well controlled loading system are essential for useful and meaningful results in a reactor vessel model. Where plenty of data is expected in the results, automated data generation should be incorporated in the model.

Internal pressure tests and thermal tests (of RCPV and PCPV's) each require rather different instruments. Each will be discussed separately.

2.6.1 Instrumentation for Internal Pressure Test

Types of Gauges and other Instruments

- (i) Resistance strain gauges, bonded on the outer surfaces of the model.
- (ii) Strain gauges embedded in concrete.
- (iii) Resistance strain gauges bonded on prestressing tendons (for PCPV's).
- (iv) Load transducers (or load cells) at the prestressing tendon anchorage (for PCPV's).
- (v) Crack detection gauges or strips (long single-element bonded strain gauges).
- (vi) Concrete embedded gauges for crack detection.
- (vii) Deflection gauges (bonded resistance strain gauges on phosphor-bronze strips).
- (viii) Pressure transducers (to record internal pressure).
- (ix) Photoelastic coating on concrete to indicate location and

growth of initial cracking.

(x) Dial gauges for excessive deflections. (Figs. 2.2 and 2.3 show a typical layout of instruments in a PCPV, employed by the Kajima Corporation (Ref. 2.1)).

The embedded gauges used in their model were "elastic resistance wire strain gauges sandwiched between two acryl resin plates, waterproof-coated and covered with silica sands to improve bond strength with concrete". These were installed on the reinforcement cages prior to concrete pouring; only about 1% were defective by testing time. This is satisfactory.

2.6.2 Automated Data Generation

A system, shown schematically in Fig. 2.4, controlled and processed by computer, generates the required data. The system scans and records data from each of all the gauges automatically, and in seconds. The data output can be punched on paper tape, or typed out straight by the computer terminal software.

Such a system takes some time to set up; and requires plenty of patience, but the final speed of data acquisition makes it all worthwhile.

2.6.3 Instrumentation for Thermal Tests

The purposes of instrumentation in these tests are:

(i) To measure the temperature distribution of the model when heated.

(ii) To measure the strain distribution and displacements when heated; and for PCPV's, to measure the same under prestressing.

As mentioned earlier, measured results should be compared with analysed results at every stage of the test.

Types of Gauges Used (Ref. 2.2)

(i) Carlson Gauge:- Essentially an electric resistance wire strain gauge; could be used also to measure temperature variations.

(ii) Vibrating Wire Gauge:- The principal of this gauge is that the strain is proportional to the natural frequency of the stretched wire inside the gauge body. Any thermal expansion of the concrete is cancelled by the thermal expansion co-efficient of the gauge.

(iii) BS Gauge:- Consists of a metal membrane with an electric resistance strain gauge glued onto both faces. Co-efficient of expansion of metal coincides with that of concrete. Its fragile, so it should be embedded in mortar.

(iv) Copper - Constantan Thermocouple:- Used to measure temperature at different points of the model. Can be used inside the model (containing hot water, say) at the inner surface of the model, embedded in concrete, at the outer surface of model, and in air. Such a thermocouple can be connected to the automatic data generating system.

Layout of Gauges

In such a test, radial stresses are expected to be much smaller than circumferential or meridional stresses, hence gauges in the radial directions can be neglected. Also, the circumferential and meridional stresses are expected to be maximum at both surfaces and be zero near the centre of the wall thicknesses. This governs further any meaningful layout.

Figs. 2.5 and 2.6 indicate typical layouts of gauges and thermocouples.

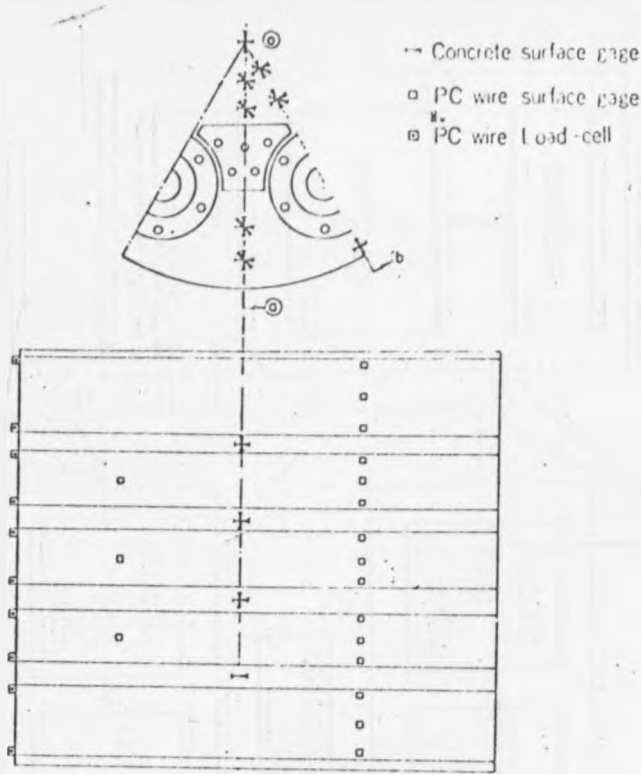


Fig. 22 Locations of Surface Gages

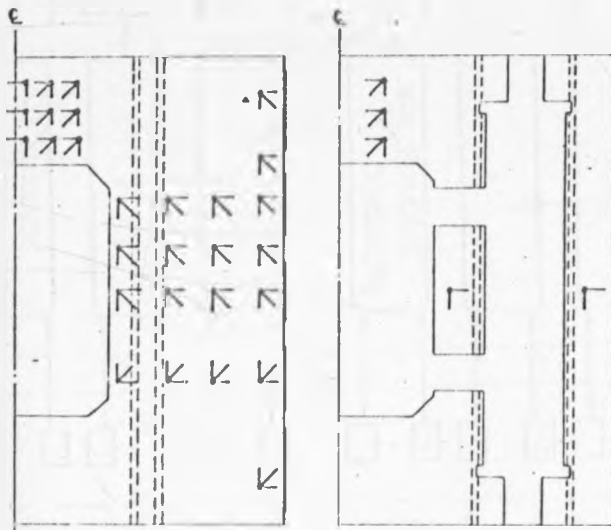
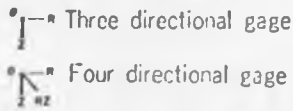
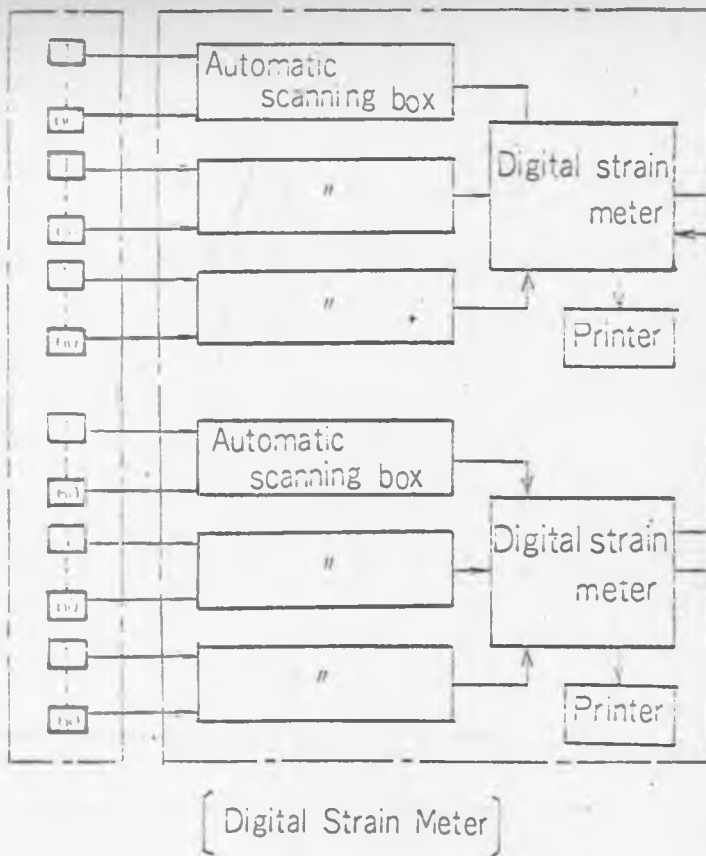
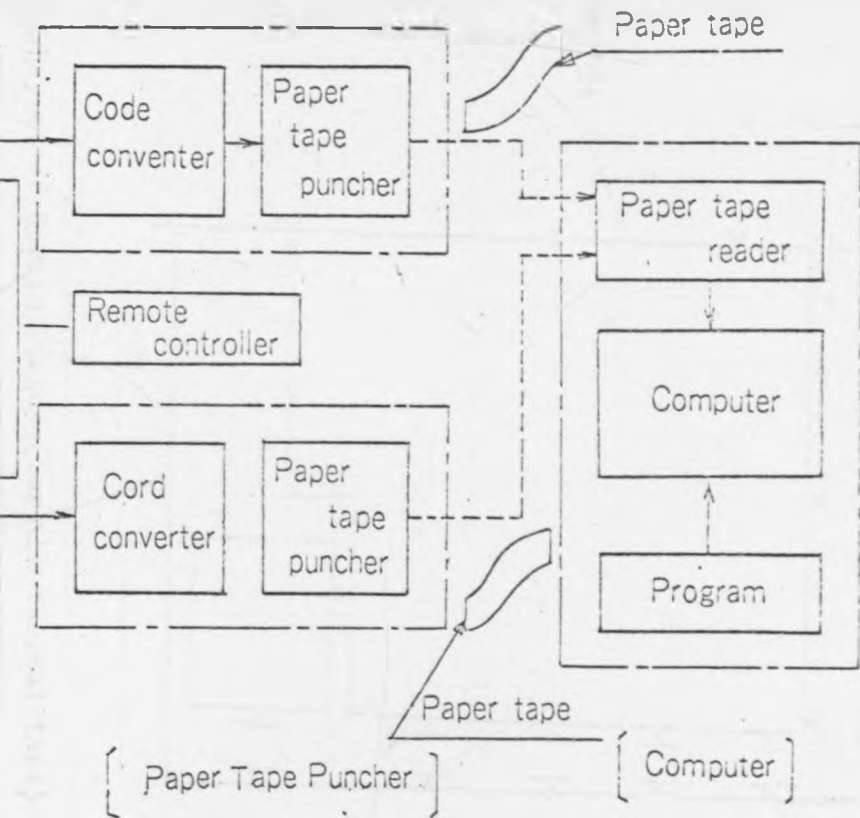


Fig. 23 Locations of Embedded Gages

Fig. 2.4 Data Acquisition System Diagram





x Hoop
— Longitudinal

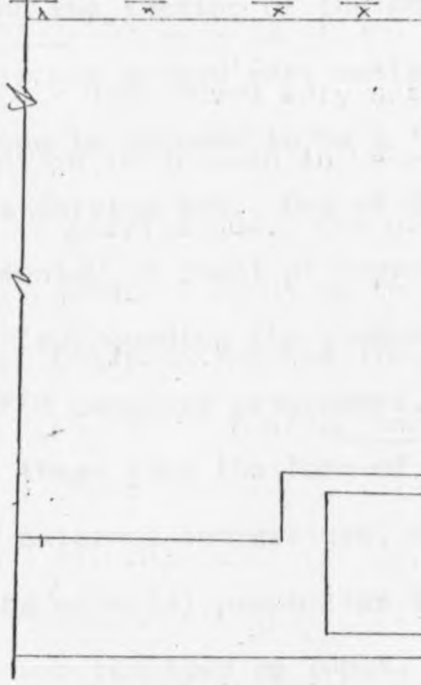
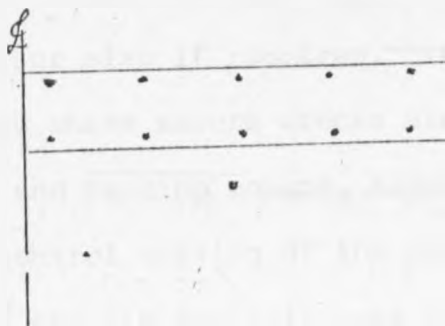


Fig. 2.5 Layout of Strain Gauges. (for the the



2.7 The FEM Analysis

A mathematical analysis of the prototype is necessary for comparing results during the testing of the model. The Finite Elements Method (FEM) of analysis has proved very satisfactory for this purpose.

When the prototype is assumed to be a 'thin' shell, a two-dimensional analysis is carried out. One of the walls is divided into a finite number of elements. A count of these elements, together with a count of the 'nodes' (surrounding the element) is used as part of the input of existing FEM computer programmes. The boundary conditions are then established - these take the form of internal pressure, external pressure, internal and external temperature, etc. These constitute further input. Also the material properties (e.g. Young's Modulus, Poisson's ratio, etc.) are required as input. The programme assumes a 'continuous medium' over all the elements, and is used to compute deformations, axial loads, moments, stresses, etc. (depending on the particular programme). The same procedure can be carried out for the roof slab, and the floor slab if required. Indeed this analysis is very useful at regions where severe cracks are expected - where the values of deflection and bending moment, together with the local axial force are needed to control testing of the model.

The results of the FEM analysis must be obtained before testing of model commences, and should be available at all stages of testing. Should there be a discrepancy between the model results and the FEM analysis ones, that anomaly should be checked out and taken into account before further testing proceeds.

More elaborate programmes assume the reactor vessel to be a 'thick' shell. The FEM is then a three-dimensional one. These are more exact. Normally a 'sector' of the vessel is taken (a 30° or 45° symmetrical section, i.e.) The elements become hexahedral, with more nodes per element. This method is very advantageous because it

takes into account the thickness of the walls, which is one of the most important features of the reactor vessel. Furthermore, the behaviour of the areas where the roof slab meet the walls can be more fully analysed and understood.

Most FEM programmes can carry out elastic or elasto-plastic analyses. The latter are more important in this context, since they yield information after cracking has occurred.

The FEM type of analysis is discussed more fully in Chapter 4.

CHAPTER 3

CONSTRUCTION OF THE REINFORCED CONCRETE REACTOR VESSEL MODEL

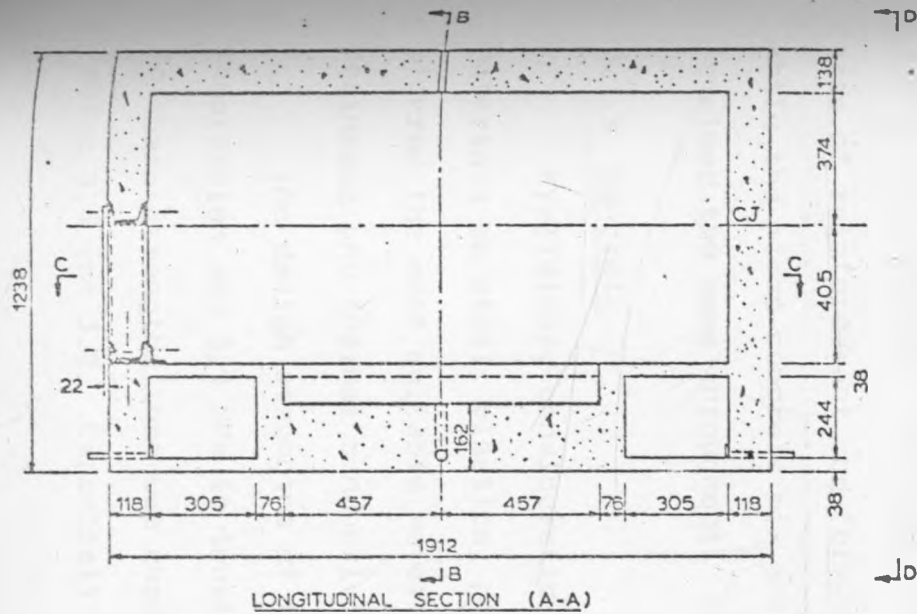
3.1 Planning and Design

3.1.1 Planning

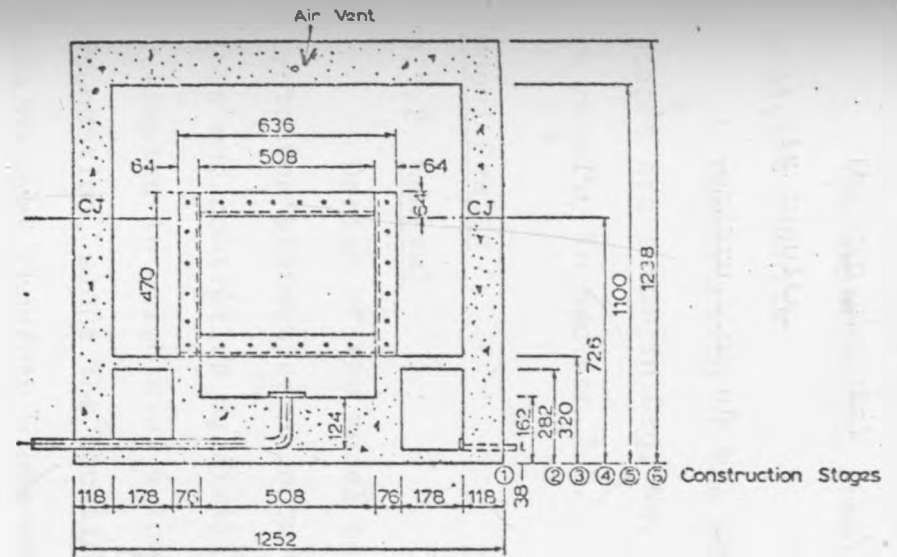
The prototype reactor vessel on which the model is based is typical of the containment structures constructed for small scale experimental reactor vessels.

This prototype structure is essentially a 'thick' shell, occupying a plan area of 24m by 15m and rising to a height of 15m; with walls 1.5m thick to provide shielding. These walls enclose 8 edge 'hollow cells' (referred to as cavities, too), and a large central cavity (11m x 6m) where the reactor sits. After consideration of the size of model, reinforcement, available space and the acceptable limits of scale in micro-concrete models, a scale factor of 1 in 12 was chosen. A model, then, occupying a plan area of 2m by 1.25m and a height of 1.24m, with 118mm thick walls was to be built in the Hydraulics Laboratory, School of Civil Engineering, University of Sydney. Fig. 3.1 shows its layout.

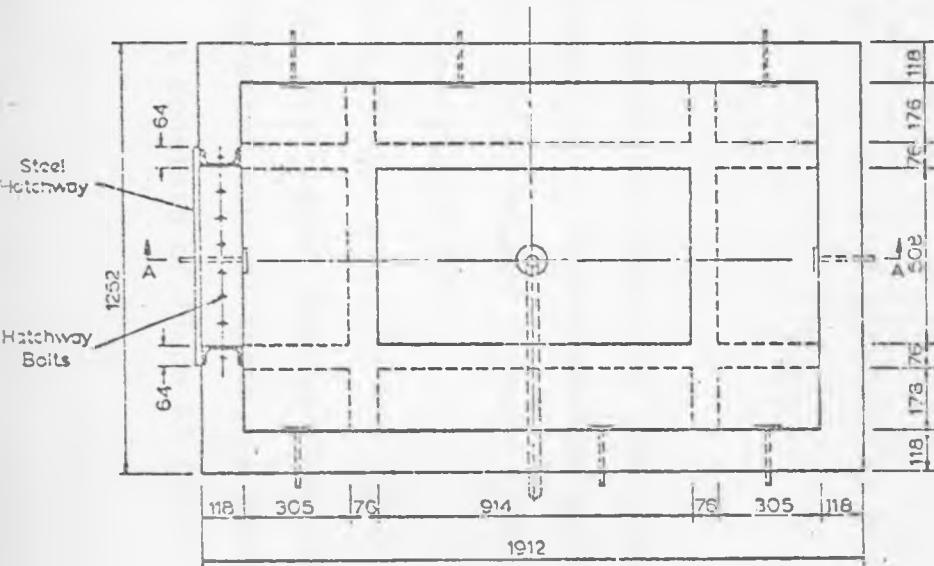
'Micro-concrete', consisting of 'Napean' Sand, cement and water, was to be used. The reinforcing bars chosen were 2mm diameter round steel rods, to be used all throughout the model. Using steel bars of the same diameter throughout saved fabrication time of reinforcement. Instrumentation was to be considered during each of the different stages of construction. A Finite Element Method (FEM) analysis was used on the vessel to give a guide to the expected strains, stresses, moments, deflections at different points. This indicated areas prone to cracking and possible leakage zones. During testing, air pressure was to be used initially, then water pressure (with a controlled head), till



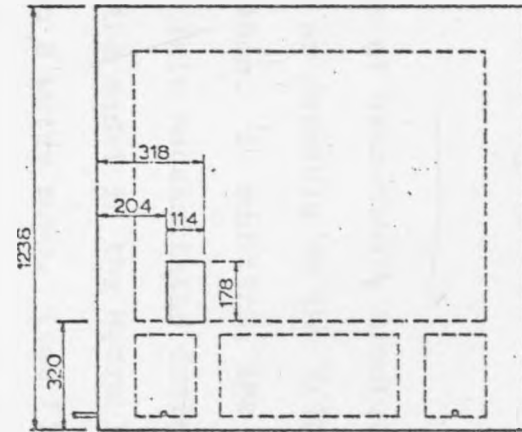
LONGITUDINAL SECTION (A-A)



TRANSVERSE SECTION (B-B)



TYPICAL PLAN (C-C)



END ELEVATION (D-D)

NOTES

1. All Dimensions in mm
2. CJ = Construction Joint
3. For Details of Steel Hatchway See Drg No 5
4. For Details of Formwork See Drg. No 2,3,4,5
5. For Details of Steel Reinforcement See Drg. No 4,5

Fig. 3.1 General Layout of Model

DEPARTMENT OF CIVIL ENGINEERING			
UNIVERSITY OF SYDNEY			
PROJECT	REACTOR CELL MODEL		
TITLE	GENERAL LAYOUT		
DRG. NO.	01	SCALE	1:1
DESIGNED	A/1	DRAWN	A/1 DATE 12.2.78

cracking occurred. (The prototype was designed to withstand an internal explosion pressure approximated to 100KPa).

The experimental results were then to be compared to the FEM analysis results.

Construction of the model was planned in six (6) stages. These stages are shown in Drg. No. 3. Each Construction stage is discussed in detail, in section 3.2.

Model Design

3.1.2 General

Design of the model consists of essentially simulating the prototype properties as accurately as possible to the 1/12 scale model. This was controlled by similitude laws. In addition, the model was estimated to weigh over 4 tonnes. This necessitated designing the foundation, since the location of the model in the Hydraulics Laboratory was on weak concrete slabs covering a water sump. (see Fig. 3.2)

Finally, formwork for easy placing and vibration of concrete, had to be designed. For each of the 6 stages of construction, therefore, area of reinforcement and formwork dimensions had to be calculated; while the micro-concrete mix and the diameter of reinforcing bars remained the same throughout.

3.1.3 Concrete

Preliminary considerations eliminated the use of such modelling materials as steel, plastics, plaster, etc. Micro-concrete was considered the most suitable material, for purposes of crack, creep, shrinkage and thermal conductivity investigations.

The design strengths of the prototype concrete were 31MPa in compression and 3.1 MPa in tension. The micro-concrete mix corresponding to these strengths that was chosen, after several tests, is shown in Tables 3.1 and 3.2. Essentially, it consists of 'Type A' (Portland)

cement, Napean sand with a maximum particle size of 3.2mm, and a 'water to cement' ratio (W/C) of 0.65. This gave the required workability and strength at 28 days. The modulus of elasticity, E_c , of this micro-concrete approximated to 2.1×10^4 MPa at 28 days. This material is also referred to merely as 'mortar' in this thesis. During construction, it was to be placed in smooth finished plywood formwork, and vibrated using a 10mm diameter, miniature poker vibrator.

As a check on strength before casting, a trial mix of the mortar was made. Cylinders of it, 100mm in diameter and 200mm high (100 x 200mm cylinders), were made and tested at 7 days for compression and tensile strengths. (The Australian Standard procedures of 'concrete strength determination' - parts 9 and 10 (1972 and 1973) - were used. This employs the 'Brazil' or splitting indirect test for tensile strength).

Typical test results are shown in Appendix 3A.

3.1.4 Reinforcement

As mentioned earlier, 2mm diameter steel rods were used throughout the model as reinforcement. The area of reinforcement was computed by the equation:

$$A_{rp} = \sum A_{r_m}^2 \dots \dots \dots 3.1$$

(notation as before, Section 1.6, Table 1.1).

This equation satisfies area requirements only. As the correct scale relationship between bar dimensions could not be obtained, bond similitude is not exact. This can have an effect on crack widths and distribution. However the number of bars in the model were sometimes less, and sometimes more than the prototype number. It was thought that this fact would diminish the problem.

In the case of reinforcement fabrics, meshes and cages where A_{rp} is given in mm^2/m , the equation was modified to:

$$A_{rp} = \lambda_l A_{r_m} \dots\dots\dots 3.2$$

for dimensional homogeneity.

After several tests, the average yield stress of the steel wires was established as $\sigma_y = 390\text{MPa}$. (The prototype steel has a design yield stress of $\sigma_y = 380\text{MPa}$). The modulus of elasticity $E_r = 3.22 \times 10^4 \text{MPa}$, was also determined.

The general layout of the reinforcement was along the prototype lines, excepting of course, diameter and spacing of bars. Joints in meshes, cages and fabrics were glued or spot-welded. A minimum bar spacing of 15mm (equivalent to 180mm on the prototype) was imposed to ease placing of the micro-concrete. But even with this constraint, the heavily reinforced reactor vessel presented problems in fabrication, with many, many wires criss-crossing all around the model, (see Plate 1).

During construction some of these problems were overcome by steel 'templates' as guides in spacing; these are discussed in more detail in Section 3.2.1.

3.1.5 Foundation

The foundation of the model had to be designed to take a load in excess of 4 tonnes, resting over a sump. A set of 5 taper flange beams (152 x 76) spanning the sump and supported on strong concrete walls, was used, (see Fig. 3.2). This arrangement took the load off the slabs covering the sump, raised the base of the model for easier fabrication, and provided anchorage for formwork during the initial stages of construction. The beams were placed on steel plates and positioned with gypsum plaster. Levelling of beams was done by a spirit level before the plaster set.

This foundation being set, a form-board was bolted on top, forming the model base, and at the same time simulating a permanent sandstone foundation of the prototype.

3.1.6 Formwork

Ply form boards, 18mm thick, with a smooth finish, were used as a formwork. For the initial stages of construction, the boards were placed and fixed in position with bolts, pipes and nuts; as shown in Plates 1, 3 and Fig. 3.3. Wooden boxes were made up and placed to form the vessel cavities, during the placing of the mortar. Fig. 3.4 shows details of these boxes.

Maximum Aggregate Size	3.2mm
Design Compressive Strength (28 days)	31 MPa
Design Tensile Strength (28 days)	3.1 MPa
Design Elastic Modulus (28 days)	2.1×10^4 MPa
Shrinkage	High
Type of Sand	Napean
Type of Cement	Type A Portland

TABLE 3.1 MICRO-CONCRETE MIX DESIGN AND CHARACTERISTICS

Water to Cement Ratio	Water to Sand Ratio	Ingredients by Weight (kg) per batch		
		Water	Type 'A' Cement	Napean Sand
0.65	0.2	11	16.9	55

TABLE 3.2 MICRO-CONCRETE MIX PROPORTIONS

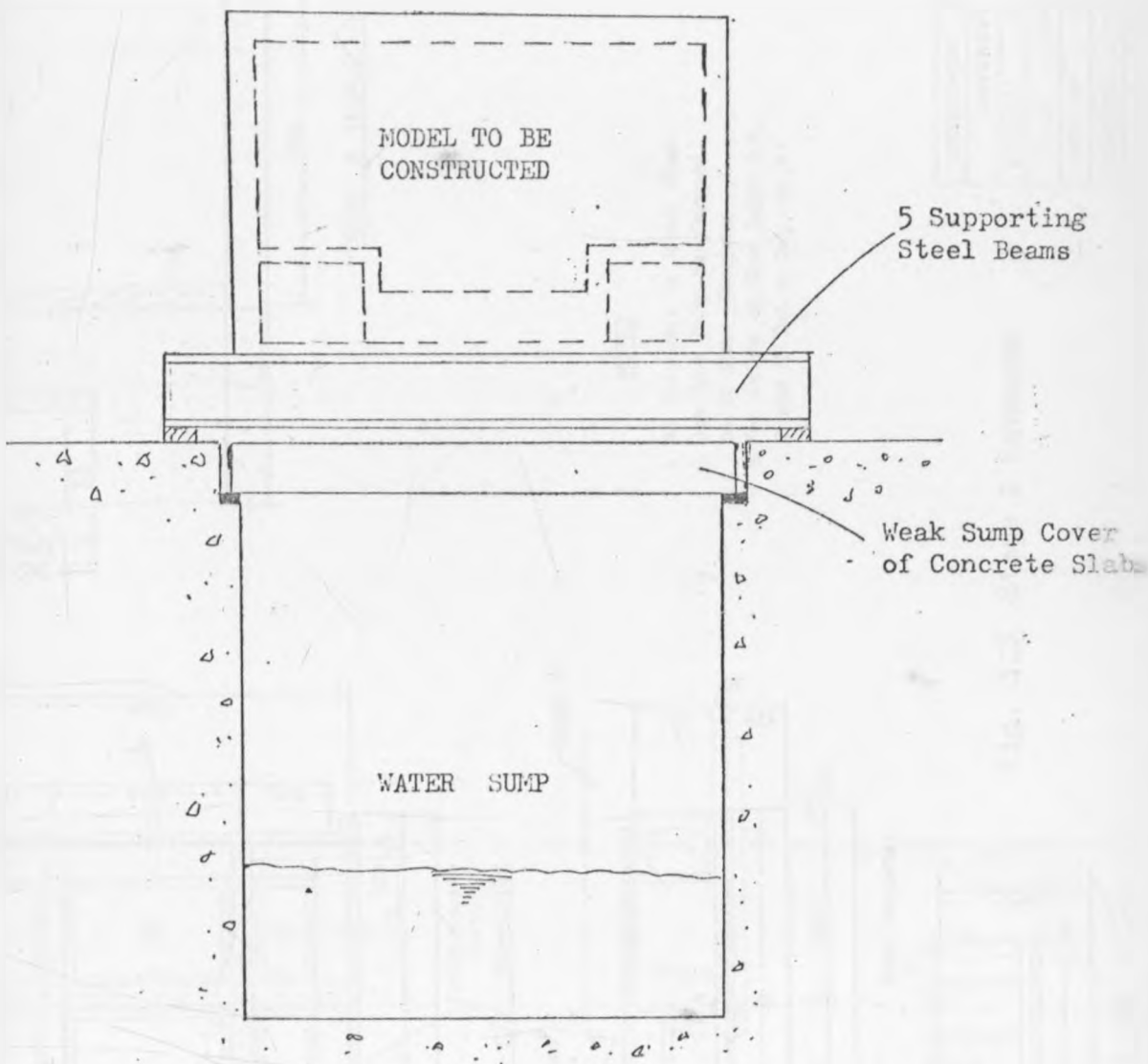
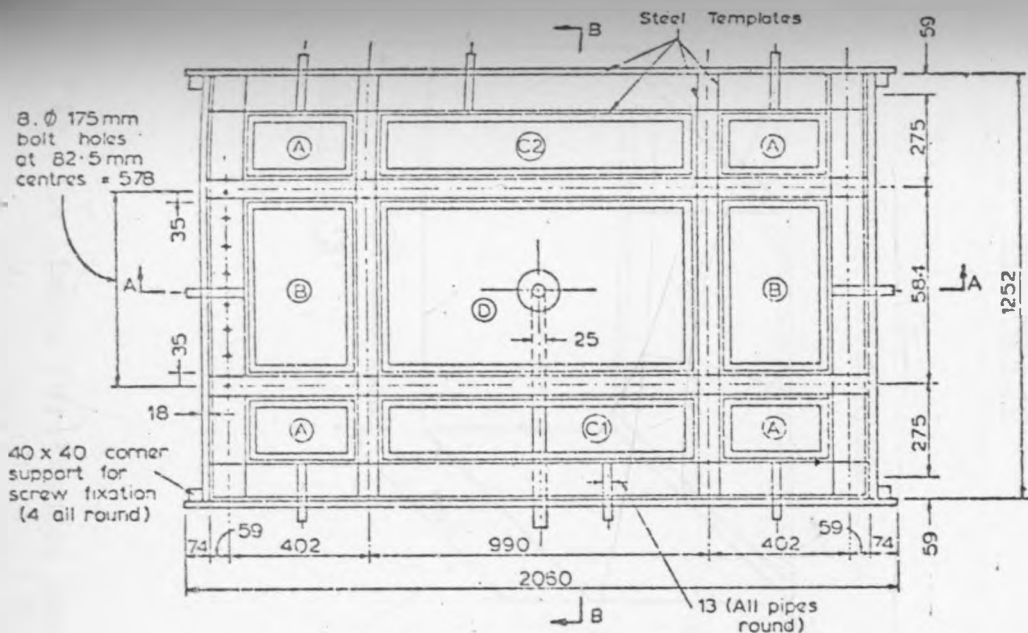
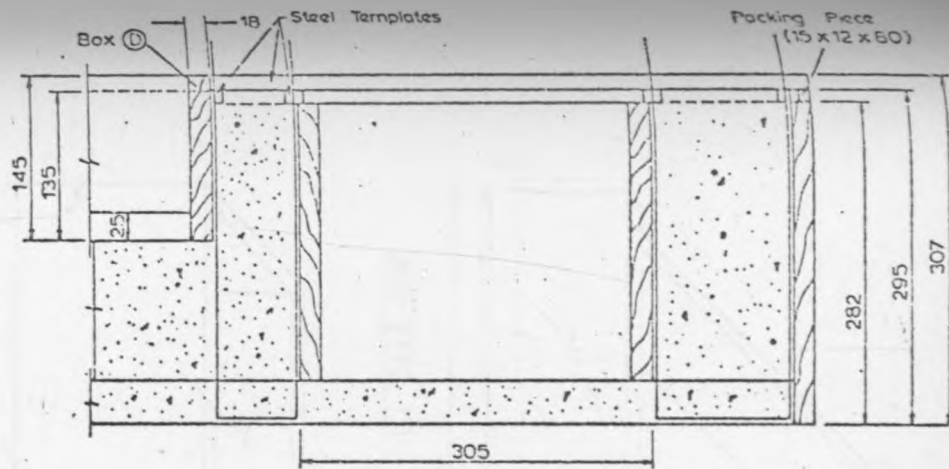


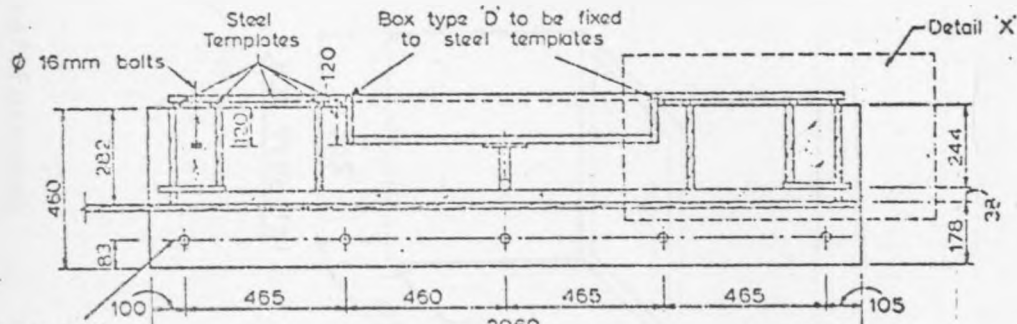
Fig. 3.2 Section through Foundation for Model



PLAN - SHOWING FORMWORK AND STEEL TEMPLATES

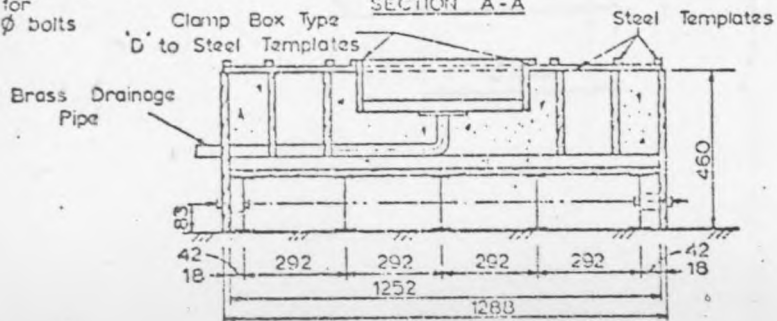


DETAIL X (SCALE 1:3)



SECTION A-A

5.16mm Ø holes for 12mm Ø bolts



SECTION B-B

NOTES

1. All Formwork is 18mm Thick
2. Box Type D to be Clamped on to Steel Templates
3. For Details of Box Types A,B, C and D Ref. to Drg No. 3

Fig. 3.3. Stage 2 Formwork

DEPARTMENT OF CIVIL ENGINEERING				
UNIVERSITY OF SYDNEY				
PROJECT	REACTOR CELL MODEL			
TITLE	STAGE 2 FORMWORK ASSEMBLY			
DRG. NO	2	SCALES	1:10, 1:3	
DESIGNED	AM	DRAWN	AM	DATE 26.2.76

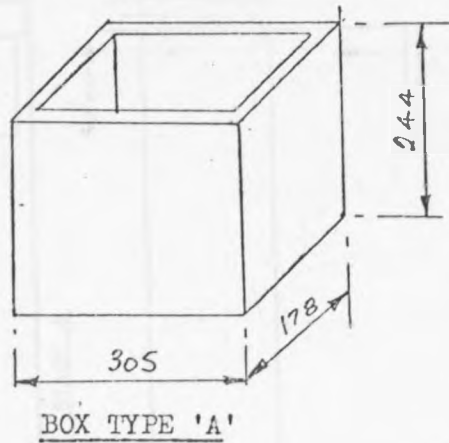
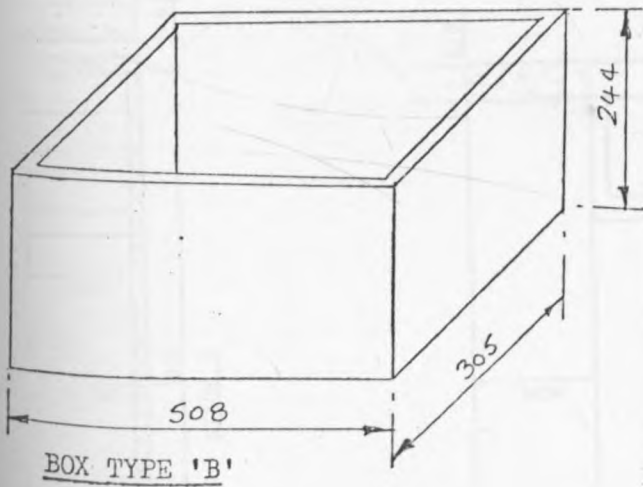
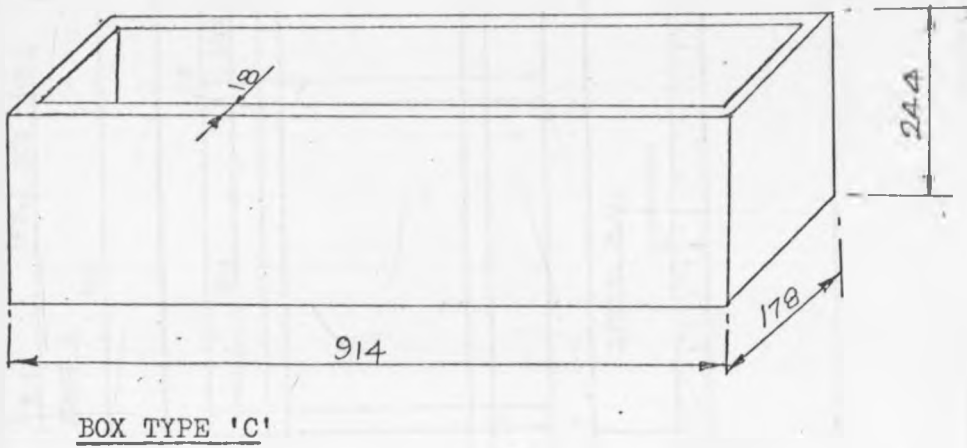
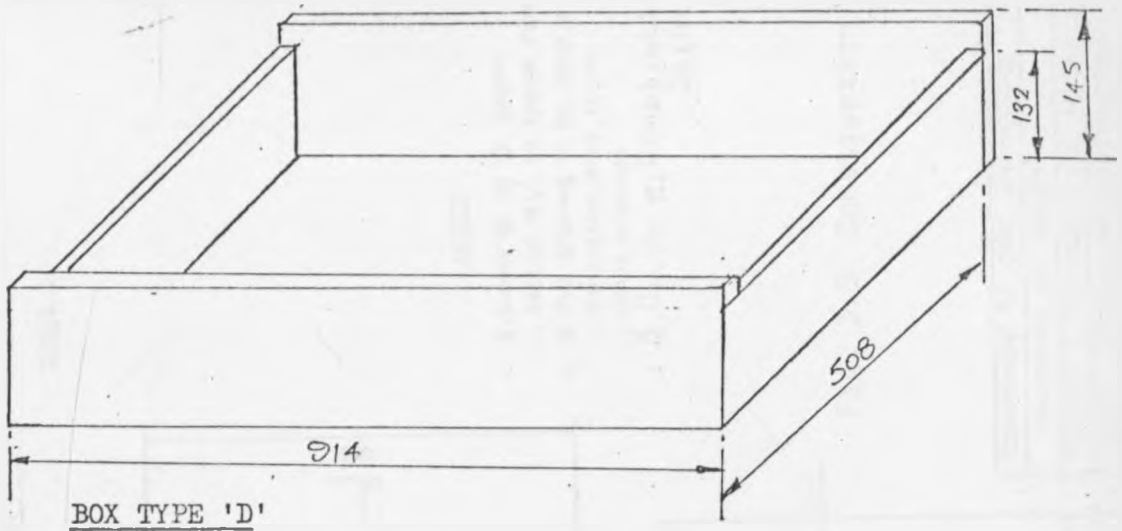
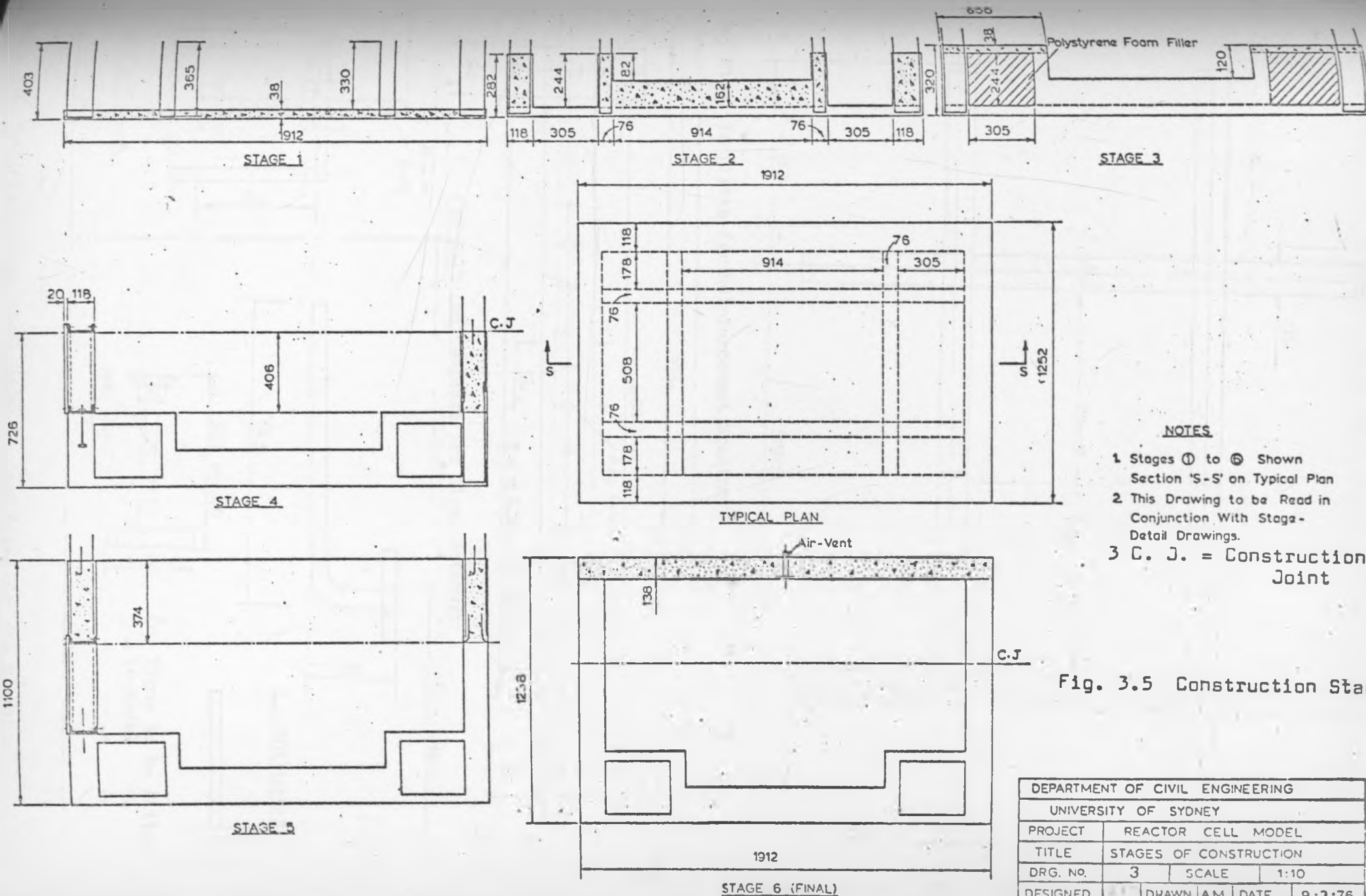


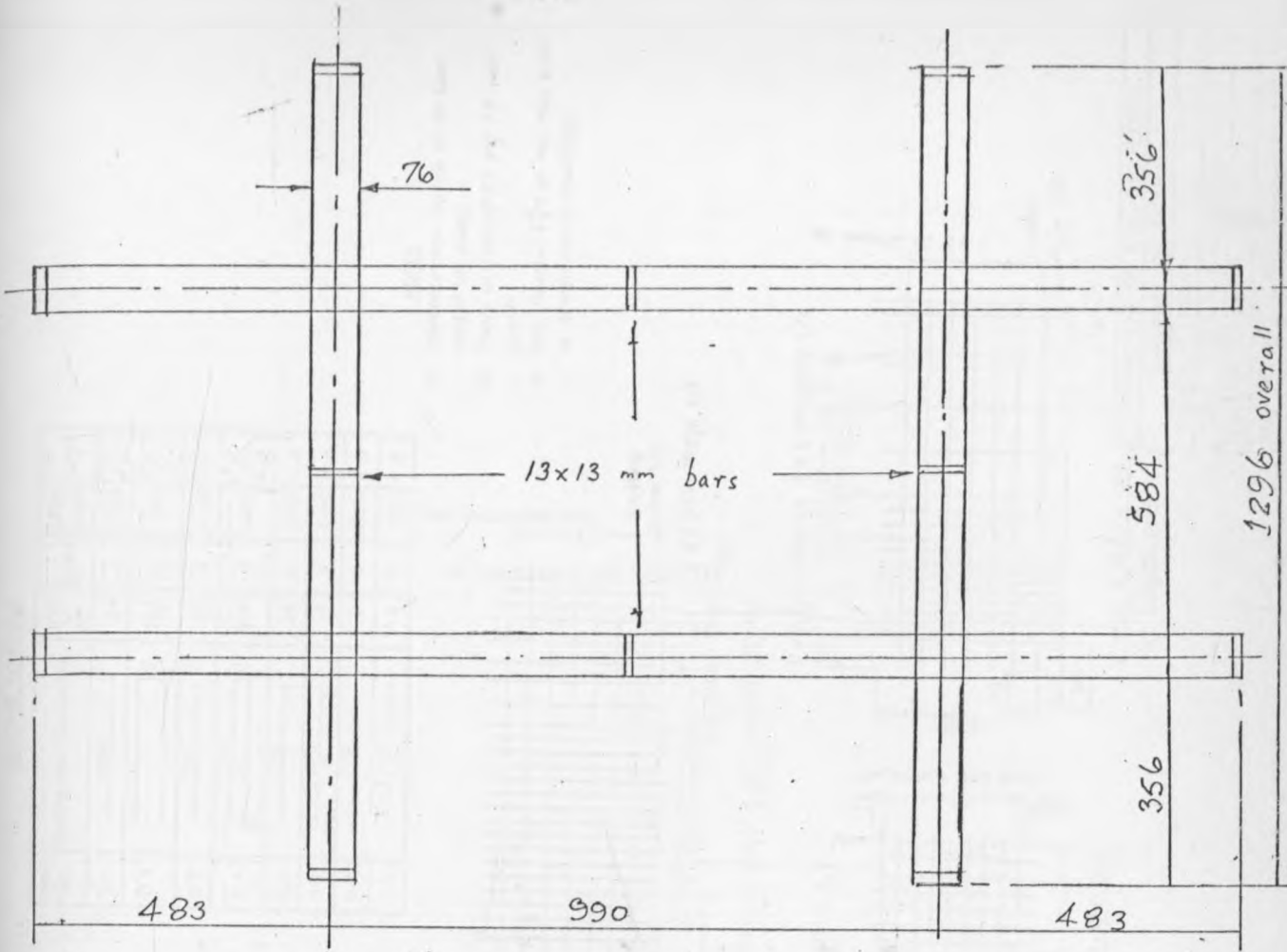
Fig. 3.4 Boxes for 'Vessel Cavities' Formwork



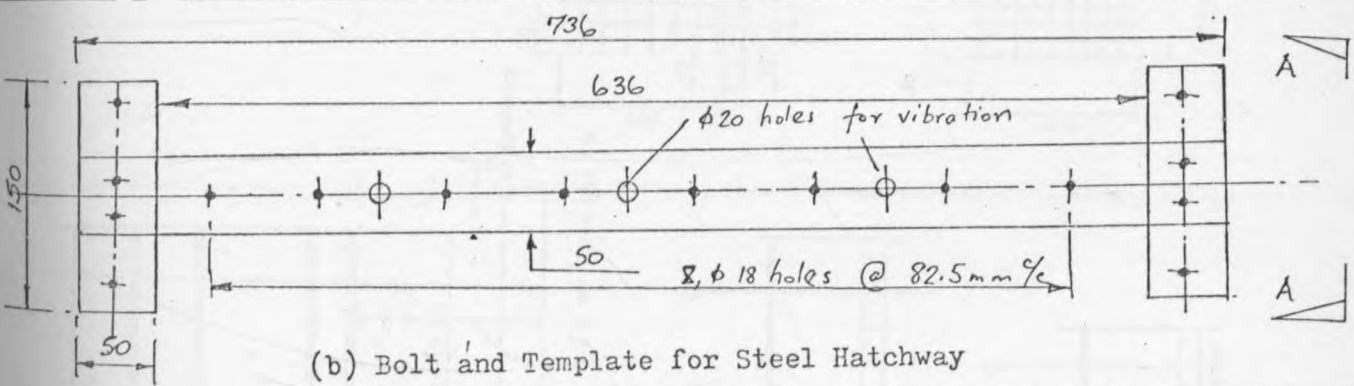
- NOTES**
- 1 Stages ① to ⑥ Shown Section 'S-S' on Typical Plan
 - 2 This Drawing to be Read in Conjunction With Stage- Detail Drawings.
 - 3 C. J. = Construction Joint

Fig. 3.5 Construction Stages

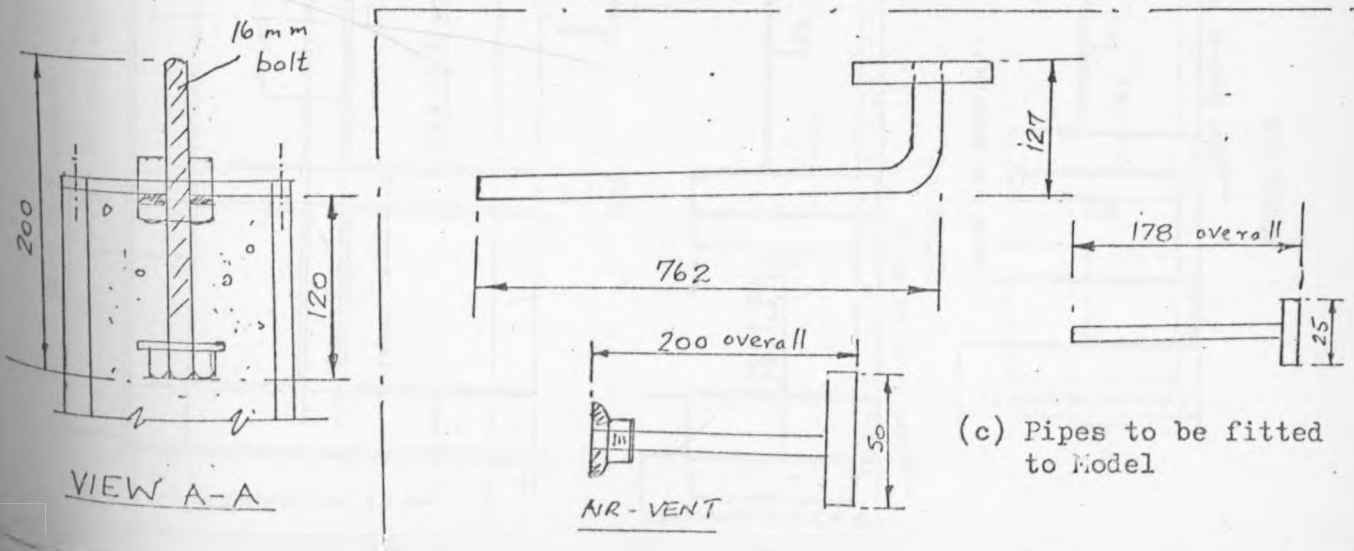
DEPARTMENT OF CIVIL ENGINEERING			
UNIVERSITY OF SYDNEY			
PROJECT	REACTOR CELL MODEL		
TITLE	STAGES OF CONSTRUCTION		
DRG. NO.	3	SCALE	1:10
DESIGNED		DRAWN	A.M. DATE 9.3.76



(a) Steel Templates for Reinforcement Spacing

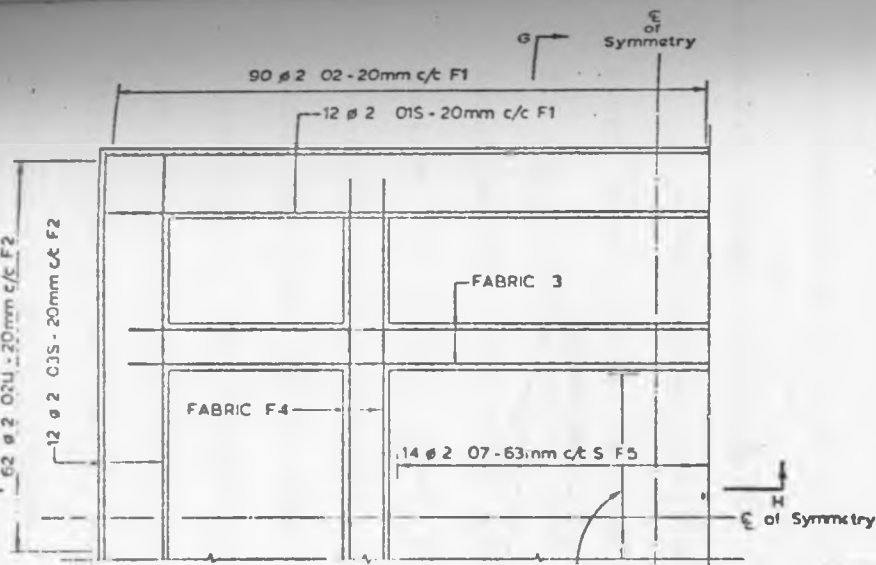


(b) Bolt and Template for Steel Hatchway

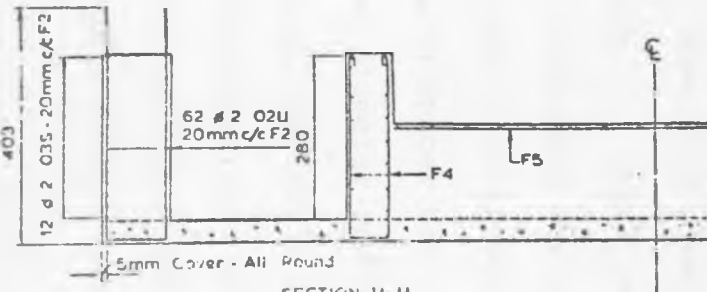


(c) Pipes to be fitted to Model

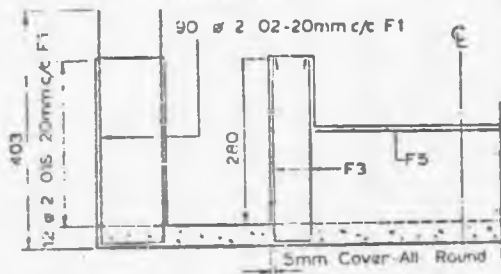
FIG. 3.6 Steel Templates, Steel Hatchway, and Pipes for the Model



PLAN



SECTION F-F



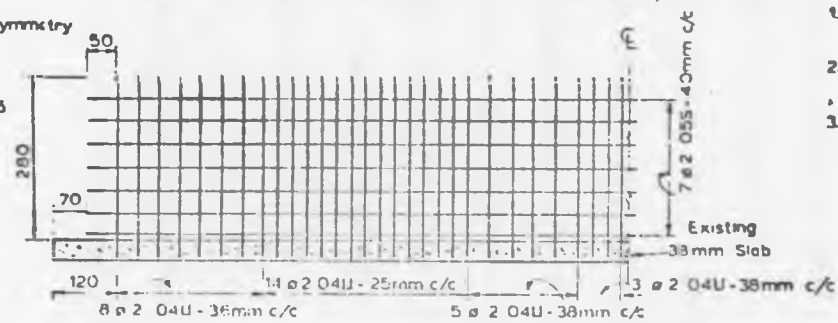
SECTION G-G

BENDING SCHEDULE

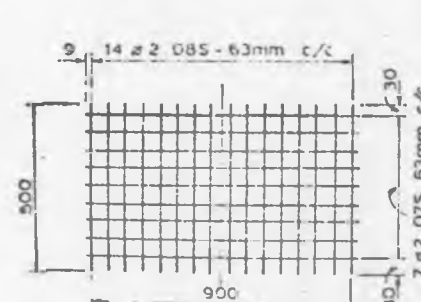
Mk. NO.	Bending and Dimensions	Total No Off	Shape	Cutting Length	Label
01	1890	24	S	1890	F 1
02	1110	304	U	910	F 1 & F 2
03	1230	24	S	1230	F 2
04	800	376	U	800	F 3 & F 4
05	1770	28	S	1770	F 3
06	1110	28	S	1110	F 4
07	900	7	S	900	F 5
08	500	14	S	500	F 5

NOTES

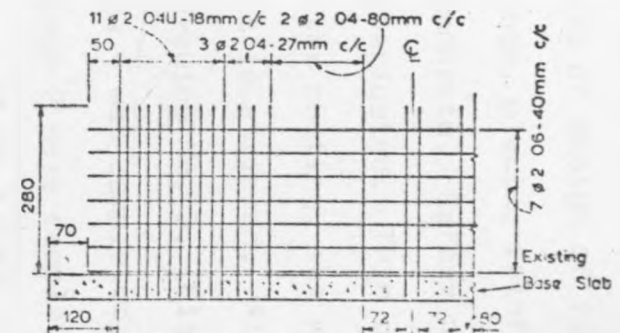
1. Reinforcement Fabrics to be Spot Welded at Joints.
2. Views of Fabrics F1 and F2 not Shown.
3. One Quarter ($\frac{1}{4}$) of the Plan View is Shown, due to Symmetry.



FABRIC 3 (F3) - 4 OFF (LONG BEAM)



FABRIC 5 (F5) - ONE OFF



FABRIC 4 (F4) 4 OFF (TRANS. BEAM)

DEPARTMENT OF CIVIL ENGINEERING			
UNIVERSITY OF SYDNEY			
PROJECT	REACTOR CELL MODEL		
TITLE	STAGE 2 REINFORCEMENT DETAILS		
DRG. I. NO.	04	SCALE	1:5
DESIGNED	AM	DRAWN	AM
DATE	2 3 77		

3.2 CONSTRUCTION AND CONSTRUCTION STAGES OF THE MODEL

The six stages of model construction mentioned earlier will now be considered in detail. Each stage consists of design of reinforcement and formwork, preparing working drawings, placing reinforcement and formwork in place, and casting with micro-concrete. Before pouring the mortar, the next stage up is thoroughly investigated. This obviates problems in continuity and instrumentation. After casting, the mortar is cured for no less than 5 days, after which it is stripped. All construction stages are shown diagrammatically in Drawing No. 3, (Fig. 3.5).

By the time of writing this thesis, stage 1 was completed; and all the required preparations and design for stage 2 were completed - however, it was still under fabrication. Stages 3 to 6 were being planned. I will present these four stages as I think they should be constructed, attempting solutions to problems that are peculiar to each stage.

For meaningful results, the instrumentation for each stage must be given careful consideration. Section 3.2.7 has been devoted to suggestions on this question.

3.2.1 Stage 1 (Fig. 3.7)

A reinforced concrete slab, 38mm thick, was built. The layout of steel reinforcement is shown in Plate 1. Steel templates shown in Fig. 3.6 and Plates 3 and 4, were used. They were mainly used for spacing requirements. A typical template consisted of two open square hollow section (13 x 13mm) steel tubes, with spacer bars at the ends and at mid-span. Clearance holes (for 2mm diameter rods) were then laid out along the tubes at the exact spacing, previously calculated. Through these holes, the U-shaped reinforcing bars were passed. As shown in the Fig. 3.6, four (4) of these templates arranged together fixed a firm frame of reference, around which the different items of the model were checked for placement.

Formwork consisted of edge boards bolted to the foundation steel beams. Wooden strips, 38mm high were then bolted to the foundation board, at the ends of the slab. Strong fixity was important for thorough vibration of mortar.

During casting, 6 (100 x 200mm) cylinders were made along-side each batch of mortar, for a check on strength. The results obtained were in good agreement with required strengths. Appendix 3B shows the test details and results.

Casting the 1.9m by 1.25m slab with micro-concrete was done in three continuous sections over a period of 8 hours. A smooth surface was finished (by trowel), and where walls or beams were to be built for stage 2, laitance was removed to facilitate good construction joints.

The slab was cured with water for 5 days and was stripped after 7 days.

3.2.2 Stage 2 (Fig. 3.8)

Four inner beams and the vessel walls were to be built (Drg. No. 2) to a height of 282mm. Drawing numbers 2 and 4 show details of formwork, fixations, layout and details of the reinforcement. The vessel cavities were created by form boxes, which at the same time gave a good finish to the beams. The edge and end boards were strongly fixed to the beams. The edge and end boards were strongly fixed as in Stage 1.

Steel templates discussed for Stage 1 were used; this time for clamping formwork in position also. Reinforcement meshes joints were to be made using a portable spot-welder.

Due to the anticipation of possible leakage in slabs and beams under pressure, 15mm diameter pipes were to be placed in each of the 8 edge cavities of the models, as shown on Drg. No. 1.

Also to facilitate a water-pressure test, a central 25mm pipe, fitted with an outer tap, was to be placed in the central cavity (where the reactor sits in the prototype). This was to allow the displacement of air during filling with water; and also to take a pressure gauge

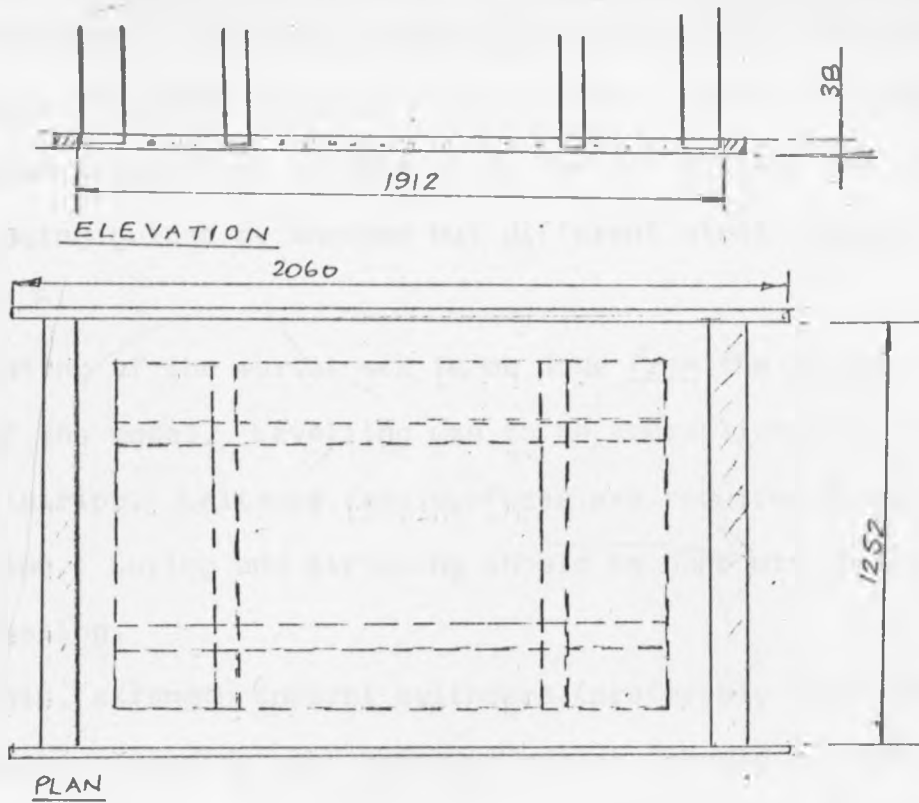


Fig. 3.7 Construction Stage 1

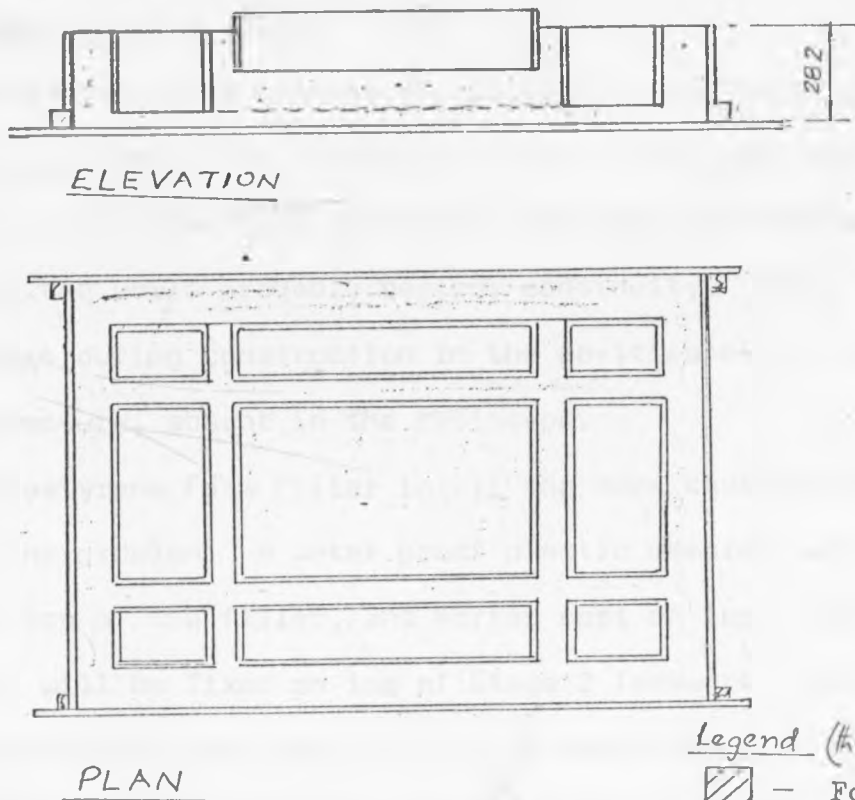


Fig. .9 Construction Stage 2

For Stage 4, a steel hatchway for access into the model was to be built. For this purpose, 8 steel bolts, 200mm in length, were to be placed in position at this stage for its fixity; the exact location being guided by another but different steel template shown in Fig. 3.6. . . .

Casting of the mortar was to be done from the inside to the outside of the model. Levelling was to be accomplished by designed levelling strips. Laitance free surfaces are required for continuing construction. Curing and stripping should be done within the first week of casting.

Again, strength control cylinders (preferably 50mm diameter by 100mm length) alongside each batch of mortar, should be made and tested. Any variation in strength should be taken into account in all future calculations.

3.2.3 Stage 3 (Fig. 3.9)

This stage will consist of building a reinforced concrete slab, 38mm thick, covering the 8 edge cavities of the model structure. Pre-cast slabs could have been an answer, but they were not used in the prototype, and would probably destroy continuity. Also, any supports for formwork during construction in the cavities might add strength to the structure, absent in the prototype.

Polystyrene Foam filler in all the edge cavities is proposed to solve the problem. A water proof plastic membrane will then be placed on top of the filler, and mortar cast on top. Wooden strips, 38mm high, will be fixed on top of Stage 2 formwork, round the periphery and on the central box (box type 'D'); - see Figs. 3.4 and 3.9.

Proposed reinforcement details are laid out in Fig. 3.10.

As before, a check on strength of each batch of mix would be made by at least 6 test cylinders of mortar. Stage 4 is considered

before casting. Steel templates will be used for reinforcement spacing.

This stage will bring the model to a height of 320mm above the foundation line.

3.2.4 Stage 4 (Fig. 3.11)

The steel hatchway shown in Fig. 3.12, (for access into the model) will be installed. Also the walls of the model will be raised by 406mm; preparations for a 'construction joint' at this level made. This joint will be made by 50mm by 500mm aluminium plates placed vertically at the centre-lines of the walls (see Fig. 3.11). These are to be cast in with the reinforcement, but of course being near the neutral axis, should add no extra strength.

Formwork will consist of ply form boards, 18mm thick, 406mm high, fixed above the Stage 3 formwork (except for box type 'D' (Fig. 3.4), which should be now removed). The same boards should also be placed on the inside of the vessel wall and fixed to the steel templates (screwed, bolted or clamped). Fig. 3.13 indicates the sizes of the boards to be cut.

The steel hatchway area should be left clear of wooden formwork.

Steel reinforcement (shown in Fig. 3.14) will be spot-welded in position (before fixing the form boards). Rods should protrude above the formwork level to facilitate a splicing of at least 25mm.

The steel hatchway will be placed in position using bolts that were installed during Stage 2. This should be done before any casting of mortar is done.

The aluminium plates, providing the construction joints, will then be placed in position. Any embedded instrumentation should also be placed in position, at this juncture.

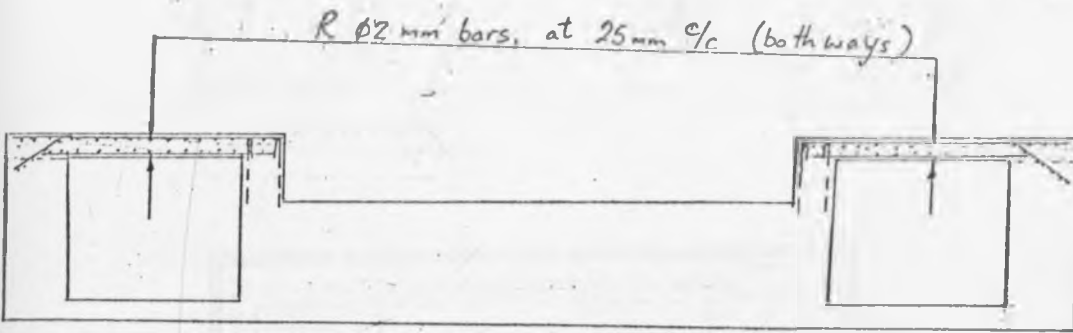


Fig. 3.10 Layout of Reinforcement for Stage 3

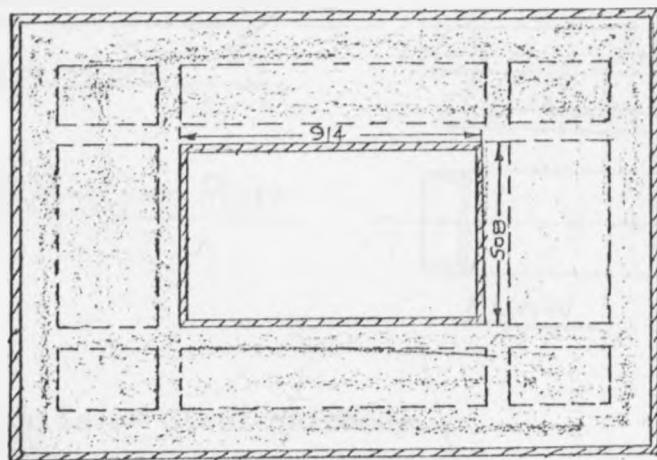
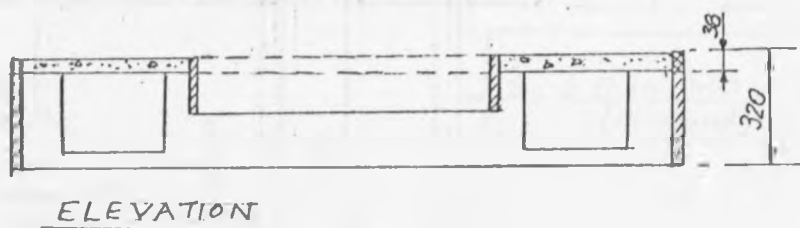


Fig. 3.9 Construction Stage 3

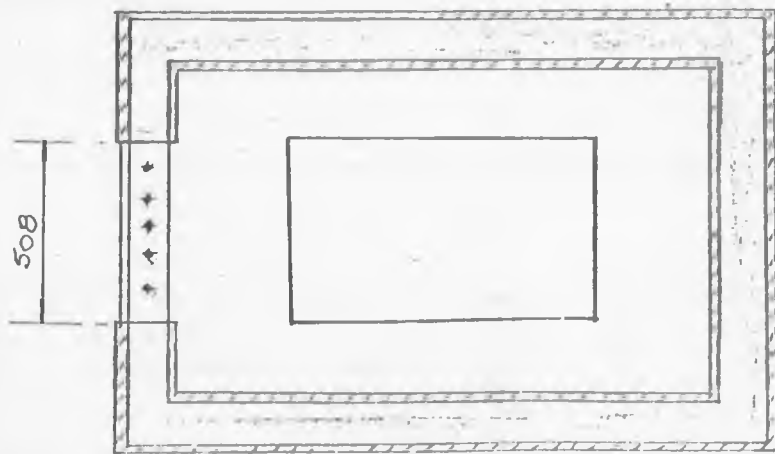
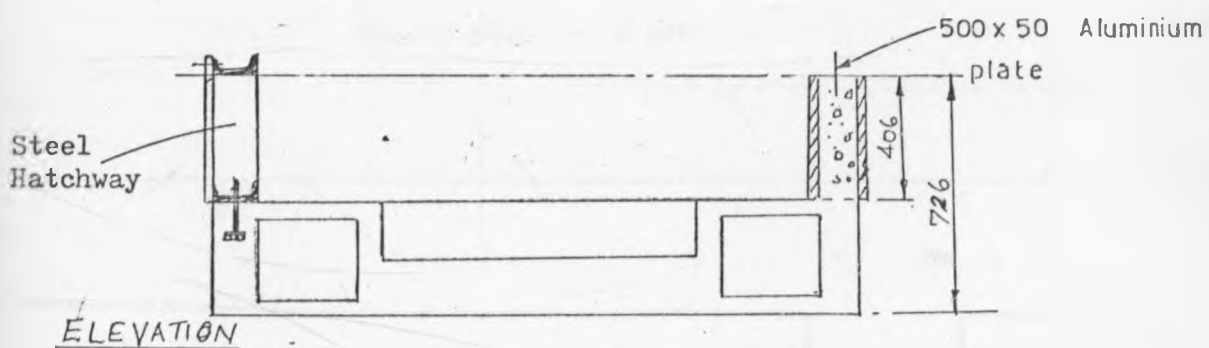


Fig. 3.11 Construction Stage 4

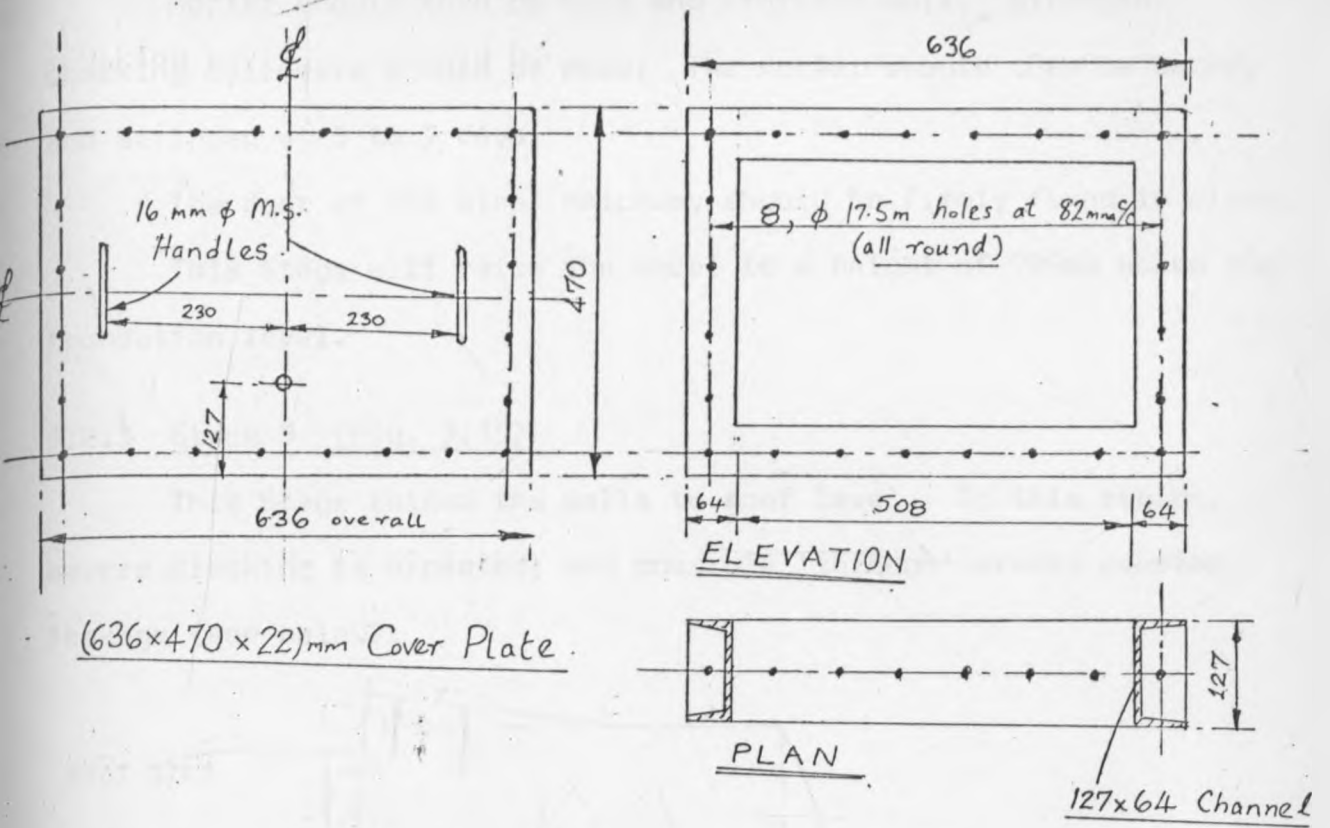


Fig. 3.12 Details of Steel Hatchway

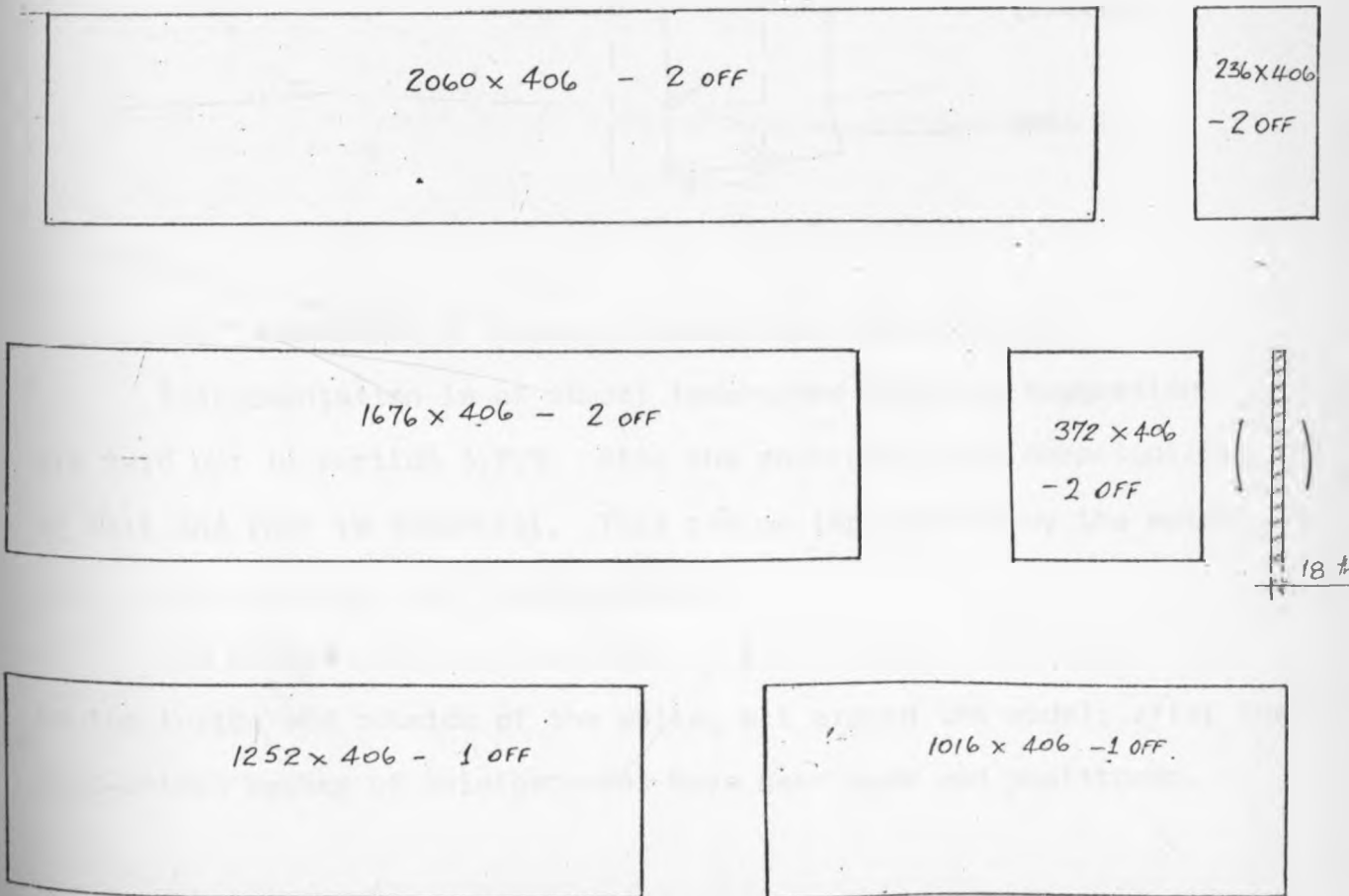


Fig. 3.13 Boards for Stage 4 Formwork (all 18mm thick)

Mortar should then be cast and vibrated well. Strength-checking cylinders should be made. The mortar should then be cured, and stripped at 5 to 7 days.

The door of the steel hatchway should be firmly fixed in place.

This Stage will raise the model to a height of 726mm above the foundation level.

3.2.5 Stage 5 (Fig. 3.15)

This Stage raised the walls to roof level. In this region, severe cracking is expected; and possibly 'through' cracks causing leakage (see below).

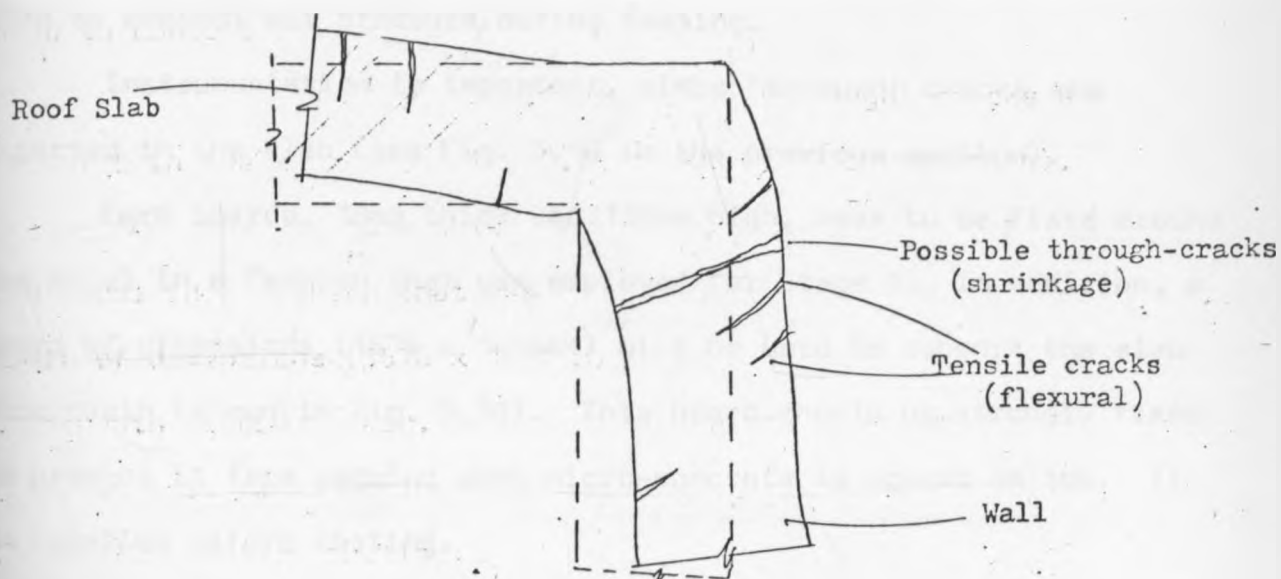


Fig. 3.16. Formation of Cracks at Wall/Roof intersection

Instrumentation is of utmost importance here and suggestions are laid out in section 3.2.7. Also the continuity and compatibility of wall and roof is essential. This can be implemented by the mutual work of the wall and roof reinforcement.

The construction will consist of formboards, 374mm high, fixed on the inside and outside of the walls, all around the model; after the spot-welded meshes of reinforcement have been made and positioned.

Aluminium plates for a construction joint (cf. Stage 4); and any gauges for instrumentation should be placed firmly in place. Mortar should then be poured, vibrated, cured and stripped. The layout of formwork and reinforcement is shown in Figs. 3.15 and 3.17.

Completion of this Stage will bring the model to a height of 1.1m above the foundation level.

3.2.6 Stage 6 (Fig. 3.18) (Final)

This stage will comprise of building a roof slab, 138mm thick, for the model. The slab covers the entire model; and has dimensions 1.9m x 1.25m. At the centre of the slab will be an 'air-vent' pipe, used to control air pressure during testing.

Instrumentation is important, since 'through' cracks are expected in the slab (see Fig. 3.16 in the previous section).

Form boards, 18mm thick and 138mm high, have to be fixed around the model in a fashion that was employed for Stage 1. In addition, a board of dimensions (1676 x 1016mm) will be used to support the slab underneath (shown in Fig. 3.18). This board should be strongly fixed to prevent it from sagging when micro-concrete is poured on top. It is levelled before casting.

Reinforcement details are shown in Fig. 3.19. Continuity of wall to roof is established by reinforcement.

After the 'air-vent' has been placed in position, the instrumentation checked, and the formwork fixed, the mortar then should be cast, levelled, cured and stripped after 8 days.

The construction joint mentioned in the preceding Stage will be in conjunction with the roof slab.

Completion of the roof slab completes the model construction. This brings the model to its full height of 1.238m above the foundation level.

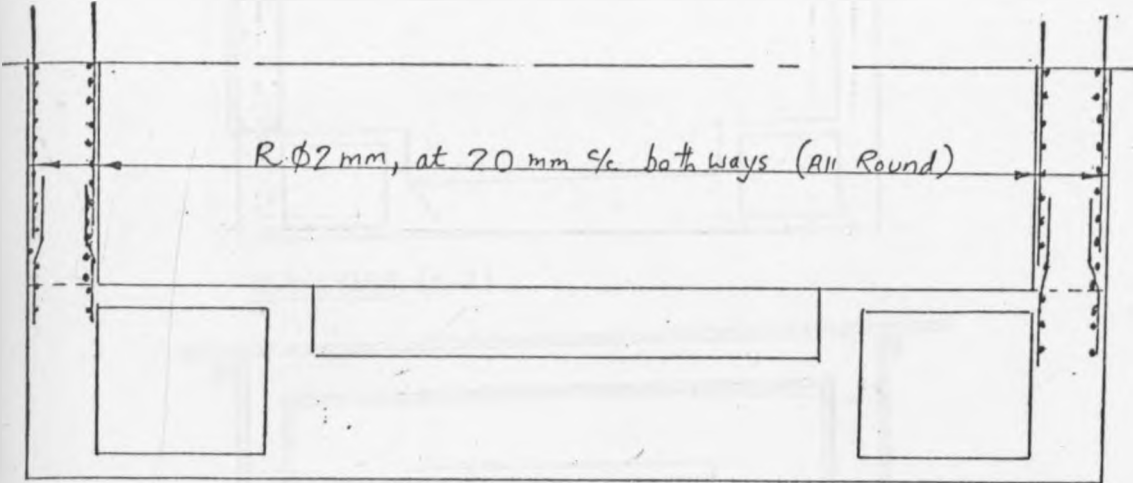


Fig. 3.14 Layout of Reinforcement for Stage 4

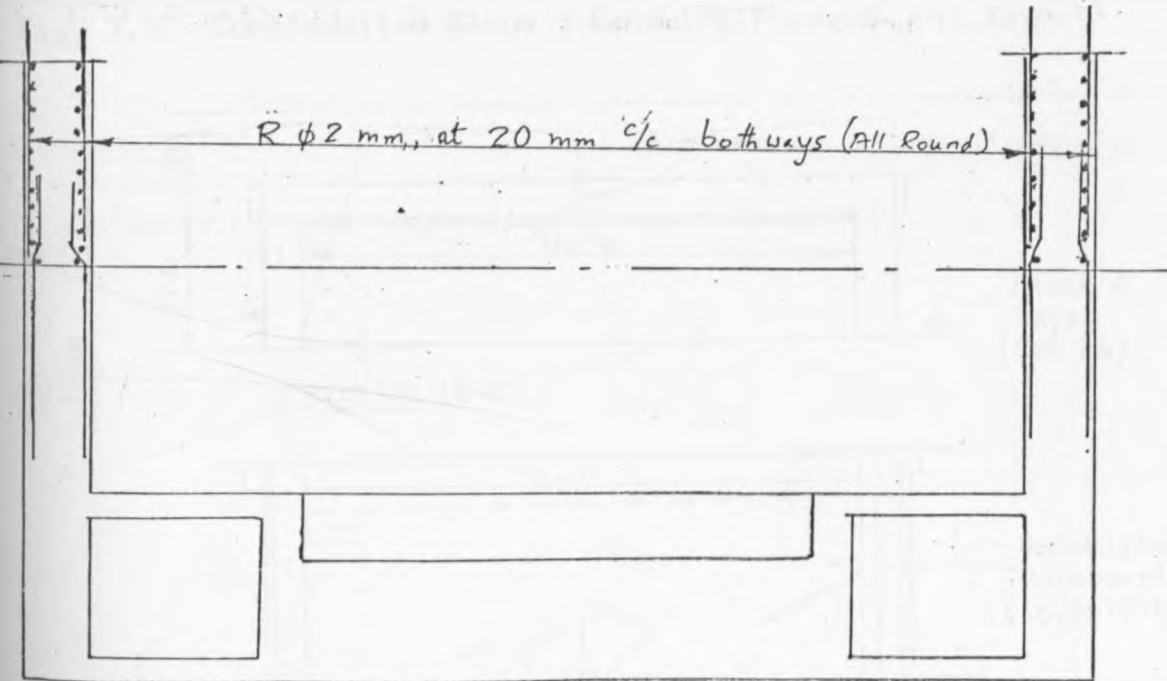
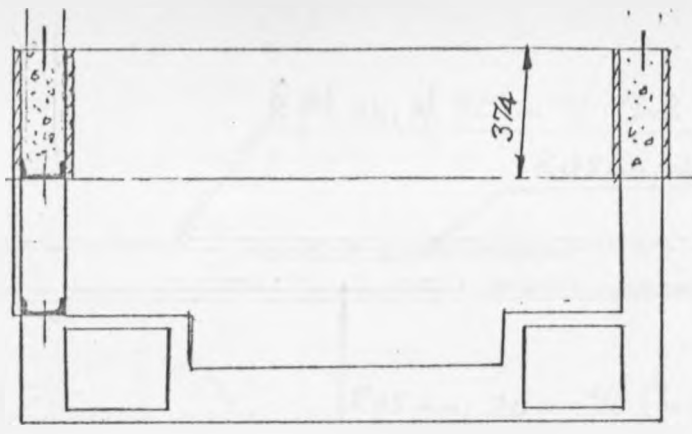
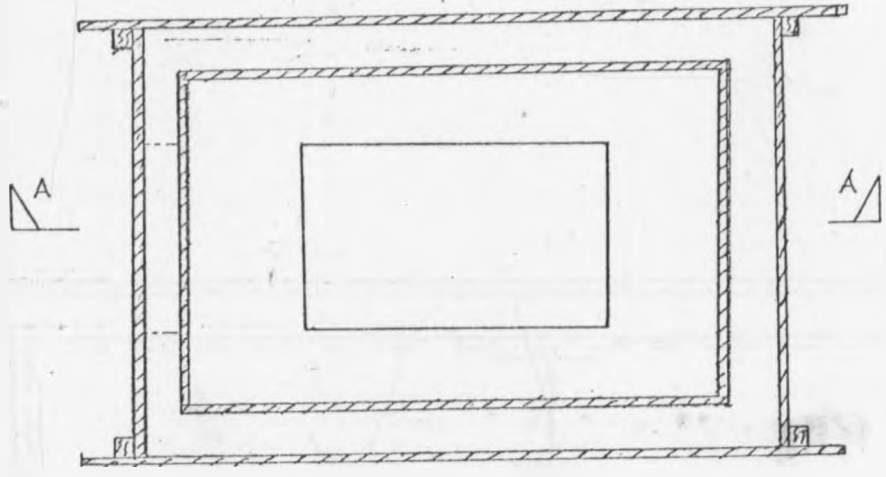


Fig. 3.17 Layout of Reinforcement for Stage 5

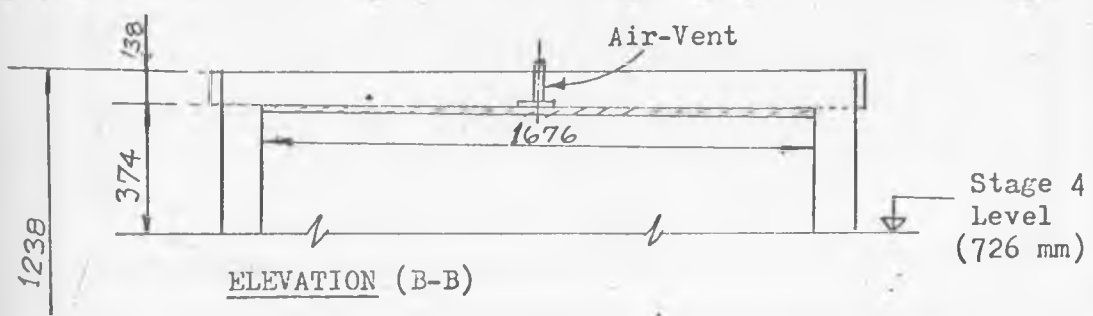


ELEVATION (A-A)



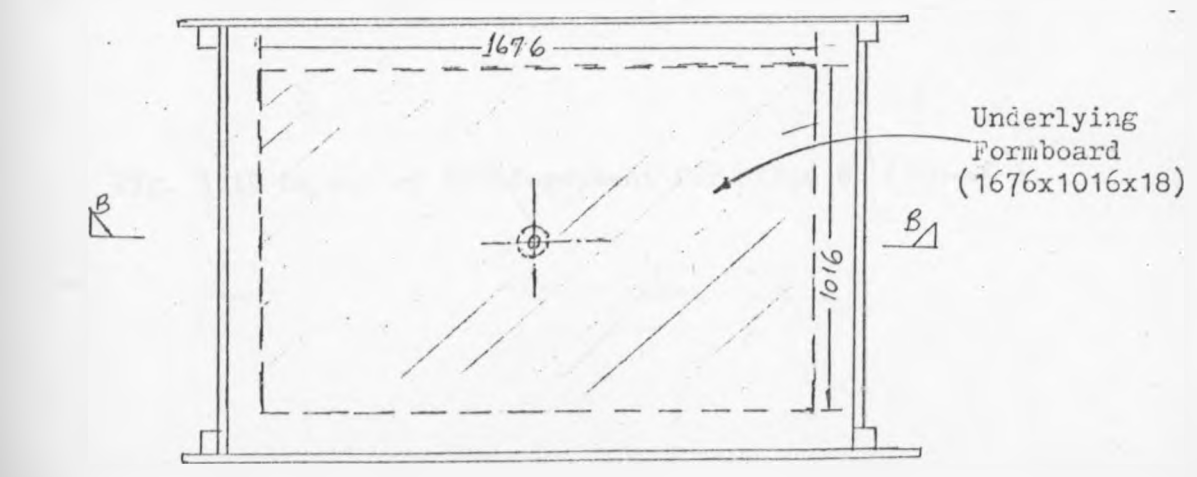
PLAN

Fig. 3.15 Construction Stage 5 (showing formwork and layout)



ELEVATION (B-B)

Stage 4 Level (726 mm)



PLAN

Underlying Formboard (1676x1016x18)

Fig. 3.18 Construction Stage 6 (Final) with formwork and layout

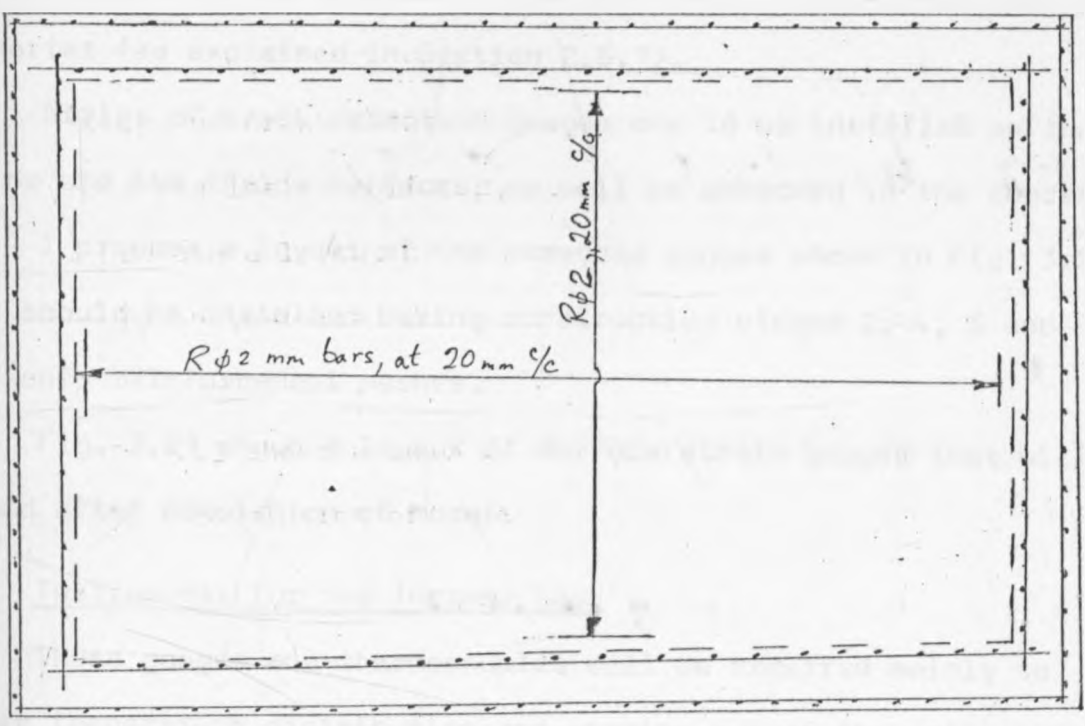
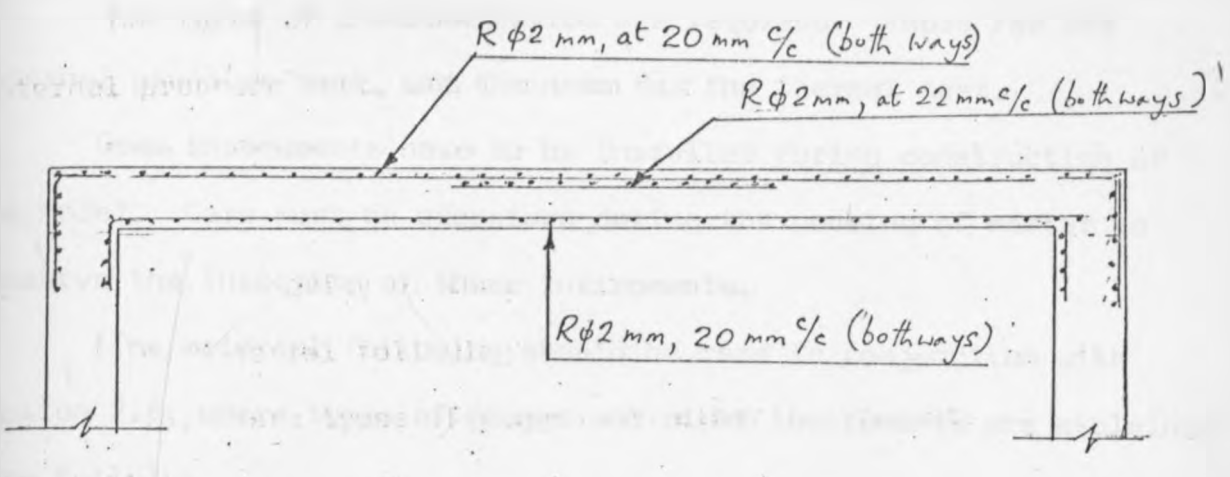


Fig. 3.19 Layout of Reinforcement for Stage 6 (Final)

3.2.7 Proposed Instrumentation

Two types of instrumentation are required: Those for the internal pressure test, and the ones for the thermal test.

Some instruments have to be installed during construction of the model. Care must be exercised during the pouring of mortar to preserve the integrity of these instruments.

(The material following should be read in conjunction with Section 2.6, where types of gauges and other instruments are explained more fully).

(a) Instruments for the Internal Pressure Test

Resistance strain gauges may be used to measure strains. These will be placed on the micro-concrete surface, and also embedded into the mortar (as explained in Section 2.6.1).

Strips of crack detection gauges are to be installed on the outside and the inside surfaces, as well as embedded in the concrete.

I propose a layout of the embedded gauges shown in Fig. 3.20. These should be installed during construction stages 2, 4, 5 and 6; fixed onto reinforcement meshes.

Fig. 3.21 shows a layout of surface strain gauges that will be mounted after completion of model.

(b) Instruments for the Thermal Test

These gauges and thermocouples will be required mainly to measure temperature distribution and strains across the walls and roof slab.

I suggest that Carlson gauges, 'vibrating wire' gauges and 'copper-constantan' thermocouples (discussed in Section 2.6.3), be used.

A layout of these instruments is shown in Figs. 3.22 and 3.23.

The embedded gauges should be fixed to the aluminium plates used for the construction joint, as well as the reinforcement cages, during the

appropriate construction stages.

(c) Data Acquisition

An 'automatic data generation' system shown in Fig. 2.4 (Section 2.6.2) is recommended for record of the numerous measurements to be encountered during the test.

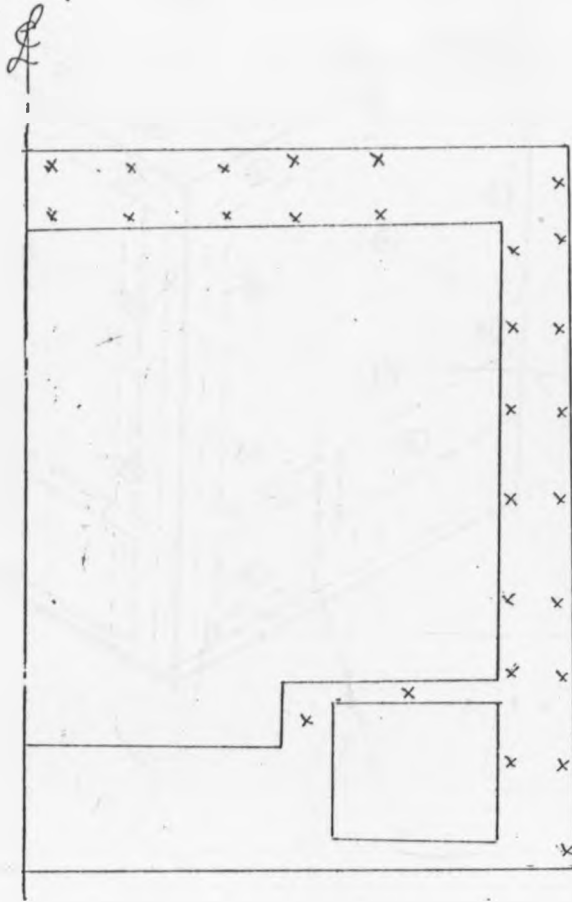


Fig. 3.20 Embedded Gauges for Internal Pressure Test

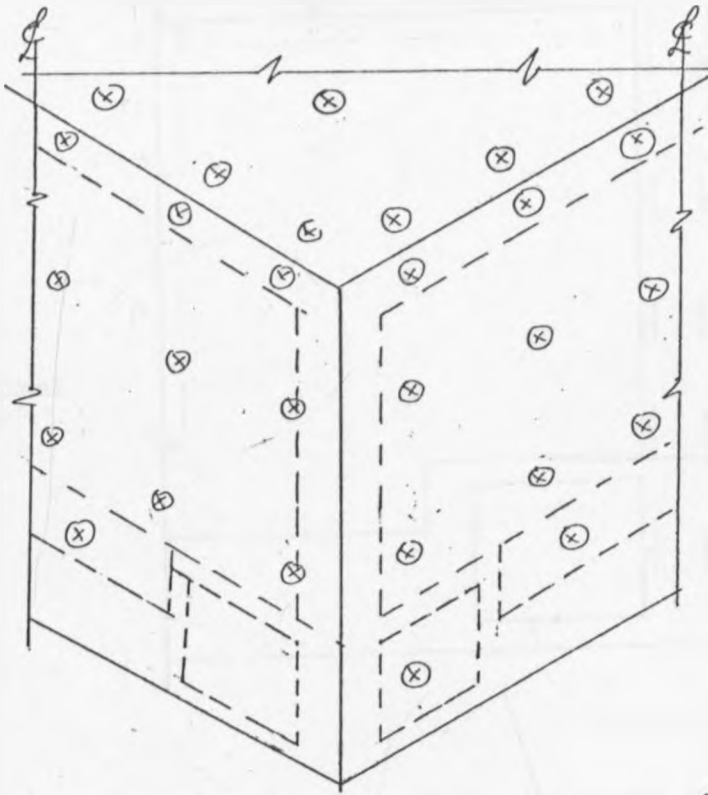


Fig. 3.21 Proposed Surface Strain Gauges Location
for the Internal Pressure Test

Longitudinal
Hoop

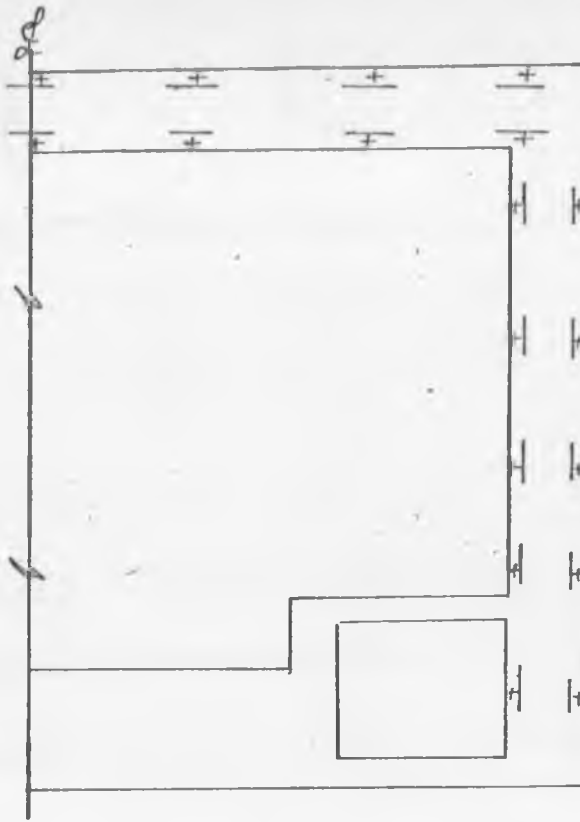


Fig. 3.22 Proposed Location of Strain Gauges for thermal test

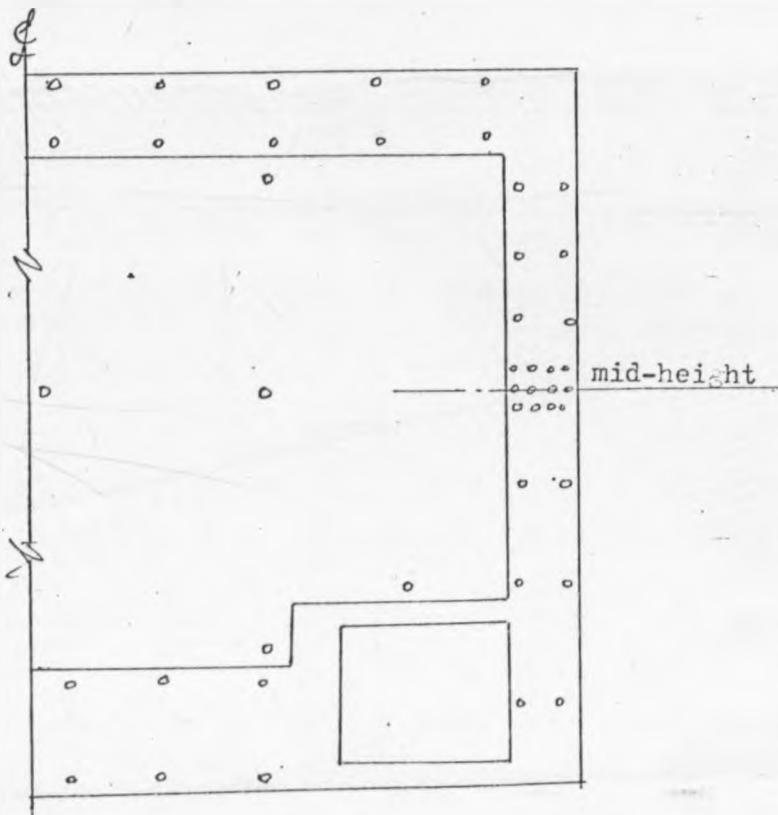


Fig. 3.23 Proposed Location of Thermocouples for thermal test.

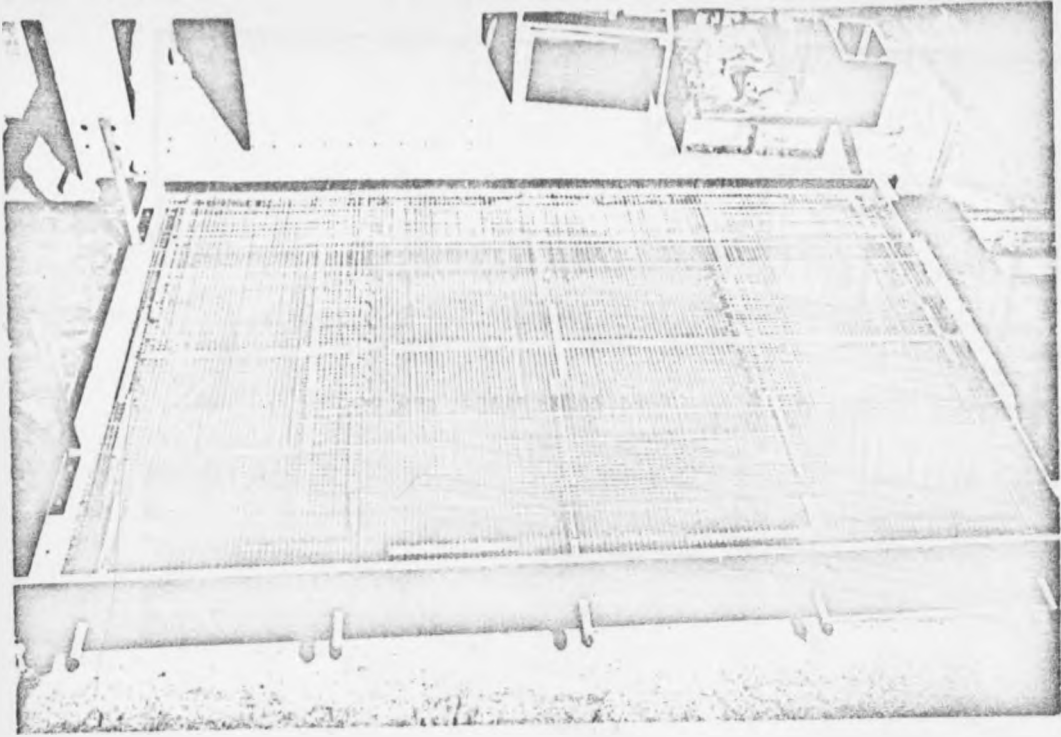


PLATE 1 REINFORCEMENT IN BASE - GENERAL ARRANGEMENT

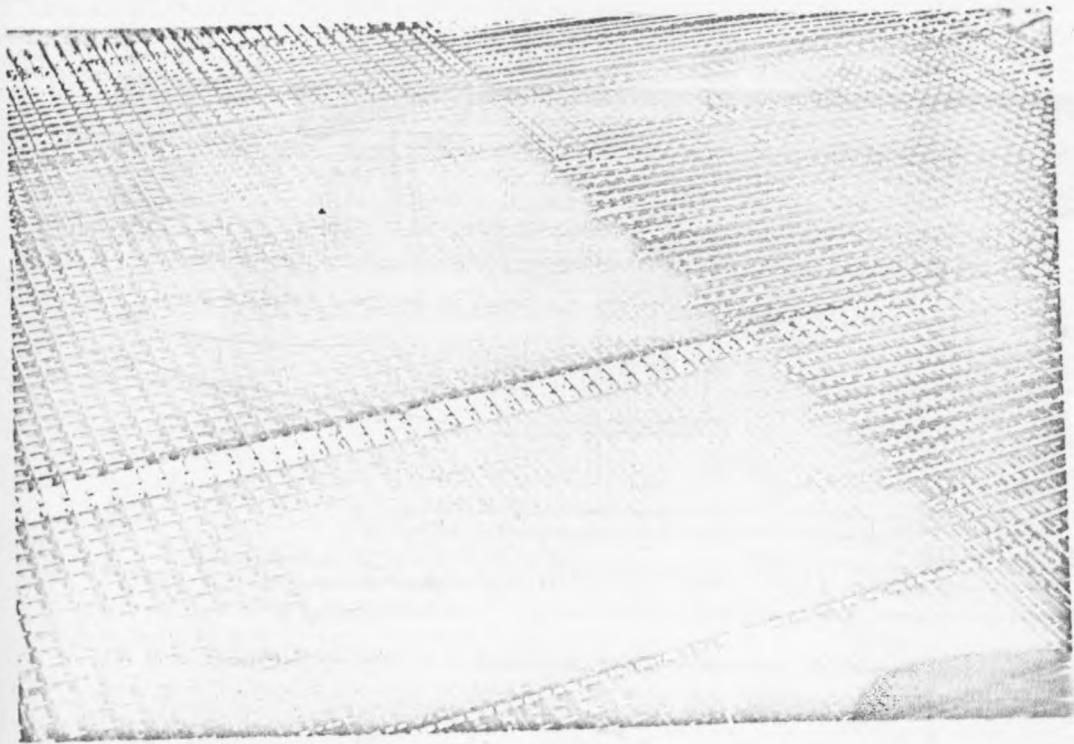


PLATE 2 DETAIL OF BASE REINFORCEMENT UNDER REACTOR

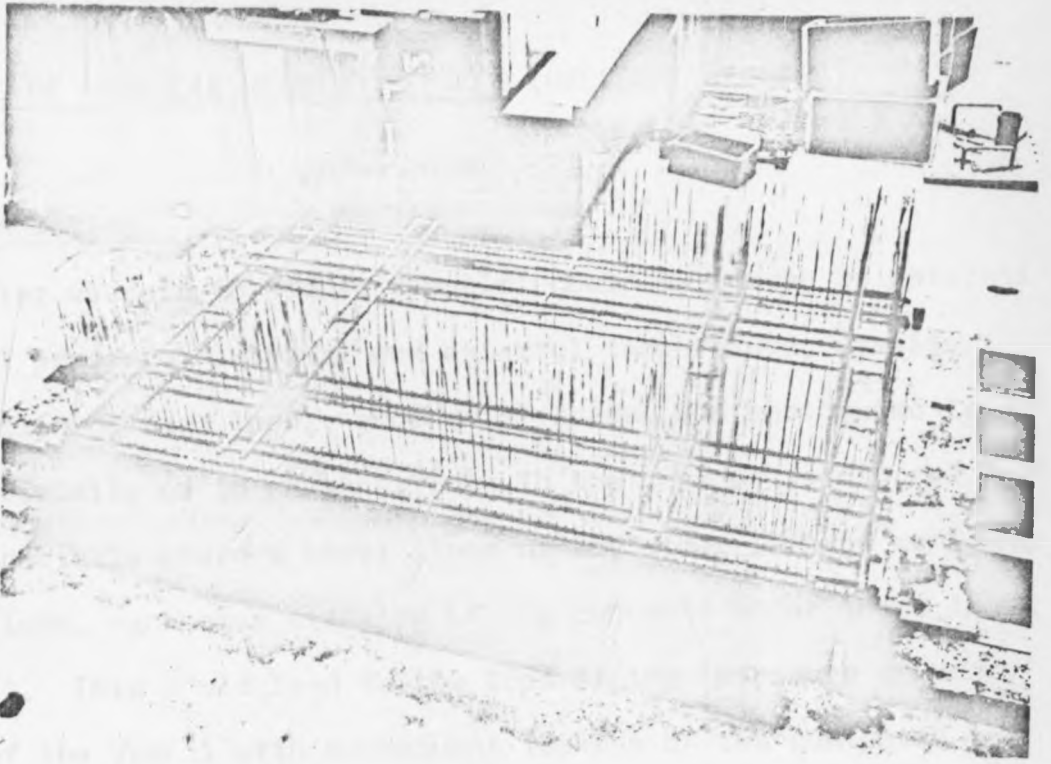


PLATE 3 WALL REINFORCEMENT ABOVE BASE

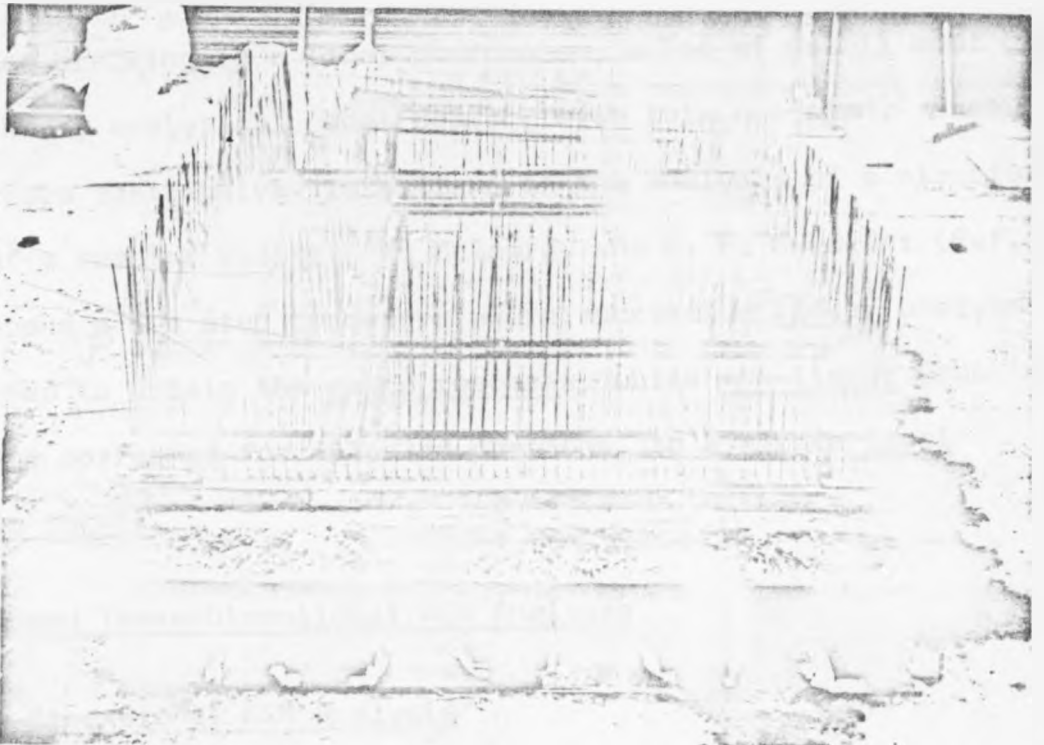


PLATE 4 WALL REINFORCEMENT ABOVE BASE

THE ANALYSIS OF CONCRETE REACTOR VESSELS (PRESSURE VESSELS)

4.1 Introduction

Reactor vessels (pressure vessels) could be loaded by internal and external pressure, internal and external temperature, gravity loading (including dead load), accidental loads, and earthquake loads, acting individually or in combination. In the case of reinforced concrete vessels, especially where a steel liner or any other leakage membrane is not provided, excessive cracking of the concrete under these loads could result. This could lead to the loss of the 'pressure boundary' integrity of the vessel with subsequent leakage of the contents.

Since the pressure vessel considered in this thesis is a reinforced concrete one with no steel liners, most of this chapter will be devoted to the analysis of cracking. The Finite Elements Method (FEM) of analysis is considered to be the most suitable for analysing a problem of such complexity.

Since cracking is a local phenomenon, a lot of detail must be included in any analytical model dealing with this question. Such detail imposes restrictive limitations on the analysis of a structure the size of a reactor vessel. R. McGeorge and L. F. Swec Jnr (Ref. 4.1) have developed a two step procedure where successive linear analyses are performed to obtain the gross response, while non-linear cracking analyses are performed for selected portions, to evaluate local cracking in detail.

4.2 Two and Three-Dimensional FEM Analyses

4.2.1 Two-Dimensional FEM Analysis

This method of analysis assumes that the vessel is a 'thin' shell.

Each wall or slab is analysed as a two-dimensional 'plate' - with well refined boundary conditions. A finite number of quadrilateral elements is arranged on the plate surface, joined by the 'nodes' (surrounding each element). Compatibility of deformation between neighbouring elements should be satisfied for a precise 'continuum' model in the analysis. The modulus of elasticity of concrete, the compressive and tensile strengths of concrete, Poisson's ratio, the loadings (pressure, temperature, etc.) and boundary constraints constitute the input for a FEM computer programme designed to analyse pressure vessels. The output of the programme yields longitudinal and hoop stresses and moments, deformations and deflections; as well as shears, axial loads, etc. as required.

Typical input elements are shown in Fig. 4.1 and typical results in Fig. 4.2a, 4.2b.

This method can be used for elastic as well as elastic-plastic analysis. The results shown in Fig. 4.2 are 'elastic' results obtained for the reactor vessel considered in this thesis. (192 elements, 217 nodes required solution of 1005 equations.)

A Slab and Wall Elastic Analyses Programme (namely 'SWEAP') was used here (Ref. 4.5). It utilises quadratic displacement plane stress and plate bending finite elements in association with compatible column, beam and line elements. The isoparametric 8-node elements adopted are shown to be accurate for elastic structural analyses.

A similar elasto-plastic analysis was used by the Kajima Corporation PCPV Research and Development Group in Japan in September, 1973. (Ref. 2) The analysis was utilised for the following purposes:-

(i) To predict the model behaviour under overpressure.

(ii) To follow the crack propagation sequence in relation to the pressure.

(iii) To verify that the vessel has a progressive fracture mode.

The particular programme used here performed analysis after

cracking of concrete and yield of steel. Also non-linear stress-strain characteristics were assumed and idealised for steel and concrete. In addition, idealised 'bond-slip' characteristics were programmed for the reinforcement.

To convert the problem from a three- to a two-dimensional one, Young's modulus was corrected by a factor 'a', defined as:

$$a = d_2/d_3 \dots \dots \dots 4.1$$

d_3 : three-dimensional radial displacement

d_2 : two-dimensional radial displacement with Young's modulus uncorrected.

With this correction, the radial displacements under the two- and three-dimensional analyses became identical.

It should be noted, however, that the two-dimensional model takes no account of:

(i) The three-dimensional stresses within the 'plate' thickness

(ii) Cracks due to the anisotropic nature of material, important for shrinkage, construction joints, etc.

(iii) The 'doming' action which may increase slab stiffness.

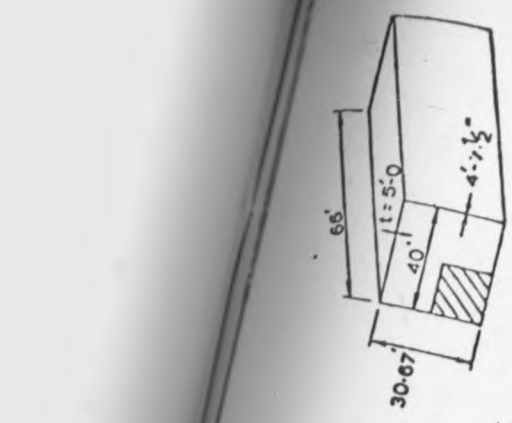
(iv) The influence of creep.

(v) The dynamic nature of pressures due to abnormal loading.

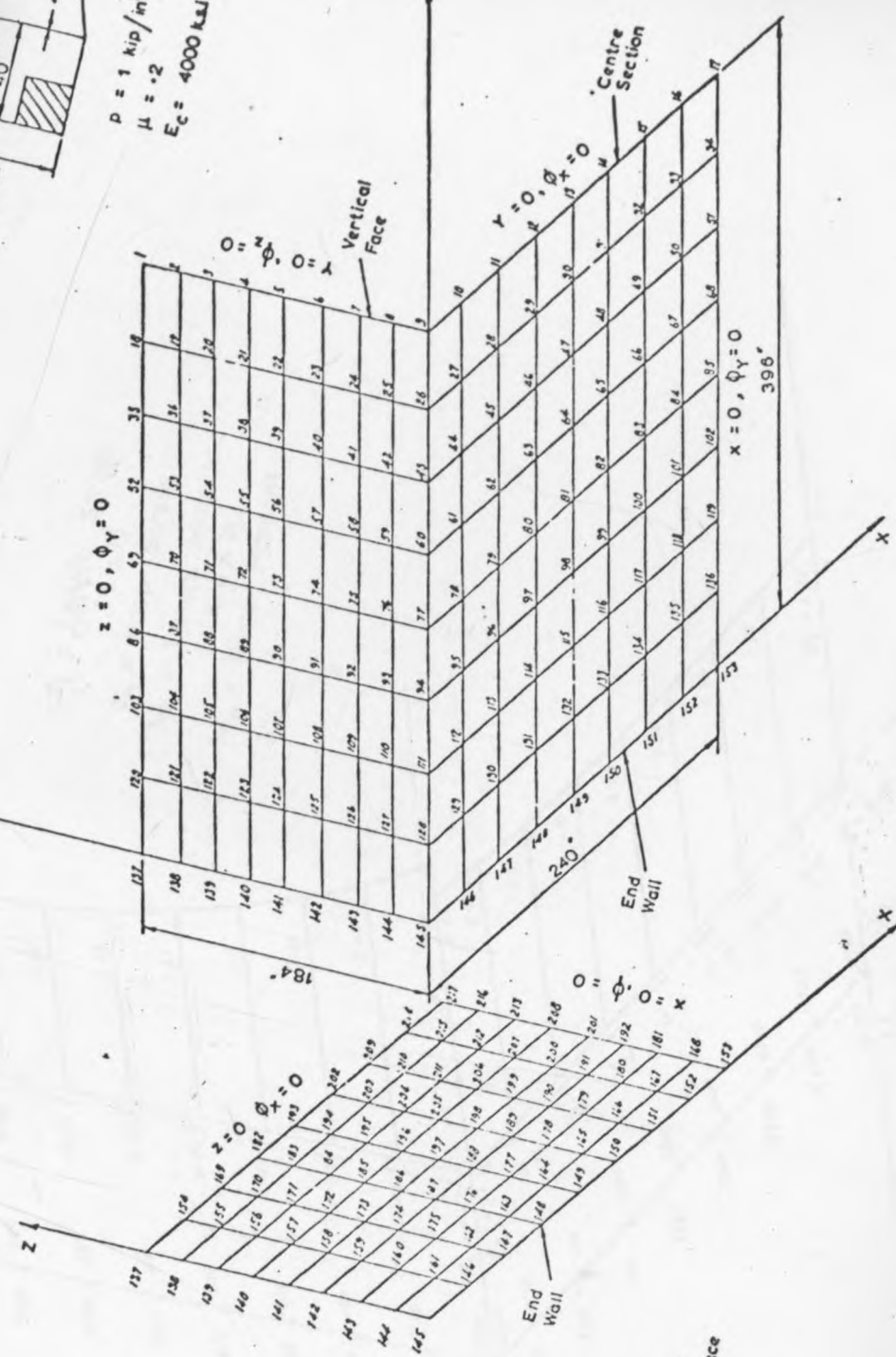
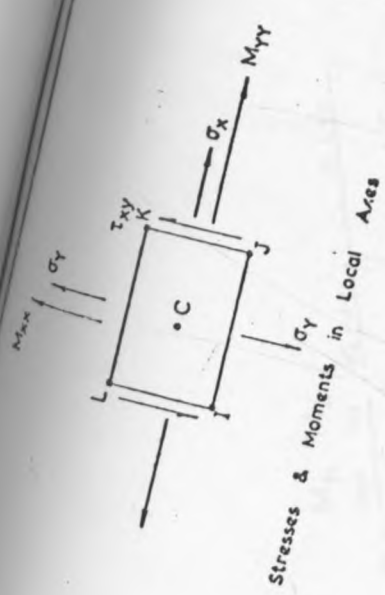
4.2.2 Three-Dimensional FEM Analysis

This method analyses the pressure vessel as a 'thick' shell.

The computer programmes for this method are more elaborate and more accurate. The elements are hexahedral, and the nodes are more in number. Instead of a thin plate as in the two-dimensional analysis, a solid free-body - representative of the entire structure - is analysed. In the case of a cylindrical vessel, this can be a 30° or 45° or 90° sector. Fig. 4.3 shows a 30° degree sector analysed by the Kajima Corporation Group (referred to in the last Section 4.2.1).



$p = 1 \text{ kip/m}^2$
 $\mu = .2$
 $E_c = 4000 \text{ ksi}$



Note:
 $\phi_y = 0$ on end wall
 $\phi_x = 0$ on vertical face
 $\phi_z = 0$ on horizontal face

FIG. 17 FINITE ELEMENT MESH OF '019' ELEMENTS

FIGURE 4.1

FIG. A2 - CENTRE SECTION

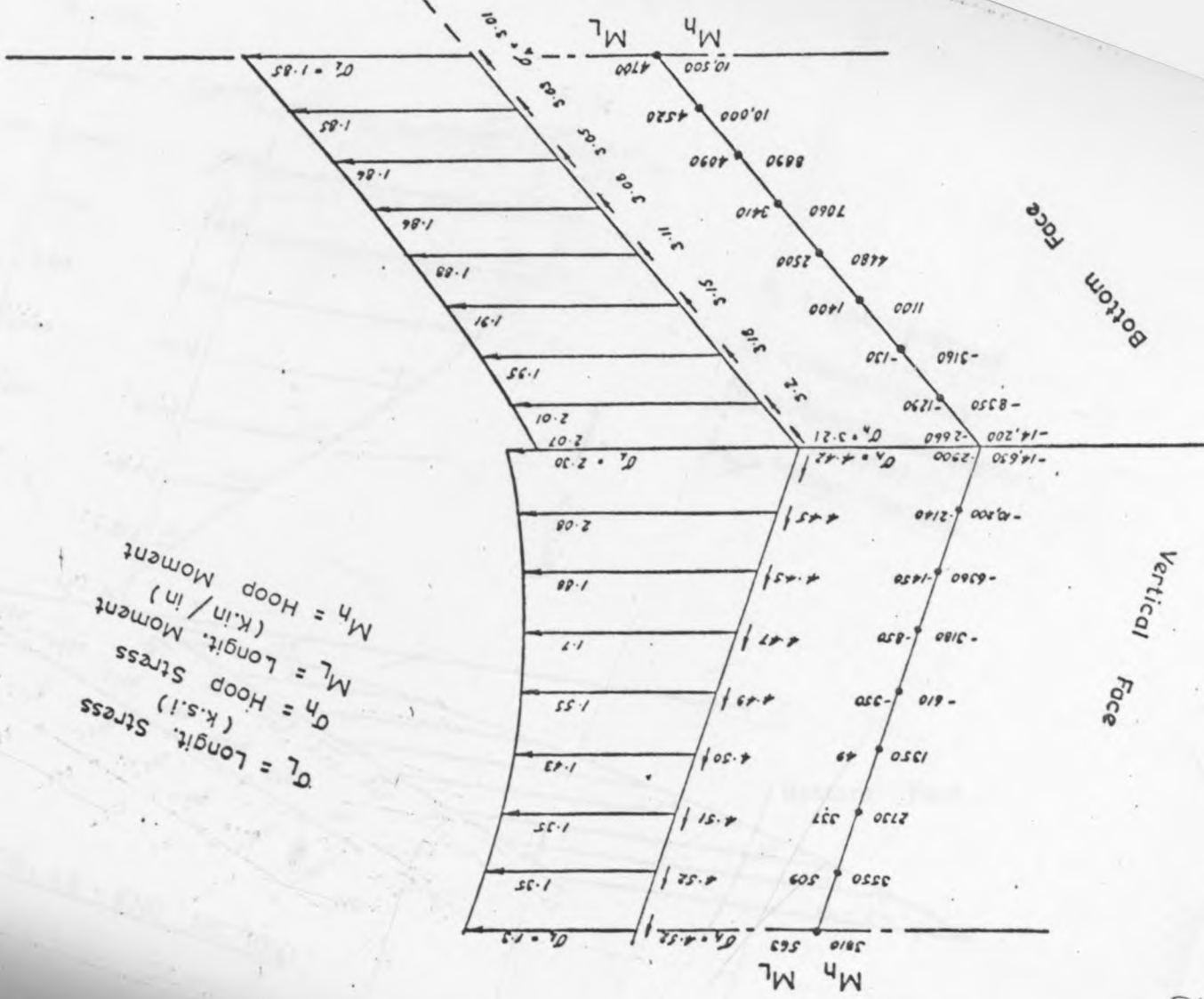


FIGURE 4.2(a)

σ_L = Longitud. Stress (k.s.i.)
 σ_h = Hoop Stress (k.s.i.)
 M_L = Longitud. Moment (k.in/in)
 M_h = Hoop Moment (k.in/in)

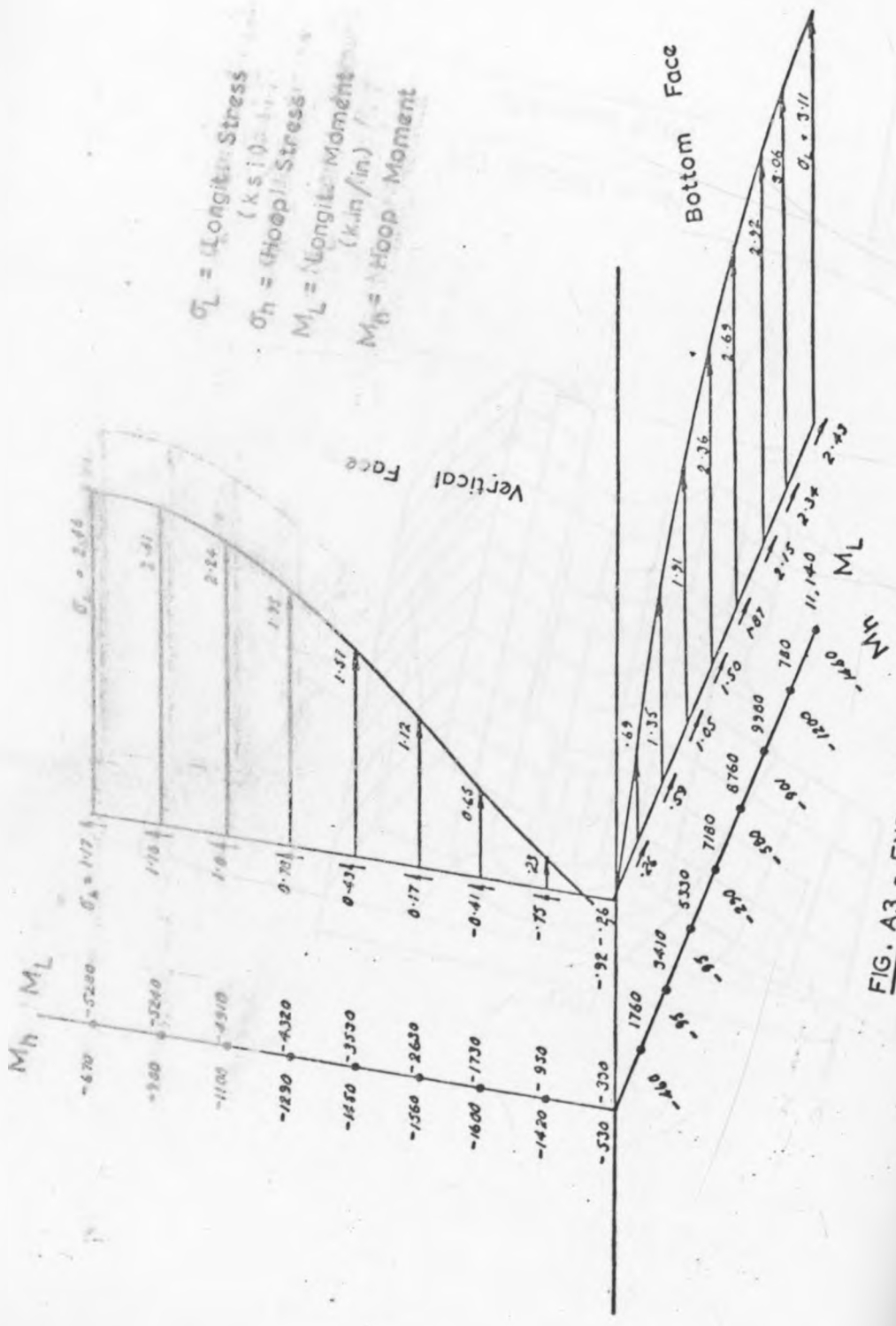
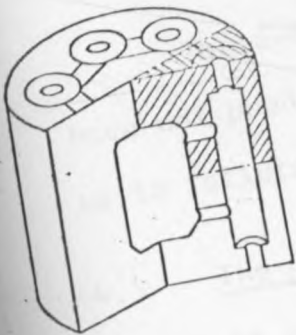
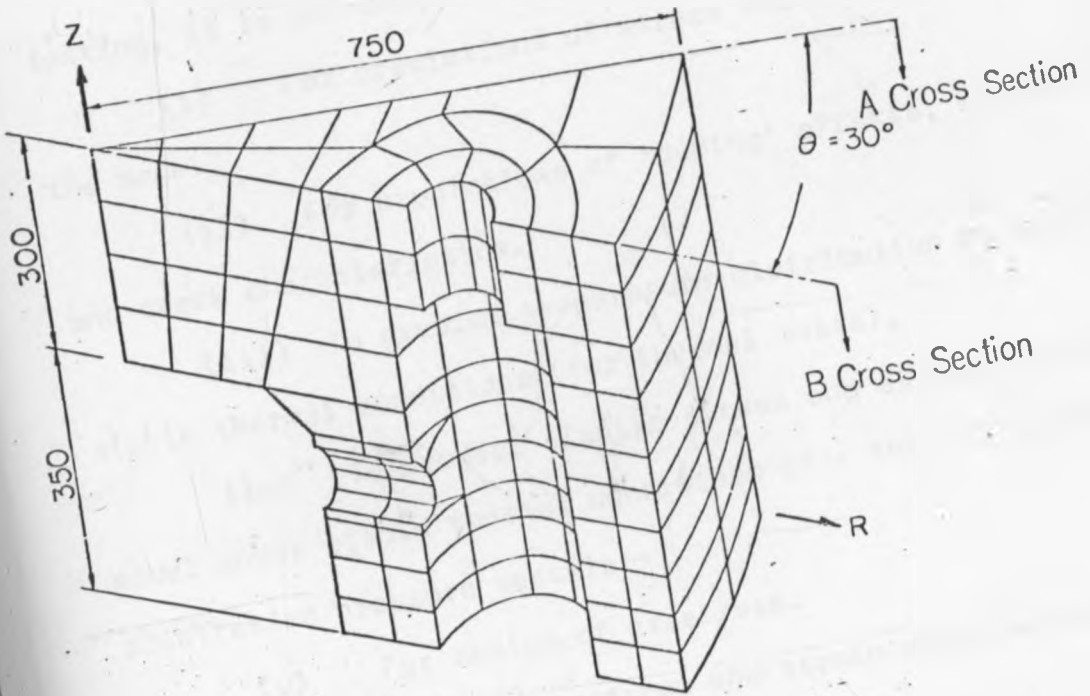


FIG. A.3 - END SECTION



No. of Elements 124

No. of Nodes 920

Fig. 4.3 Three Dimensional Finite Element Division of the Model

We note that a mere 124 elements created 920 nodes. Compatibility of deformation is satisfied between neighbouring curved surfaces, this representing a precise 'continuum' model.

The three-dimensional FEM model tends to be restricted to an elastic analysis, to give the gross response of the entire structure.

When the analysis is carried out as a guide in model design and testing, it is normally utilised as follows:-

- (i) For predictions of stress and strain distributions of the model.
- (ii) For predictions of 'doming' effects, severe crack regions, and crack characteristics.
- (iii) To predict temperature distribution of model under stable thermal conditions (for thermal tests).
- (iv) To predict elastic stress and strain distribution of model under stable thermal conditions (for thermal tests); and for prestressed pressure vessels:-
 - (v) For design of prestress.
 - (vi) To predict stress and strain distribution under prestress; and of most importance,
 - (vii) For comparison with results during testing.

Three-dimensional programmes investigating post-elastic phenomena have not been well-developed to date; behaviour beyond elasticity up to failure is best observed by the built-model itself.

4.3 The General Analytical Scheme for Cracking

As mentioned earlier, cracking of reinforced concrete is a local, non-linear phenomenon requiring a detailed analytical mathematical model. Crack widths, cracking penetrations and distribution need to be determined. The computational effort involved for detailed crack analysis for a large reactor vessel is clearly prohibitive.

To overcome this size restriction, an iterative analytical scheme shown in Fig. 4.4 may be used. This was suggested by McGeorge and Swec (Ref. 4.1). Linear analyses of the complete structure are performed using equivalent structural properties to obtain the gross structural response. Non-linear cracking analyses are then performed for selected portions, using appropriate boundary conditions, to evaluate local cracking. Compatibility of behaviour between the linear and non-linear analyses may be achieved through iteration, allowing an extrapolation of local cracking results to predict cracking over the entire structure.

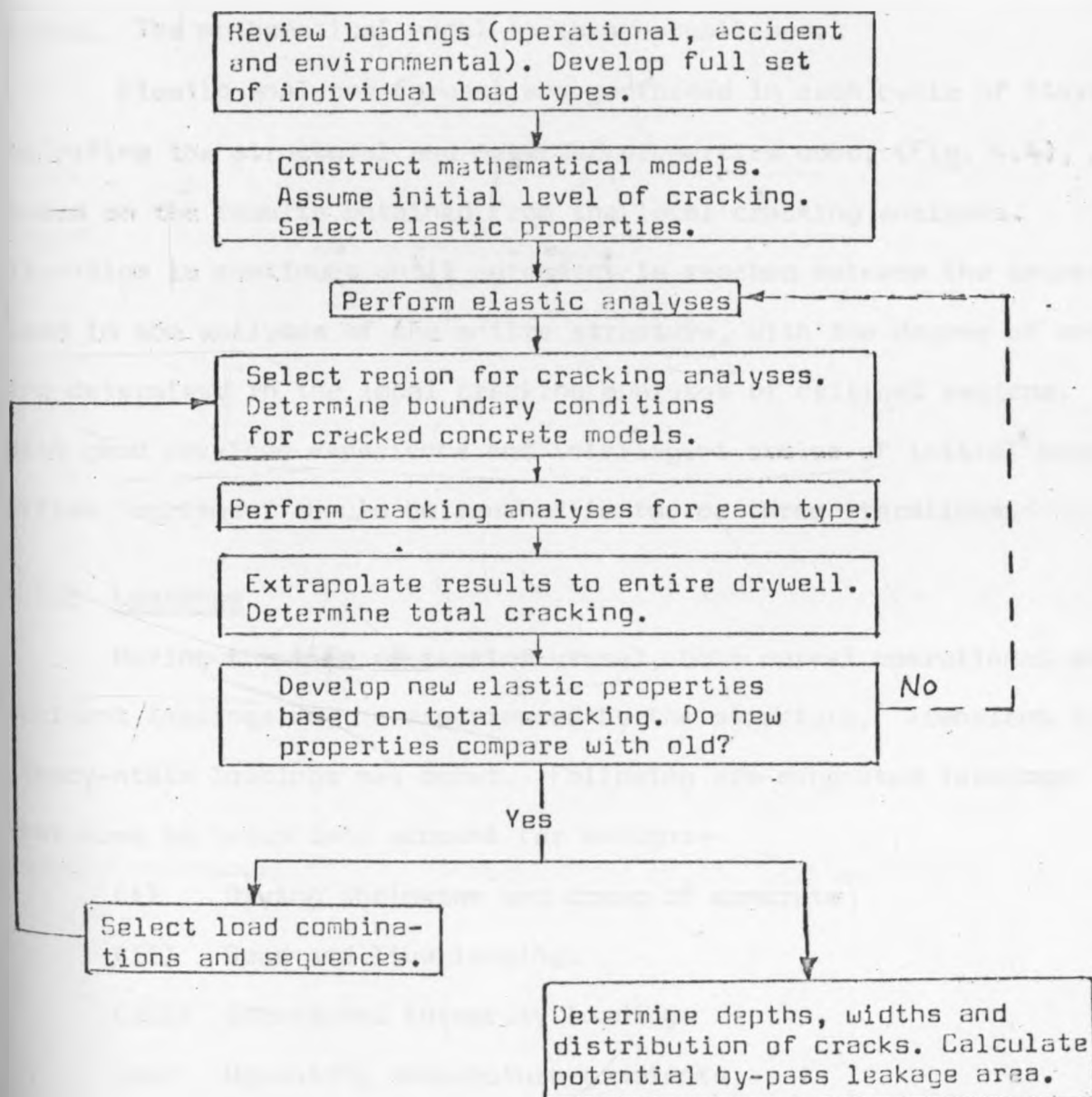


Fig. 4.4 The General Analytical Procedure for Cracking
(McGeorge and Swec)

The FEM, described previously, can be used both for the analysis of the complete structure, as well as for the detailed analysis of local regions or structural components. Indeed all the analyses indicated in Fig. 4.4 can be carried out by this method.

4.4 Elastic Analysis of the Entire Reinforced Concrete Structure

4.4.1 Outline

Once the structure dimensions are established, and the material properties are idealised, an element (or a sector) of the structure is divided into finite elements to complete the computer programme input. The mathematical model is then established.

Elastic analyses (gross) are performed in each cycle of iteration to refine the structural and material properties used, (Fig. 4.4), based on the results obtained from the local cracking analyses. Iteration is continued until agreement is reached between the properties used in the analyses of the entire structure, with the degree of cracking determined in the local cracking analyses of critical regions. With good previous experience and intelligent choice of initial properties, agreement should be reached in two or three iterations.

4.4.2 Loadings

During the life of reactor vessel, both normal operational and accident loadings may be experienced by the structure. Transient and steady-state loadings may occur. Following are suggested loadings that must be taken into account for design:-

- (i) Drying shrinkage and creep of concrete
- (ii) Dead and live loading.
- (iii) Structural integrity loading.
- (iv) Operating temperature gradients
- (v) Small break accident (SBA) pressure and thermal transients

(vi) Design basis accident (DBA) pressure and thermal transients.

(vii) The safe shutdown earthquake (SSE) loading.

Drying shrinkage of concrete is a time-dependant aspect associated with moisture loss from the concrete. It occurs first on the outside and then on the inside of a concrete section. Creep will occur simultaneously with shrinkage in concrete walls and slabs, resulting in some relief of the stresses induced by shrinkage. This aspect is of importance only in the early life of the structure, up to 2 - 3 years.

Pressure and temperature transient loadings of the structure occur for both SBA and DBA accident conditions. The pressure loading associated with the DBA can then be selected from the peak value of the DBA and SBA time histories. The temperature value for the loading is selected similarly.

The safe-shutdown-earthquake value depends on the geographic area of interest. For East Africa, a horizontal ground acceleration of 0.40g would be selected for the tectonic Western and East Rift Valleys, and 0.20g value elsewhere. For the reactor vessel considered in this thesis, the risk of destructive earthquake was assumed to be negligible.

4.4.3 The Analysis

The box-like structure under static internal pressure (and a steady-state thermal load), is anticipated to have a structural behaviour exhibiting three distinct phases:-

(i) The Elastic phase, where the stresses in the reinforcement are less than the yield stress.

(ii) The Elasto-Plastic one, where yield stresses and extensive

flexural cracking develop in regions of maximum bending moment.

(iii) The Plastic phase, where 'yield line' mechanisms develop, followed by additional load resistance due to membrane action of reinforcement, caused by excessive deflections.

In the Elastic Phase, the resistance of the uncracked slab may be greater than that of the cracked one, due to the very small percentage of tensile reinforcement provided only on the basis of restricting crack widths. This is an undesirable characteristic as collapse may occur abruptly immediately on cracking. The analytical results under increasing load, therefore, depend on the tensile strength of concrete, and already existing cracks.

4.5 Local Cracked Concrete-Analysis

4.5.1 Outline

One of the fundamental characteristics of reinforced concrete is that the full tensile capacity of the material is achieved only when cracking of the concrete occurs; this resulting in the development of the necessary strains in the reinforcement. In the analysis, the non-linear material properties must be considered as well as the complex failure criteria. Discontinuity effects in development and propagation of cracks through the material are also present, and need consideration.

Work published by M. A. Taylor and others, in 1972 (Ref. 4.3), develops a plane-strain finite element, used to investigate the behaviour of reinforced concrete, subject to arbitrary static loading, in great detail. The element has the following features:-

- (i) Linear strain characteristics.
- (ii) Loading and unloading conditions.
- (iii) A non-linear, constitutive law for concrete, (based on damage theory concepts and biaxial test data).

(iv) A biaxial failure criterion, which predicts the point and orientation of cracking.

(v) Occurrence of crack propagation along any element boundary, but continuity of reinforcement across cracks.

(vi) Redistribution of internal stresses after occurrence of crack propagation.

(vii) Modelling of 'reinforcement to concrete' bond by a continuous series of springs, parallel and perpendicular to the reinforcing bars, allowing for moderate slip according to the piecewise linear law.

4.5.2 Cracked-Concrete Model

This model is comprised of plane-strain finite elements just described. Typical vertical and horizontal sections of the structure wall or/and roof slab are chosen. The model consists of a combination of plane-strain quadrilateral elements of unit thickness representing the concrete, and one-dimensional 'beam' elements representing the active reinforcement; (see below).

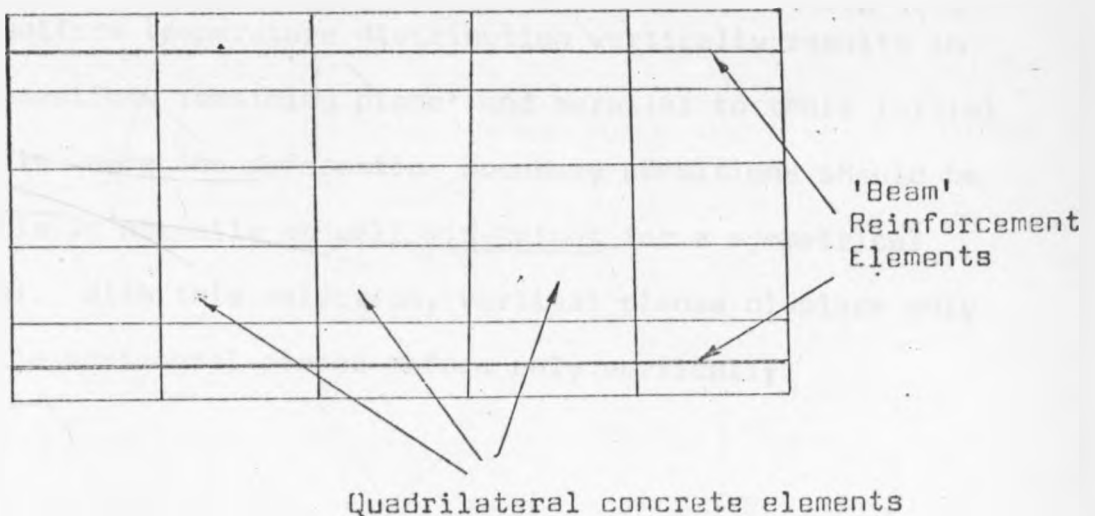


Fig. 4.5 Finite Element Model for Cracked Concrete

Since cracking is only allowed to occur in the plane of the model, the three-dimensional cracking behaviour is determined by performing cracking analyses on both the horizontal and vertical models for each set of loading conditions.

The three-dimensional stress distributions obtained from each of the elastic analyses are reviewed and regions of maximum tensile stress identified for each loading type, and selected loading combinations. The distributions of normal and shear stress through wall thickness (and roof slab) are then obtained in these regions at locations corresponding to the end faces of the cracked concrete model; and are used as direct loadings to the cracking model. Equilibrium of loading is achieved by applying appropriate body forces over the surface area, as well as externally applied loads. This procedure enables accurate duplication of elastic stress distribution for these regions of interest.

For shrinkage and temperature loadings, crack concrete analyses can be performed directly with deformation rather than force boundary conditions. In the region of the structure (wall or slab) where the essentially uniform temperature distribution vertically results in 'plane cross-sections remaining plane' and parallel to their initial orientation, is where the deformation boundary conditions should be selected. This is normally at wall mid-height for a symmetrical reactor vessel. With this selection, vertical planes displace only radially, while horizontal planes deform only vertically.

4.6 The Analysis for this Specific Vessel

The idealised structure shown in Fig. 4.1, for the input of the programme 'SWEAP' (Section 4.2.1) is a simple, thin shell model, assuming elastic and isotropic thin plates rigidly connected at the edges. Due to symmetry, only 1/8 of the structure is input.

Input are an internal pressure $P = 6900\text{kPa}$, Poisson's ratio $\nu = 0.2$, and the modulus of elasticity of concrete, $E_c = 28\text{MPa}$. The compressive and tensile strengths of the concrete are taken as 32MPa and 3.2MPa respectively.

The 'elastic' analysis of the steel and concrete stresses was carried out on selected positions of each slab, shown below.

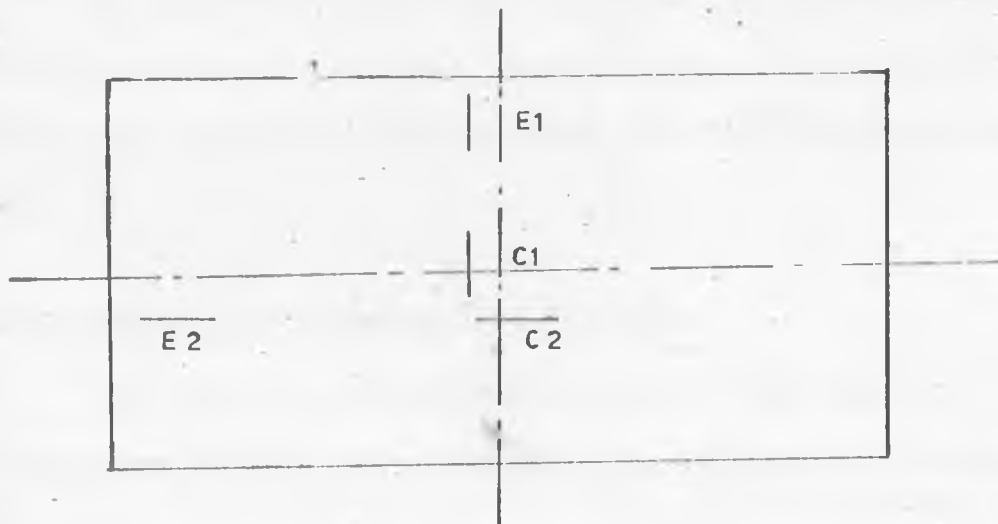


Fig. 4.6 Stress Positions of Slabs

Using the conventional working stress method, with a modular ratio of 7, the following results are obtained.

For an internal pressure of 83kPa , a maximum value of the design/yield stress ratio for the tensile reinforcement in one wall is 0.65. The maximum concrete compressive stress is 4.9MPa . Cross-sections at locations C1 and C2 are in tension; and 'through' cracks are expected, especially if precracking has occurred due to shrinkage effects. Elsewhere, no through cracks are expected.

The maximum 'uncracked' tensile stress of concrete is 2.6MPa ,

a value much less than the predicted tensile rupture strength of about 3.3MPa. It is expected, therefore, that up to this pressure (83kPa), most of the structural concrete will remain uncracked.

4.6.1 Test Pressures

The A.S.M.E. Code (Ref. 4.4) specifies a test pressure of magnitude 1.15 times the 'containment design pressure':-

$$P_t = 1.15 P_a \dots\dots\dots 4.2$$

P_t and P_a being the test pressure, and the 'abnormal' or 'incident maximum' pressure, respectively. A pressure not exceeding 100kPa was adopted on these grounds, for the structural integrity test.

4.6.2. Crack Widths Due to Test Pressure

The Australian Code of Practice AS 1480 (Ref. 4.2) crack width formula (ignoring 'tension stiffening' contribution), is:-

$$w = 3c_t \epsilon_m \dots\dots\dots 4.3$$

- where w = crack width
- c_t = concrete cover
- ϵ_m = f_s/E_s

At the test pressure of 100kPa, the maximum values of probable crack widths are shown in Table 4.1 below (for $c_t = 50\text{mm}$).

Slab	Location (Ref. Fig. 4.)	$\epsilon_m = f_s/E_s$ ($\times 10^{-6}$)	w_{max} (mm)
ROOF	E1	846	0.13
	C1	685	0.10
	E2	1108	0.17
	C2	544	0.08
TRANSVERSE WALL	E1	1289	0.19
	C1	596	0.09
	E2	1003	0.15
	C2	2860	0.04
LONGITUDINAL WALL	E1	1309	0.20
	C1	532	0.08
	E2	798	0.12
	C2	294	0.04

Table 4.1 Crack Widths for $P = 100\text{kPa}$ and $c_t = 50\text{mm}$.

Such crack widths may cause local rupture of the interior coating of the vessel, resulting in some increased leakage. However, on reduction of load, closure of cracks is expected since the reinforcement stress is theoretically below the elastic limit.

4.6.3 Collapse; Yield Line Analysis

This 'plastic' phase of behaviour will occur at pressures given in Table 4.2 below. The Orthotropic arrangement of the reinforcement, and the reduction in the collapse moment of resistance due to the axial tension forces, have been allowed for.

The effect of 'corner levers' has been ignored.

Slab	Collapse Pressure (kPa)	Collapse/Test Pressure
ROOF	276	2.76
TRANSVERSE WALL	255	2.55
LONGITUDINAL WALL	290	2.90

Table 4.2 Yield Line Collapse Pressure

It should be noted that the A.S.M.E. Code (Ref. 4.4) does not contemplate development of yield line mechanisms and membrane action with large deflections, as a design condition for concrete reactor vessels and containments.

4.6.4 Shear Strength of Slabs

No shear failure should occur prior to the full development of the yield line mechanisms. The side slabs should therefore be capable of carrying at least 255kPa.

The maximum permissible shear stress at collapse given by the Australian Code AS 1480 (Ref. 4.2) is:

$$\tau_s^* = \phi (0.33 \sqrt{f'c}) \text{ MPa, in areas with no shear reinforcement (standard notation) 4.4}$$

i.e. the allowed maximum $\tau_s = 1.5\text{MPa}$ (1505kPa).

The perimetral shear stresses for the roof and two walls are 595, 580 and 430kPa respectively due to a collapse pressure of 255kPa. This is satisfactory.

The principal tensile stresses due to shear and membrane tension are 784, 854 and 672kPa; which are satisfactory for two way slabs.

4.6.5 Results of the Two-Dimensional FEM Analysis Using the Programme 'SWEAP'

Figs. 4.2(a), (b) and 4.8(a), (b) show distributions of computed values of moments, stresses, axial forces and deflections as yielded by the 'elastic' programme 'SWEAP'. The sections shown are the three principal cross-section of the structure.

The results of deflections shown in Figs. 4.8(a) and 4.8(b) for the internal pressure of 6900kPa (1 kip/in²) provide a 'lower bound' based on the uncracked section with E_c = 28MPa. The deflection under the maximum test pressure (100kPa) would then be only:-

$$\Delta = \frac{100}{6900} \times 2.536 \times 25.4 = \underline{0.9\text{mm}}$$

An 'upper bound' estimate of deflection is made assuming that the tensile strength of concrete is negligible throughout. This gives a Δ = 7mm at the test pressure (using the bending moment FEM results). Hence:-

$$\underline{0.9\text{mm}} < \Delta < 7.0\text{mm} \dots\dots\dots 4.5$$

The actual deflection, however, depends very much on other factors like crack patterns, way of loading, local yielding. The analysis can therefore only give a probable range of deflections to be expected for the model test - see Table 4.3 below.

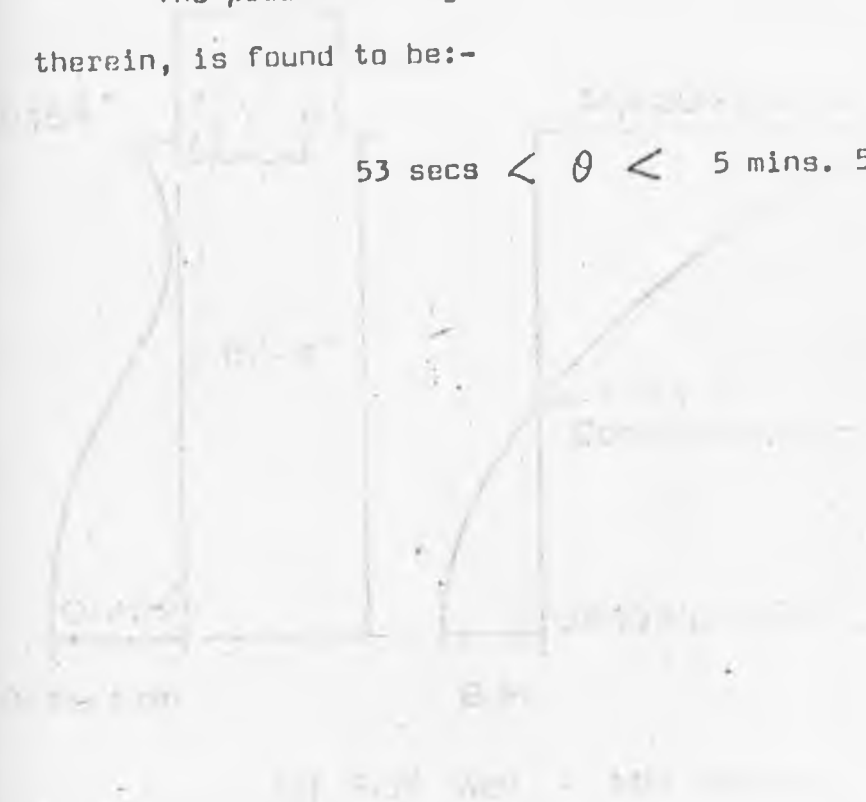
Slab	Minimum Δ (mm)	Maximum Δ (mm)
ROOF	0.90	7.0
TRANSVERSE WALL	0.15	0.7
LONGITUDINAL WALL	0.20	1.2

Table 4.3 Range of Probable Deflections at Test Pressure

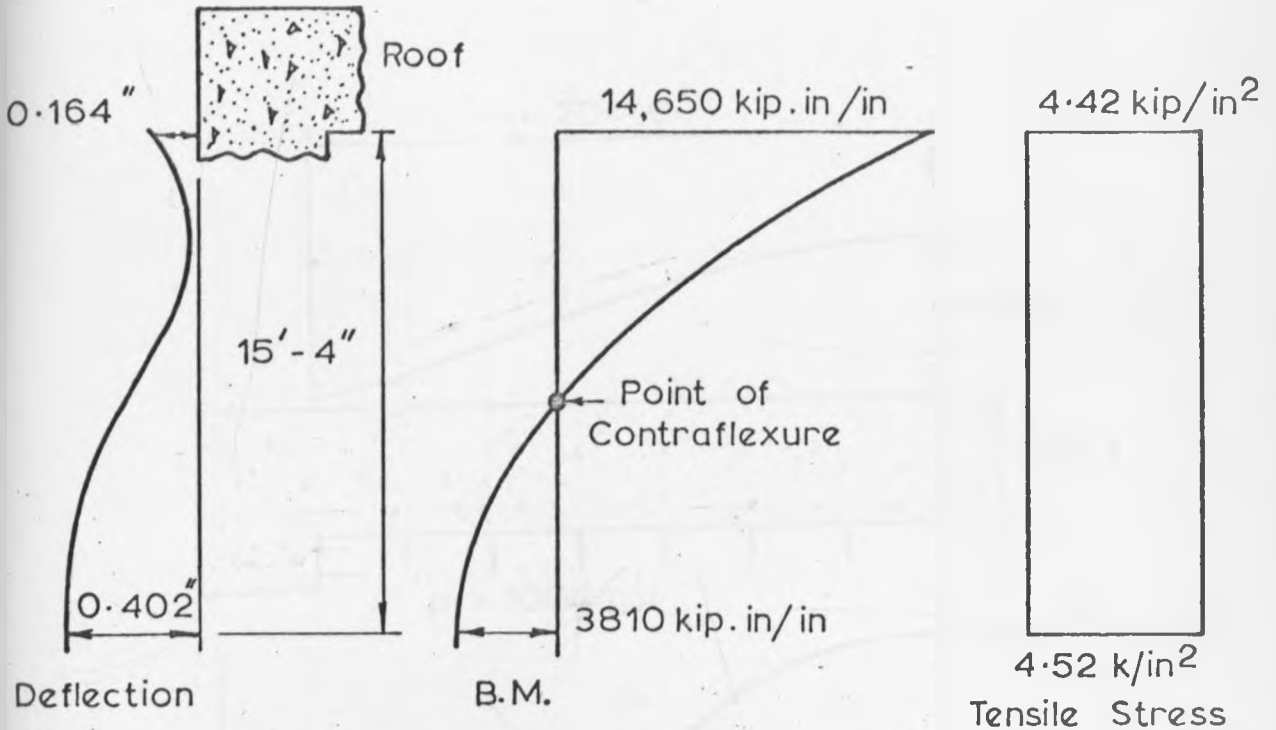
Rotations: From the B.M.D. of the FEM results (Fig. 4.8), the maximum change of slope at the point of contraflexure is approximately 2m from the inside face of the longitudinal wall.

The probable range of change of slope, by the area-moment therein, is found to be:-

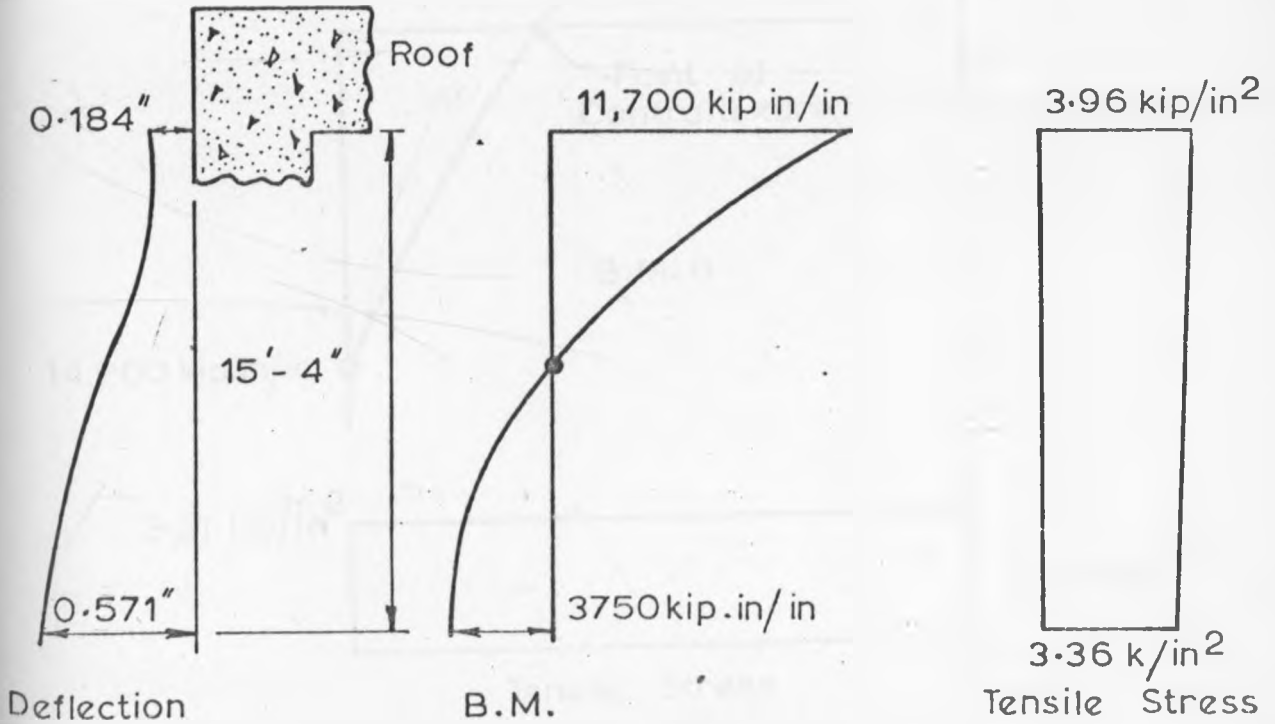
$$53 \text{ secs} < \theta < 5 \text{ mins. } 55 \text{ secs} \dots\dots\dots 4.6$$



Note: Values given due to an internal pressure of 1000psi



(a) Side Wall - Mid Section



(b) End Wall - Mid Section

FIG. 4.8 FINITE ELEMENT RESULTS

4.8(a)

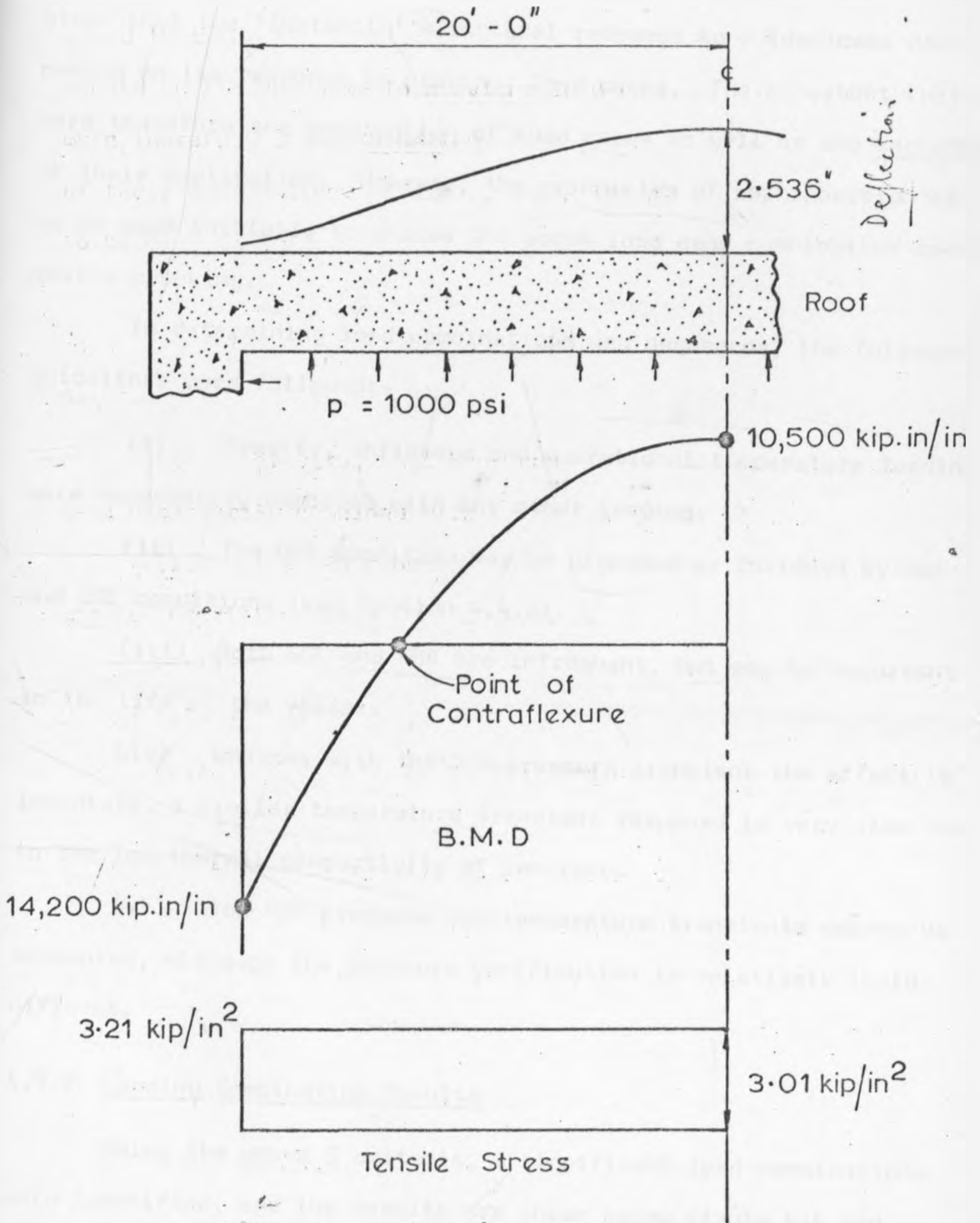


FIG. ~~AG~~ FINITE ELEMENT RESULTS

4.8(b)

4.7 Results of the Three-Dimensional FEM Analysis

(McGeorge and Swec, Ref. 4.1)

4.7.1 Introduction

In interpreting the results of this analysis, it was understood that the 'inelastic' structural response to a load case depended on its response to previous load cases. The important factors were therefore the combination of load cases as well as the sequence of their application. However, the principles of superposition had to be used initially to assess the worst load case combination causing severe cracking.

In determining load combinations and sequences, the following guidelines were followed:-

- (i) Gravity, shrinkage and operational temperature loading were necessarily combined with any other loading.
- (ii) The DBA condition may be preceded or followed by SBA and SSE conditions (see Section 4.4.2).
- (iii) Both SSE and SBA are infrequent, but may be recurrent in the life of the vessel.
- (iv) Whereas with the DBA pressure transient the effect is immediate, a similar temperature transient response is very slow due to the low thermal conductivity of concrete.
- (v) The SBA pressure and temperature transients cannot be uncoupled, although the pressure contribution is relatively insignificant.

4.7.2 Loading Combination Results

Using the above 5 criteria, 6 significant load combinations were identified, and the results are shown below (Table 4.4 and Fig. 4.7).

Combination Number	Description	Horizontal Crack Penetration (%)	Vertical Crack Penetration (%)
1	$D + S + T_0$	10 (BF)	10 (BF)
2	$D + S + T_0 + P_1$	10 (BF)	15 (BF)
3	$D + S + T_0 + E^1$	15 (BF)	10 (BF)
4	$D + S + T_0 + P_1 + E^1$	25 (BF)	15 (BF)
5	$D + S + P_2 + T_2$	<u>80</u> (OF)	<u>80</u> (OF)
6	$D + S + P_2 + T_2 + E^1$	<u>80</u> (OF)	<u>80</u> (OF)

BF - Both Faces (inner and outer)
 OF - Outer Face
 D - Gravity
 S - Shrinkage
 T_0 - Operational Temperature

T_1 - DBA Temperature Transient
 T_2 - SBA Temperature Transient
 E^1 - Seismic SSE
 P_1 - DBA Pressure Transient
 P_2 - SBA Pressure Transient

Table 4.4 Cracking Results of Load Combinations

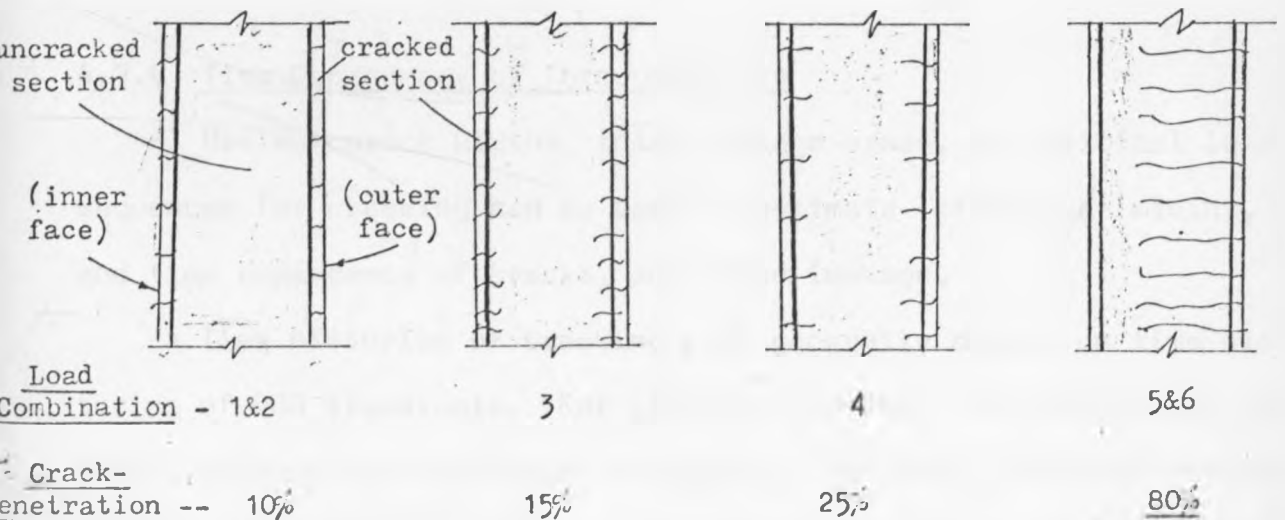


Fig. 4.7 Results of Horizontal Cracking for Various Load Combinations.

It is noted that the most severe combination did involve the SBA transient, resulting in very significant cracking (combinations 5 and 6). From these results, no 'through'-cracks are observed; indeed the cracks would be expected to close after the alleviation of the SBA conditions. However, any loading subsequent to the SBA conditions that induces significant tensile loadings could result in 'through'-cracks and potential leakage paths.

4.7.3 Load Sequence Results

The worst load combination sequences for through-cracks, identified in the analyses, are as follows:- (numbers refer to load combinations as in Table 4.4)

Sequence I: 1 - 6 - 1 - 4.

Sequence II: 1 - 5 - 1 - 3 - 1 - 6.

(note that combination 1 refers to normal operation; and 6 to accident extreme conditions).

However, potential leakage paths are only open for sequence I. In sequence II, the SBA temperature transient causes closure of inner cracks under a large induced compressive loading.

4.7.4 Time Dependency of Through-Cracks

Maximum crack widths, total leakage areas, and critical load sequences for cracking can be used to estimate 'effective' widths, and time dependency of cracks, and hence leakage.

Time histories of cracking will generally depend on time histories of DBA transients. For vertical cracking, the result will depend primarily on hoop stresses caused by the DBA pressure transient. Horizontal cracking, however, is controlled by the vertical tensile stresses of combined dead load, shrinkage, operational temperature and the DBA pressure transient.

When the DBA pressure and the SSE loads occur simultaneously, they offset the dead load compressive stresses. Hence leakage cracks only occur when both transient loading are present. The dead load stresses thus correspond to a 'threshold' stress level, below which the combined loading will not cause crack opening. This stress level varies with the height of the vessel.

The SSE loading, being cyclic, causes cracks on opposite sides to open and close alternately. So leakage is existent only on one side of the vessel, at any given instant. Seismic loading that would cause substantial leakage would be from a rather strong earth-tremor, lasting over 10 seconds. Below this level, earthquake risk is assumed negligible.

CHAPTER 5

TESTING OF MODEL, AND EXPECTED RESULTS

5.1 Introduction

The model, for which construction is outlined in Chapter 3, will be required for two basic tests:-

(i) An internal pressure test (including structural integrity and leakage evaluation).

(ii) A thermal test

Upon completion of this 1.24m high model, its interior will be completely sealed from the outside.

The two tests will be carried out separately first, within elastic limits. The two sets of test results will be then superimposed. At all load stages (with internal air-pressure), measurement will be made of leakage rate. Later, an attempt will be made to carry out both tests simultaneously, again within the elastic range. Finally, a large internal water pressure will be used to crack the model beyond the elastic limit, up to plastic behaviour and final collapse.

It should be noted that one of the major reasons why the model was constructed was to try and simulate 'proof pressure' tests that are performed on prototype reactor and pressure vessels, before they are put in use, (Ref. Chapter 6). Construction joints, temperature and shrinkage cracks, are all sources of leakage. How can these aspects be modelled? This question is a difficult one. It is hoped that the test and subsequent results will provide, if not all, at least part of the answer to the problem.

In this chapter, I will present suggestions on how the model should be loaded and tested, the procedure for some measurements, and a projected forecast of test results.

5.2 Internal Pressure Tests

5.2.1 The Air Pressure Test

The prototype structure is expected to resist an 'abnormal' (DBA) pressure of 100kPa, without yielding. From the similitude requirements for pressure (Table 1.1), since $\lambda_\sigma = 1$, the model should also be loaded with a pressure of 100kPa. In Section 2.5.1 I pointed out that air-pressures exceeding 80kPa would be dangerous to test with. This test will therefore be kept within this range of pressure, and should give an elastic response. More important is that this test will simulate the 'structural integrity test' of the prototype, with emphasis on leakage rate measurements.

The methods for these measurements will be similar to those discussed in Section 6.6. Guidelines of the A.S.M.E. Boiler and Pressure Vessel Code (Ref. 6.1) and the American National Standards Institute (A.N.S.I.) on 'Leakage Rate Testing' (Ref. 6.2) are followed, where applicable.

Compressed nitrogen cylinders, can be used for pressurising as discussed previously (Section 2.5.1) both the steel hatchway door and the simulated blast seal door should have leakage evaluations made on them. Any excessive leakage in these areas should be sealed up before further testing.

Pressure gauges on the 'air-vent', the nitrogen inlet tube(s), the 25mm outlet pipe (and possibly one on the steel hatchway), should be used to check on the uniformity of the internal pressure. Pressures up to 80kPa should be made in 3, 20kPa increments, up to 60kPa, followed by a further 2 instalments of 10kPa. The pressure at any loading stage should be held for at least thirty minutes before all readings are recorded. Unloading should be done similarly. About 4 - 5 loading-unloading cycles should remove creep effects, to make results comparable to the FEM analytical results.

Since the test should be 'elastic', any cracks that form on loading should close up upon unloading. I recommend that investigation of leakage through cracks be done, by either the 'water-submersion local leak test' or the 'vacuum test' utilising soap bubble formation in a vacuum glass cover (Ref. 6.2, Sections A.2 and A.3), followed by a leakage rate evaluation.

5.2.2 The Water Pressure Test

For reasons of safety, the water pressure test will follow on after the air-pressure test. This test should elevate the pressure from 80kPa to 100kPa; and the expected response should still be elastic.

5.2.3 Preparation

Air used in the previous test should be removed as the central cavity is filled with water. The air vent and the 25mm pipe should therefore be left open before testing commences.

Accurate methods of determining the magnitude of the 'static head' of pressure should be installed. Control valves and pressure gauges should be checked when the model is full of water, before the test begins.

5.2.4 The Test

The sequence should take this or a similar form:-

- (i) Elastic tests (to compare with analysed results)
- (ii) Crack creation tests, to check the initial crack pressure. This should get to the pressure of about 100kPa, still elastic. A thermal test should be then carried out before stages:-
 - (iii) Crack propagation tests to compare with the elasto-plastic analysis results; (100 - 200kPa).
 - (iv) Fracture test to obtain the yield and ultimate stress, as well as the ultimate failure pressure. (200kPa).

Stages (i) and (ii) I suggest be done in 20kPa loading and unloading instalments, up to 100kPa. This pressure should be obtainable from the 'elevation head' of the overhead tank in the Hydraulics Laboratory.

Four or five cycles of loading and unloading should remove the short-time creep effects from the model concrete.

Stages (iii) and (iv) of the test are discussed briefly in Section 5.6.

5.3 Creating Internal Heat

I suggest the principles of the heating system described in Section 2.5.2, (Fig. 2.1), be adopted. The system basically heats up the interior of the model, and controls the inner and outer temperatures of it, (since the model is placed in an air-conditioned chamber with its cavity continually circulated with temperature controlled water.)

Since the Hydraulics Laboratory at Sydney University is not air-conditioned, some shield of low thermal conductivity material (e.g. glass fibre) could be built around the model. The interior of this shield would then be kept at constant temperature by an improvised air-conditioning system.

The circulation required of the hot water in the model central cavity can be created by the various pipes existing on the model.

The target initially should be to maintain a constant internal temperature for at least 1 hour; and later to establish thermal stable conditions (inside and outside the model) for at least 1 week.

5.4 The Thermal Test

This test should be carried out in at least two heating cycles.

In the first cycle, a basic outer and inner temperature should be established, 20°C say. The water temperature is then raised at a rate computed using Fourier's Number (for the temperature rise rate) or Nusselt's Number (for the boundary heat transfer) or the Thermal Diffusivity, D (see Section 1.7.3). A rate of say 4°C/hour is then set.

Temperature distribution readings with time are then taken every 1 or 2 hours, until the required maximum temperature is reached (about 70°C in this case).

It should be expected that thermal strain readings may not

agree with the mathematically analysed results. This is due to creep of concrete. The creep and thermal strains get mixed up and are hard to separate precisely. This necessitates a second heating cycle, where the creep effect is assumed to be much less.

In the second (and higher) cycles, the rate of temperature rise can be increased, if required. Otherwise it is carried out as the first cycle.

Most measurements should be done at midheight of wall (for reasons discussed in Section 4.5). The temperature should not be raised too high (no higher than 70°C) since the model should remain basically elastic after this test; for comparison with the theoretical results. (In any discrepancy of strain results, another heating cycle should be carried out.)

Creep strains should be fairly small, so the strain readings should be comparable to the thermal analysis results.

Cooling should be accomplished at the same rate as heating, and unloading readings taken similarly.

5.5 A Simultaneous Thermal and Pressure Test

In this test use of air pressure is undesirable since hot air under pressure may create unprecedented explosions. The use of hot water is therefore adopted. The water creating the heat within the model cavity must be pressurised to supply a measurable internal pressure as well.

The system described in Section 2.5.2 (Fig. 2.1) is equipped with a water circulating pump. This pump should be utilised to provide a pressure head, P, given by the Bernoulli's equation (with the 'static' or 'elevation' head made zero), as follows:

$$P = \frac{v^2}{2g} + \frac{p}{\rho g} \dots\dots\dots 5.1$$

v: velocity of water in inlet duct

p: pressure exerted by the pump

Since the velocity of the water must be low and constant for a uniform inner water temperature, the total pressure head, P , will only be varied appreciably by varying the pump pressure, p .

Pressures should not exceed 50kPa and temperatures 50°C, for safety reasons. The test will therefore be 'elastic', and results obtained should compare well with the previous results obtained, by performing the two tests separately and superimposing the results.

I suggest that the pressure is elevated in 10kPa increments, and the temperature in 10°C increments. Readings then be taken after at least one hour has been allowed for conditions to stabilise.

The same instruments and devices used for the separate tests will be used for this test.

It is assumed that the previous thermal test (performed over at least two cycles), would have removed creep effects from the micro-concrete. The strains and stresses of the model walls and slabs will therefore be due to the internal loading only due to temperature and pressure.

Unloading should be done using the increments used in loading. After the last step of unloading, the model should remain untouched for 24 hours, after which period measurements should be taken in pursuit of any permanent set that might have occurred.

5.6 Testing to Failure

After all 'elastic' tests have been carried out, measurements recorded, and results compared with analytical results with satisfaction, the model will be overloaded with internal water pressure until it fails.

The purpose of this test (as outlined in Section 5.2.4), is basically to investigate crack propagation, yield and collapse mechanisms.

The test should see internal water pressures elevated from 100kPa to about 240kPa when the first yield lines should form. I suggest that loading be performed in 20kPa increments from 100kPa to 200kPa, and thereon followed by 10kPa increments up to the state of collapse. At each pressure increment level, at least 20 minutes should be allowed before all readings (of deformations, rotations, etc.) are recorded. Widths, patterns, orientation and propagation of all cracks should be recorded (by photography, say). This fact is of even greater importance at pressures above 240kPa, when yield line mechanisms are expected to start forming.

The results obtained from this test should normally not agree with computed ones. They should therefore serve as useful tools in remedying the theoretical analytical methods where they are in error.

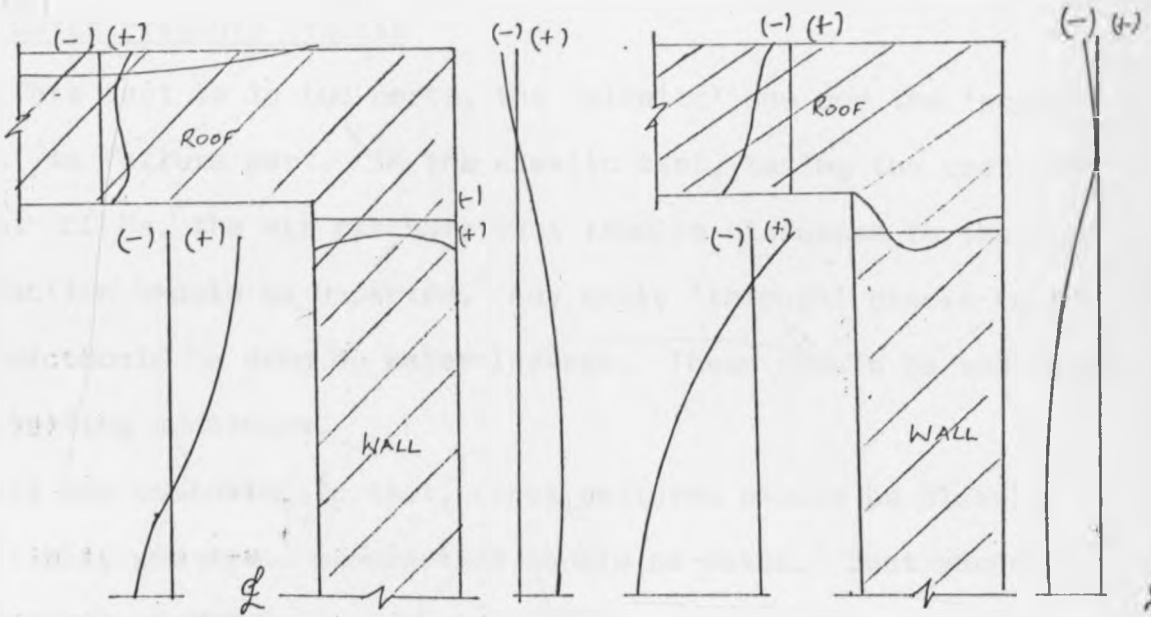
5.7 Expected Results of the Internal Pressure Tests

5.7.1 Air Pressure Results

The air pressure test is to give an elastic structural response; up to 80kPa; it also simulates the prototype structural integrity test.

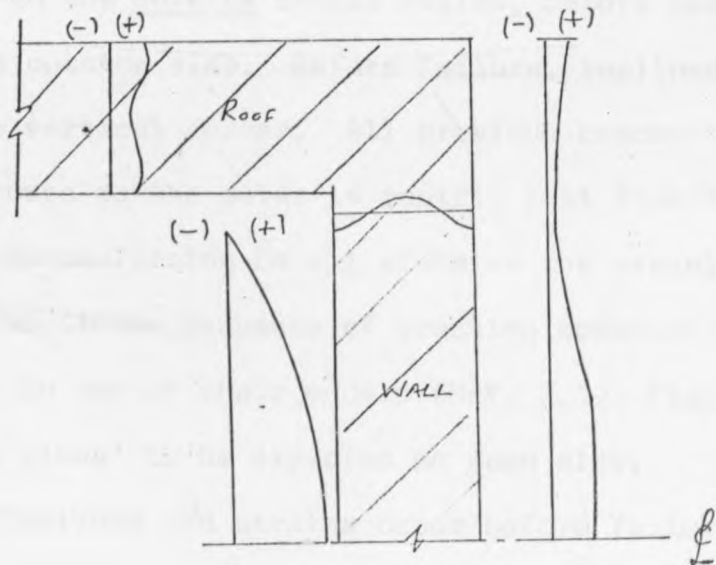
The walls and roof are expected to 'bulge' out, creating cracks of penetrations less than 30% of the wall/roof slab thickness. These should seal up upon unloading.

Strain measurements expected in the longitudinal, radial and hoop directions are shown in Figs. 5.1 (a), (b) and (c) below, for selected portions of the model structure.



(a) Longitudinal Strain

(b) Radial Strain



(c) Hoop Strain

Fig. 5.1 Expected 'Elastic' Strains Distribution

Expected deflection results are similar to those analysed by the two-dimensional FEM discussed in Chapter 4 (see Section 4.2, and Figs. 4.2(a) and 4.2(b)). If the deflections actually are as expected, areas of 'through' cracking will be established.

5.7.2 Water Pressure Results

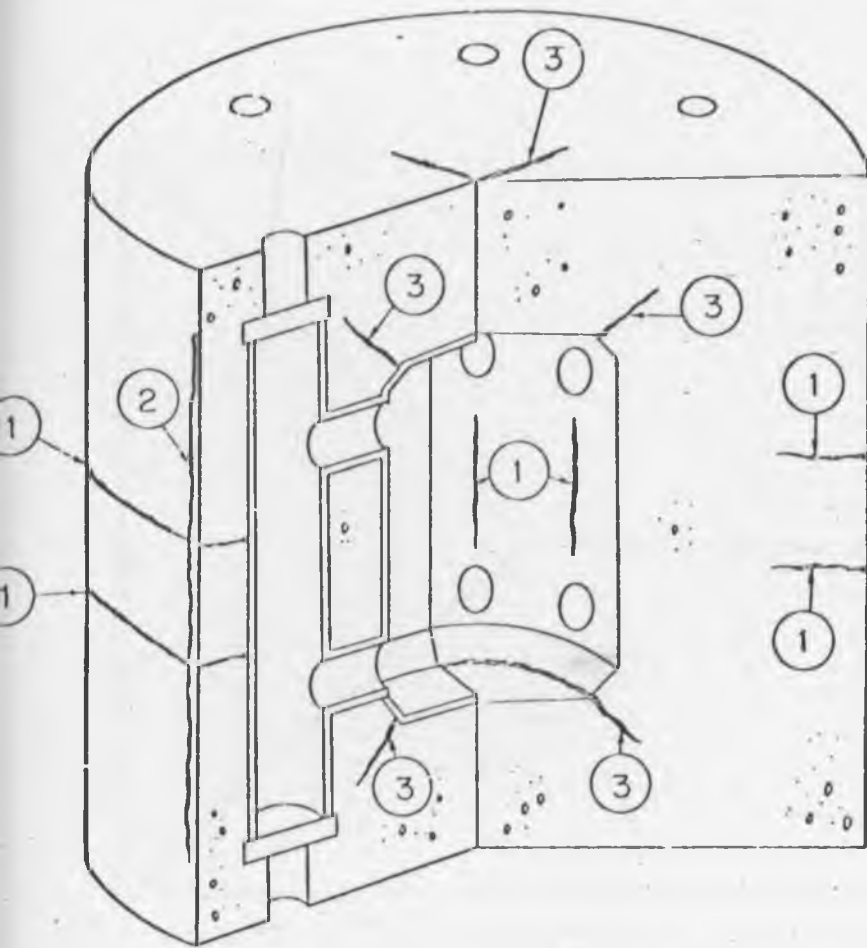
This test is in two parts, the 'elastic' one and the 'post-elastic' to failure part. In the elastic test, taking the pressure to about 100kPa, the air pressure test results discussed in the previous section should be expected. Any early 'through' cracks (not expected) should be seen by water leakage. These should be sealed up before testing continues.

In the post-elastic test, crack patterns should be clearly identifiable, and crack propagation should be noted. Just above the test pressure of 100kPa, crack widths of between 0.04mm to 0.20mm on the walls, and crack widths of up to 0.10mm on the roof, should exist.

At overpressure, excessive vertical cracking begins on the internal face, growing slowly outwards as the pressure is increased. Horizontal cracking on the outside should follow, before vertical cracks appear on the outside also. Before failure, inclined cracks at 30° to 45° to the vertical appear. All previous cracks then penetrate the wall thickness as the water is rapidly lost from the model. This leads to yield lines forming on all slabs as the vessel collapses.

Fig. 5.2 (a) shows the sequence of cracking observed by the Kajima Group (Japan) in one of their models (Ref. 2.1). Fig. 5.2 (b) indicates the 'yield lines' to be expected on each slab.

Excessive deflections and strains occur before failure - these should not agree with the analysed results. Record of these readings is therefore essential.



Sequence	Internal pressure at cracking kg/cm^2
(1)	70 ~ 80
(2)	80 ~ 90
(3)	100 ~ 110

Fig. 5.2(a) Schematic Drawing of Cracking Sequence

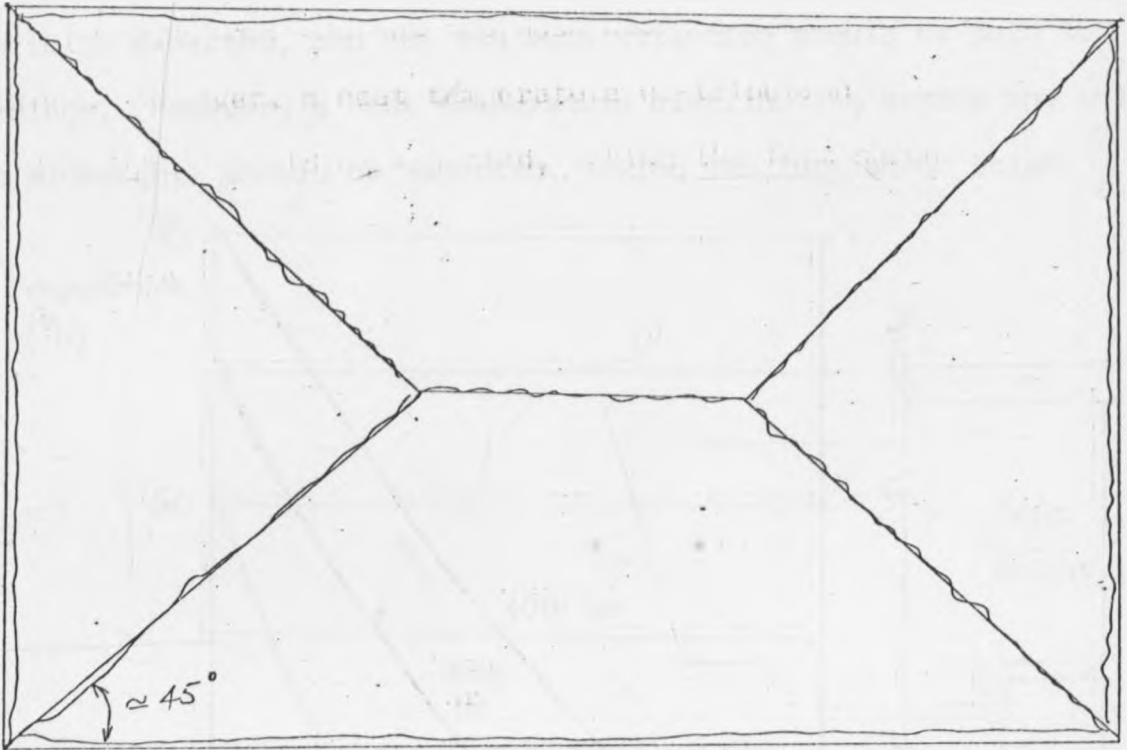


Fig. 5.2(b) Yield Lines at Failure for Wall and Roof Slabs

5.8 Expected Results of the Thermal Test

I suggested that the thermal test be done in two (or more) cycles (Section 6.4). In the first cycle, creep strains interfere with thermal strains. In the preceding cycles, this effect should be reduced, and thermal results should be expected.

So during the first cycle, 'confused' strain measurements should be expected, and not too much attention should be paid to readings. However, a neat temperature distribution across any wall (at midheight) should be expected, taking the form shown below.

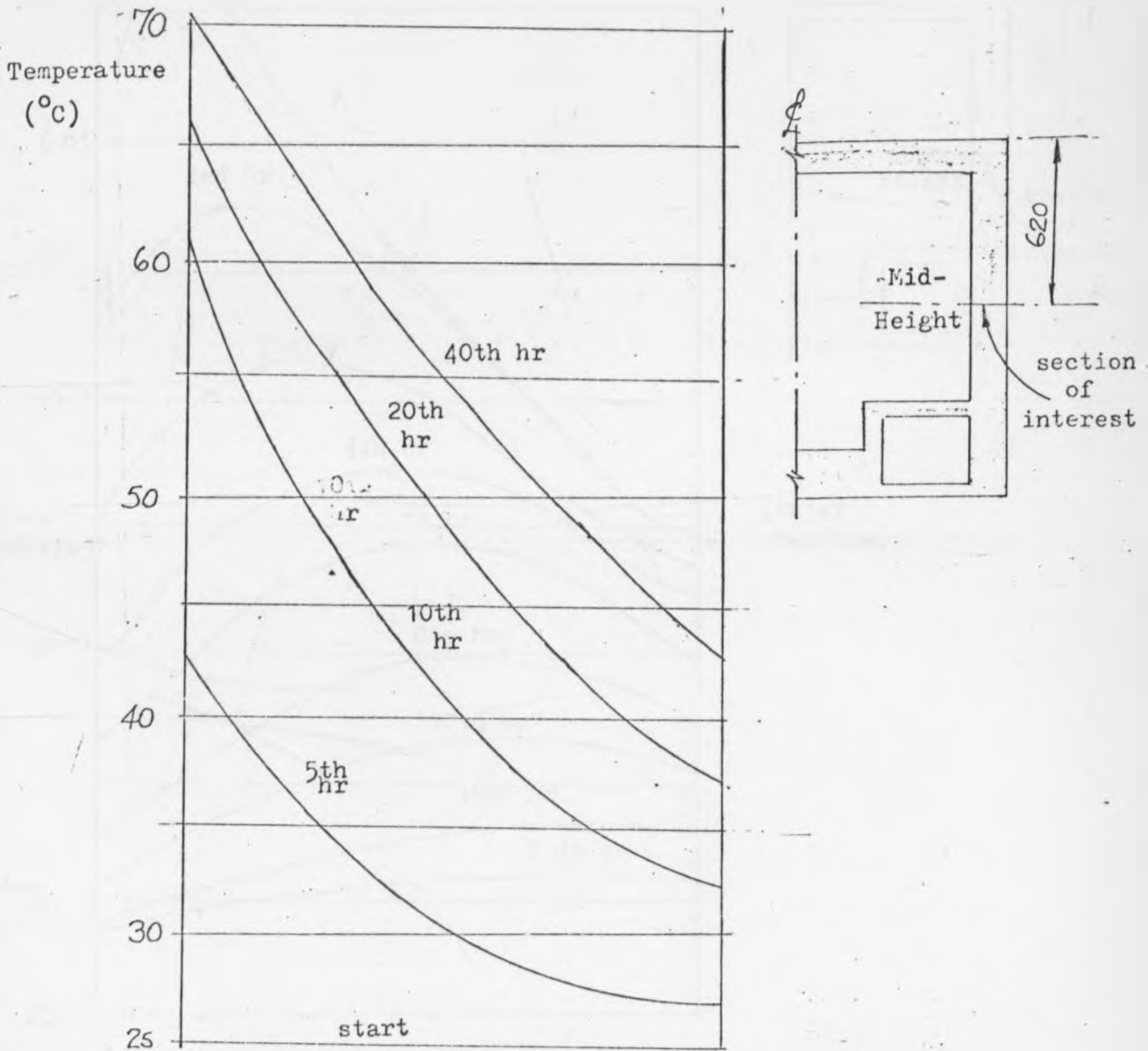


Fig. 5.3 Expected temperature distribution with time across the wall at Midheight.

During the second cycle (and any following ones), the temperature distribution should be basically the same as in the first cycle. The curves become more and more straight as the temperature is increased, and also as stable thermal conditions are maintained for longer periods of time.

On cooling, curves of the nature shown below should be expected.

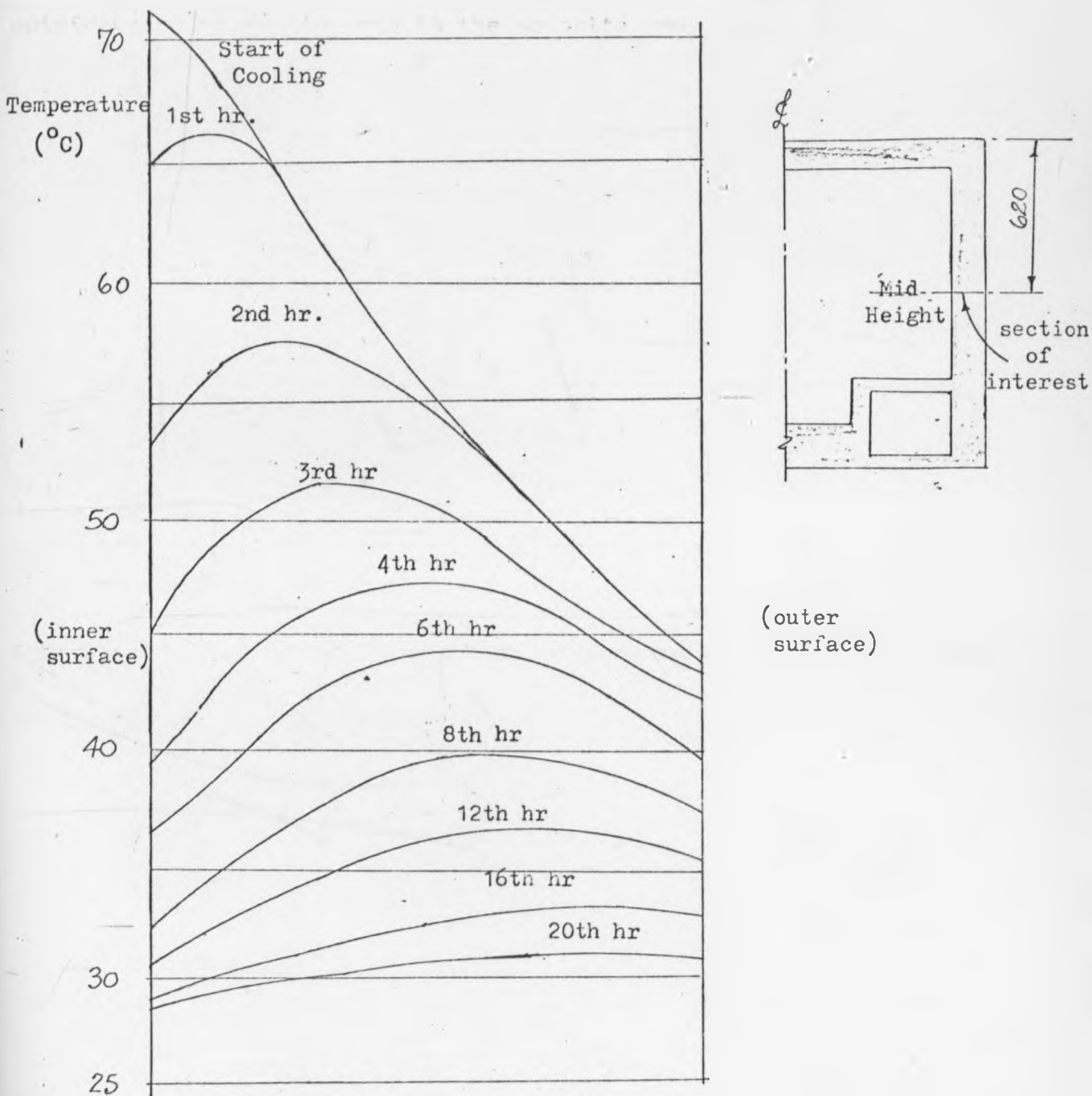


Fig. 5.4 Expected Temperature Distribution (with time).
across the wall at Midheight, on cooling.

During the second and following cycles, circumferential strains, with time should take the form shown in Figs. 5.5 and 5.6. It is noted that negative strains are induced inside, up to the peak, as the temperature is raised to the maximum testing temperature. On lowering the temperature to the original the strains rapidly reduce to the original. This response is elastic. On the outside, strains are induced in the opposite way. (Fig. 5.6).

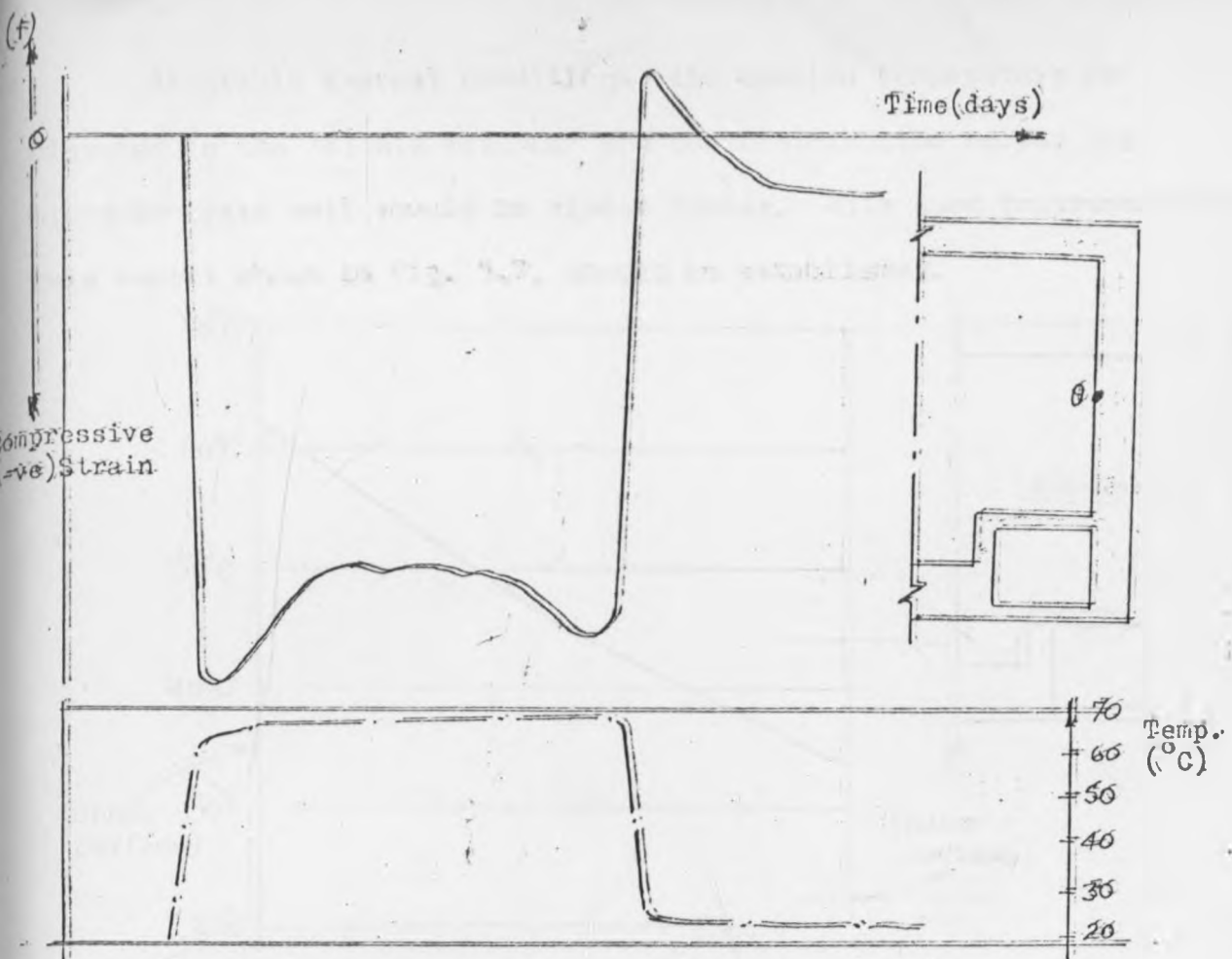


Fig. 5.5 Expected Circumferential Strain Near Inner Surface with temperature during higher heating cycles.

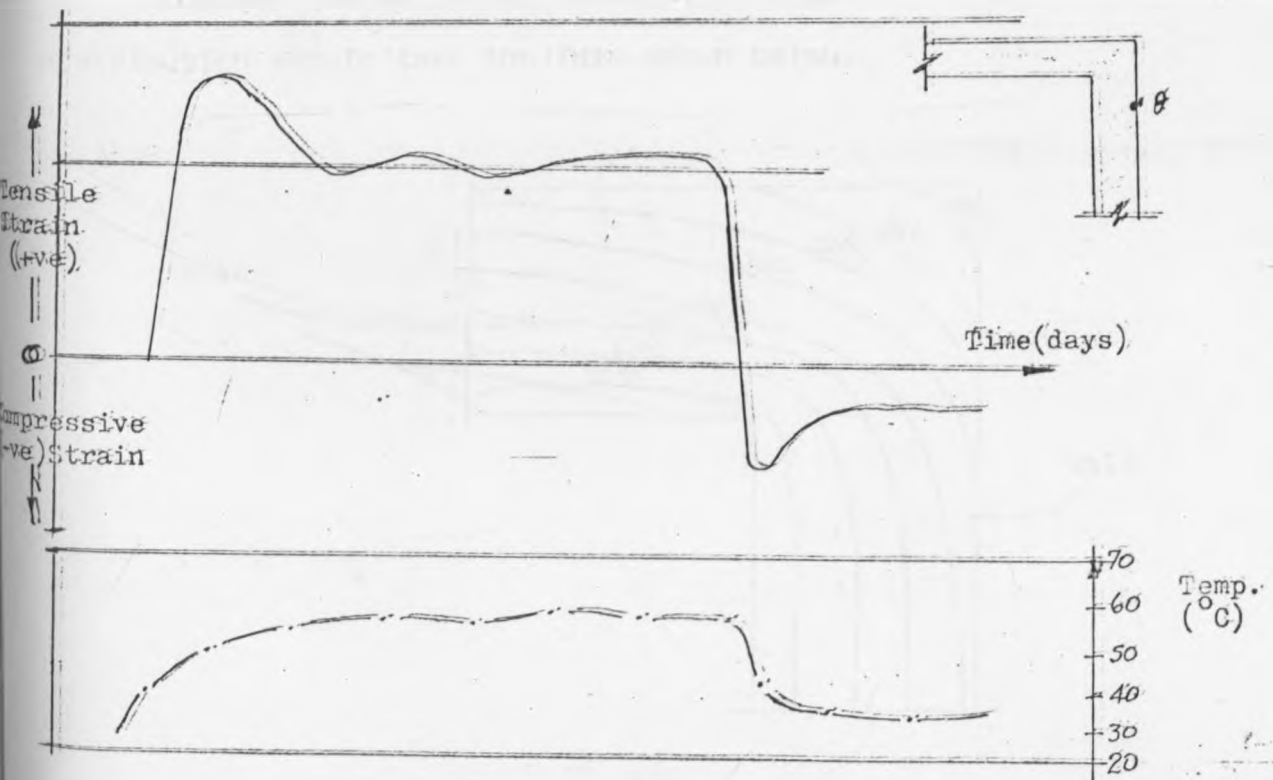


Fig. 5.6 Expected Circumferential Strain with temperature Near Outer Surface, during higher heating cycles.

At stable thermal conditions, the outside temperature is elevated to the 'stable maximum' and the distribution across the micro-concrete wall should be almost linear. With good instrumentation this aspect shown in Fig. 5.7, should be established.

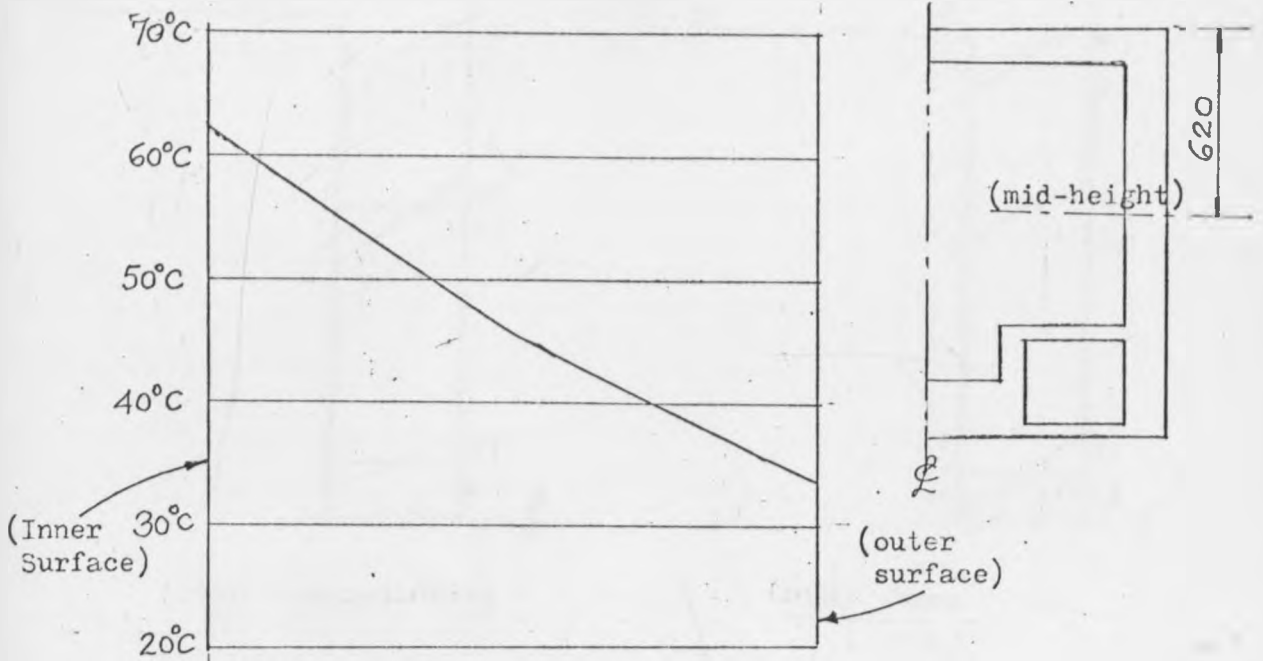


Fig. 5.7 Expected Temperature Distribution across the wall at Midheight at Stable Conditions.

Across the roof slab and wall, contours of uniform temperature distribution should take the form shown below.

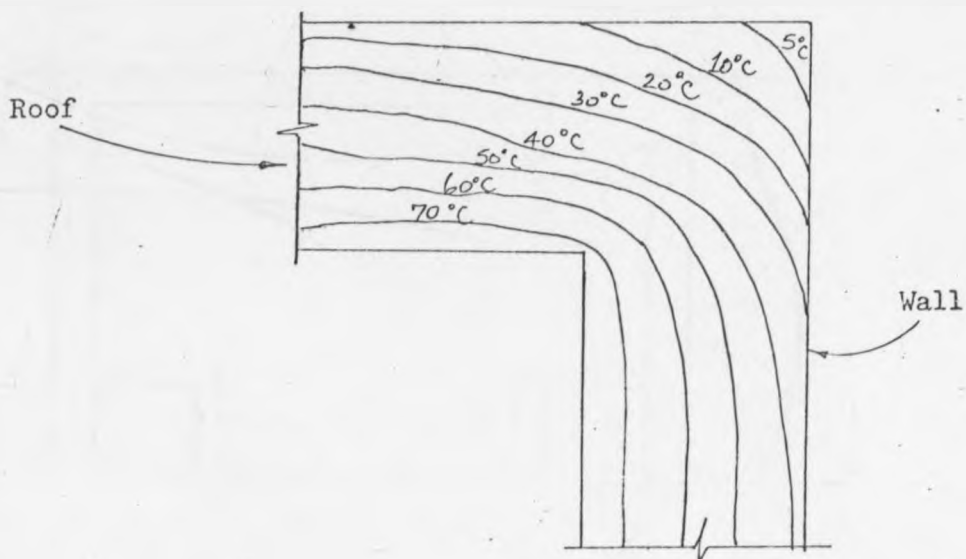


Fig. 5.8 Uniform Temperature Distribution Contours.

The internal strains caused by thermal stress to be expected are shown below

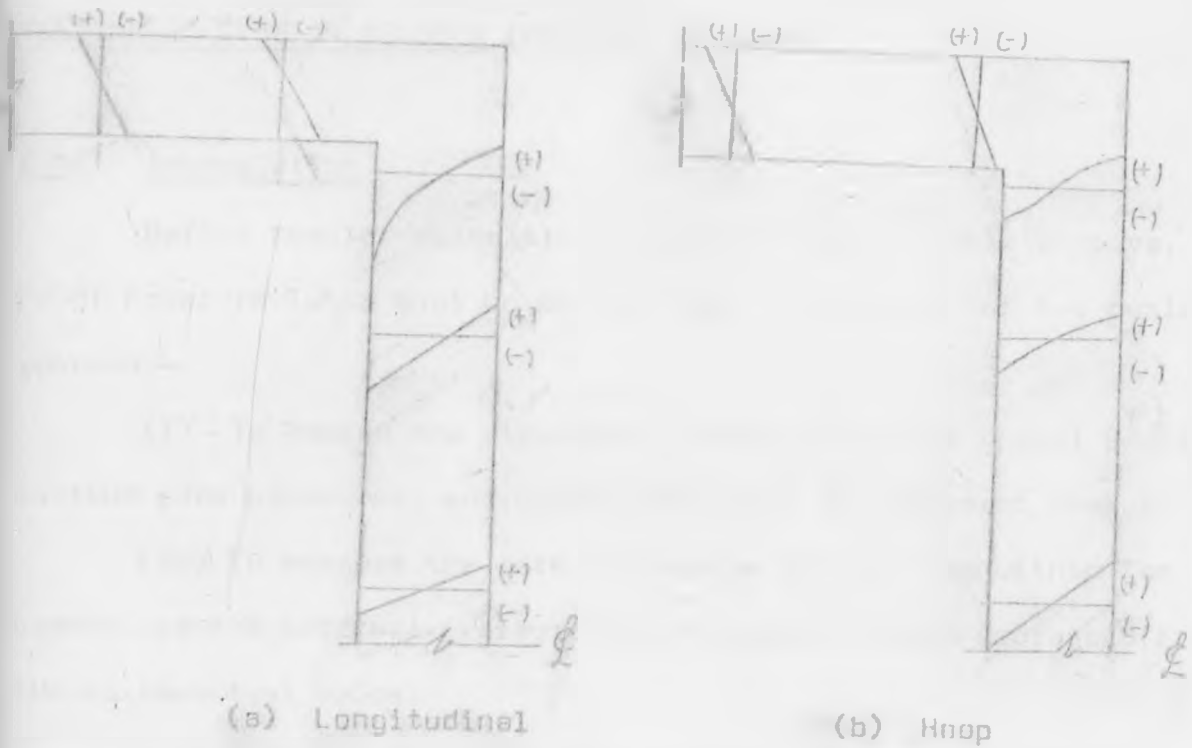


Fig. 5.9 Expected Internal Thermal Strains

Deflections under thermal load to be expected of the whole model structure is as follows.

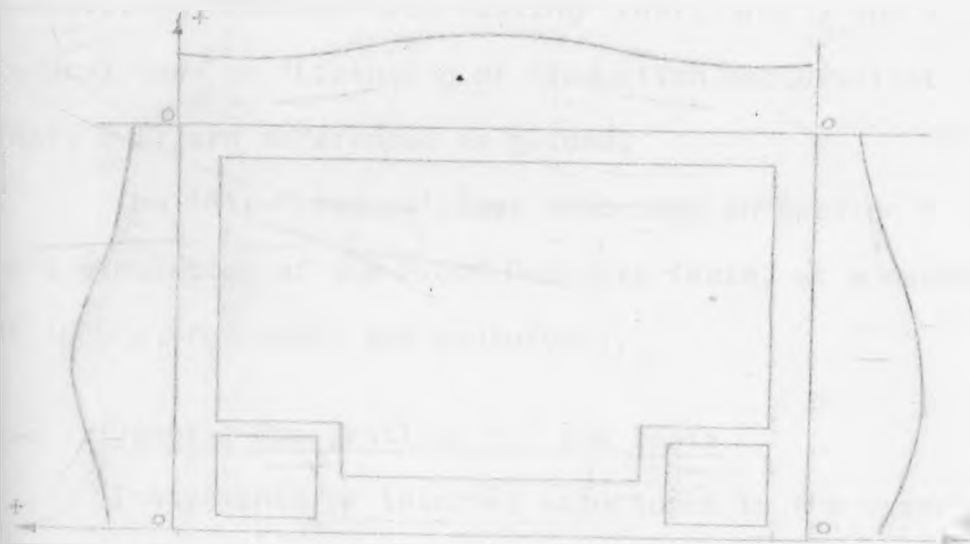


Fig. 5.10 Calculated Deflection under Thermal Load.

CHAPTER 6

TESTING OF REACTOR VESSELS (PRESSURE VESSELS)

6.1 Introduction

Before reactor vessels can be put to use of their purpose, Proof Pressure Tests must be carried out. These are for two basic reasons:-

- (i) To assess the structural integrity of the vessel under maximum peak pressures, and detect any areas of permanent damage.
- (ii) To measure the rate of leakage of air from within the vessel, as the internal pressure is increased to (and decreased from) the maximum test value.

Repetition of tests may be necessary after repairs or alterations are made to the structure, due to faults found during original tests.

In this chapter the requirements of the A.S.M.E. Boiler and Pressure Vessel Code (Section 3, Division 2), (Ref. 6.1) and the A.N.S.I. on 'Leakage Rate Testing' (Ref. 6.2) and the U.S.A. Federal Code on 'Licensing of Production and Utilization Facilities' (Ref. 6.3) are referenced as guides.

The 'Air-Pressure' Test described in Section 5.2.1 is aimed to be a simulation of the Proof Pressure Tests, at a maximum test pressure of 100kPa (for model and prototype).

6.2 General Preparations for the Tests

Instruments or internal structures in the vessel sensitive to damage by pressure differential are removed or protected. The air-conditioning system of the vessel is protected similarly.

Lines and vessels containing fluids that may become pressurised

are depressurised to prevent accidental addition of fluids to the vessel during the tests.

Environmental conditions that play an important part prior to the tests are:-

(i) Weather

(ii) Air-conditioning

A dry windless period under stable atmospheric pressure conditions is essential for the accurate test pressure control.

A four hour air-conditioning of vessel before the test, stabilises the temperature and humidity within the cell.

6.3 Test Equipment and Facilities

Readings from all deformation measuring instruments are recorded for 2 days prior to the test to ascertain stability of instruments and the environment.

During pressurisation, the air compression equipment is required to increase the pressure to the maximum test level rapidly, while maintaining a stable temperature and humidity in the vessel. For low humidity, cool night air is preferable. Indeed, compressors are normally equipped with after-coolers and dryers.

Temperature measurements are compared with a reference thermometer of established calibration; corrections are made available during the test.

The relative humidity within the cell is monitored during the test for vapour-pressure corrections (using remote wet and dry bulb thermometers).

Pressure measuring equipment (e.g. barographs) are calibrated prior to the test. For a test pressure of $P_{\max} = 100\text{kPa}$, indicating pressure gauges would need to have a range of about 200kPa.

Without special decompression facilities, personnel would not

be stationed within the pressurised vessel at pressures greater than 20kPa, for any length of time.

6.4 The Tests

'Structural Integrity' and 'Leakage Rate' are tested as described below to constitute the Proof Pressure Tests for the vessel. A test pressure of 100kPa is used for the descriptions following here-under.

6.5 The Structural Integrity Test

6.5.1 Loading

The test pressure (that is not to exceed 100kPa) is preferably applied in 6 loading stages: 4 increments of 20kPa (up to 80kPa), and 2 of 10kPa up to the total of 100kPa.

At all stages results are compared with the expected ones. In case of any anomaly, a decision must be made on whether to continue or abandon the test.

Unloading steps should be the same as the loading ones, with equal time intervals. Thirty minutes is a suggested time to hold the pressure constant before recording of deformations are made.

6.5.2 Deformation Measurement

Measurement of deformation and structural performance are in strains, rotations, deflections and crack widths and crack patterns. A concentration of strain gauges is required in areas expected to crack - e.g. construction joints and areas of maximum bending moment. Strain gauges can then be used to indicate an increase in crack width or a birth of a new crack. Recommended are vibrating wire type strain gauges, over 100mm in length, situated within the structure at critical cracking positions.

Upon removal of the concrete cover, 25mm electric resistance strain gauges are attached to the reinforcement bars, where such measurement is required.

The minimum accuracy of strain gauge measurements specified by the A.S.M.E. Code is + 5% of the maximum expected strain. For this test, + 60 micro strain.

Deflection and Rotation measurements are best carried out by optical methods. The 'optical plumbing' method using a Watt's Auto-plumb, say, equipped with an optical micrometer, is recommended, (Appendix 2, Ref. 6.4). Deflections normal to the walls and roof at the centre should be recorded; also changes in slope at chosen locations need recording.

Twenty four hours after the final depressurisation, deformations should be measured to check for any permanent set incurred by the test.

6.6 The Leakage Rate Test

6.6.1 Stages of Leakage Measurement

Three distinct stages of leakage measurement are required:

(i) The Reduced Pressure Test, carried out at a pressure not less than $0.5P_a$ (P_a = the 'abnormal' or 'incident maximum' pressure), maintained for 24 hours. In this case, a pressure of 55kPa is recommended.

(ii) The peak pressure test, 100kPa, also applied for 24 hours.

(iii) Verification of Leakage Test accuracy, for which a method described in Appendix C of Ref. 6.2 is suitable. The method requires use of a calibrated leak through a microadjustable flow valve installed at a convenient penetration. The leak system is operated immediately after the 24 hour test period, for a few hours.

6.6.2 Sequence of Tests

The reduced pressure test and the peak pressure test may be carried out separately, following each with a verification test.

If not, the tests may be carried out continuously, with verification after each 24 hour period. With this alternative, 3 to 4 days (continuous) may be required for the test.

6.6.3 Leakage Rate Measurement

The 'Absolute Method' described in Ref. 6.2 (the A.N.S.I.) is recommended. It requires measured values of direct pressure, absolute temperature and humidity, for calculation of air loss from the pressure vessel.

The percent leakage (L%) is then given by:-

$$L\% = \left(1 - \frac{T_1 P_2}{T_2 P_1} \right) * 100 \quad \dots\dots\dots 6.1$$

-subscripts '1' and '2' refer to 'start of test' and 'end of test' conditions, respectively

-T and P are the mean absolute temperature and the total absolute pressure, respectively.

A correction is made for the water-vapour pressure (P_v) variations in the atmosphere, viz:

$$L\% = \left(1 - \frac{T_1 (P_2 - P_{v2})}{T_2 (P_1 - P_{v1})} \right) * 100 \quad \dots\dots\dots 6.2$$

(A derivation of these equations is given in Appendix 6A).

Hourly leakage rates should be calculated and plotted continuously during test to reveal any gross discrepancies that may be latent.

6.6.4 Leakage at Penetrations

During the test, it is important that penetrations are located by the 'soap bubble method', say (Ref. 6.2). Leakage should then be evaluated by the 'Type A' test defined by the U.S.A. Federal Code (Ref. 6.3), on all penetrations. Indeed, it would be worthwhile to perform the 'Type B' test (from the same code) on the penetrations after the 'Type A' tests have been completed.

CHAPTER 7

DISCUSSIONS AND CONCLUSIONS

7.1 Introduction

In the preceding 6 chapters, I have presented 'A Study of Cracking in Reinforced Concrete Pressure Vessels Using Micro-Concrete Models', based on experimental and analytical results obtained from work done to date, in this field.

Pressure vessels such as water tanks, boilers and reactor vessels, all have containments that must not be allowed to leak out under any loading, particularly under internal pressure. A pressure boundary must therefore exist between the inner containments of the vessel and its environment. This boundary (such as the thick concrete wall in a reactor vessel) must maintain its integrity for all loadings; normal and accidental. The analysis and subsequent design of pressure vessels is therefore geared to prevention of excessive cracks that create leakage paths.

The discussion following will be directed particularly to Reinforced Concrete Pressure Vessels (RCPV's) - unprestressed - with particular reference to the reactor vessel considered in this thesis.

In discussing leakage through concrete, a point should be born in mind. Concrete is neither homogeneous nor isotropic. Fissures exist in the material. With shrinkage and high internal pressure, some cracks could develop around these small holes. The inevitable leakage resulting may not be dangerous, but should be assessed and ascertained to be below the magnitude given in Codes of Practice for environmental safety.

7.2 Cracking in Reinforced Concrete Pressure Vessels (RCPV's)

7.2.1 RCPV's

The main features of construction and loading for these vessels have been outlined in Chapters 2 and 4.

Loadings are basically dead loads, thermal and pressure transient loadings, shrinkage, and possibly dynamic loadings. These may act individually or in combination.

On construction, a significant feature in this particular vessel is that it is not provided with steel liners or other leakage membranes. Under a large internal pressure, this may lead to the loss of the integrity of the pressure boundary, and subsequent leakage of the containments. This aspect must be investigated in a model of the RCPV. The mathematical model developed by McGeorge and Swec (Ref. 4.1) evaluates the percentage crack penetration and subsequent leakage. Together with this mathematical analysis, a micro-concrete model is necessary to investigate regions of excessive cracking and leakage.

In the event of excessive leakage, alternatives must be sought. These would include introducing leakage membranes; or using prestressed concrete to decrease crack width and penetration.

An RCPV may have construction joints in the shielding walls. These are potential sources of leakage. A solution is to introduce a barrier in the leakage path, in the form of plates, as shown below.

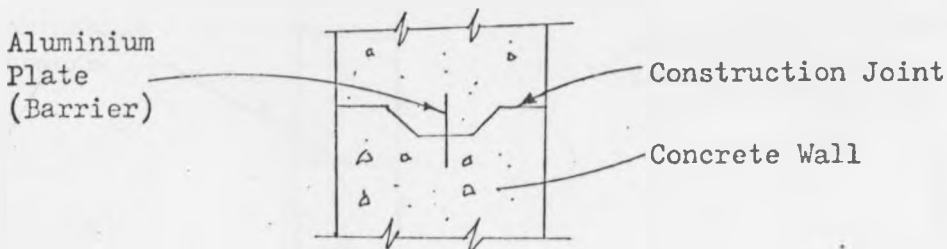


Fig. 7.1 Construction Joint with a Leakage Barrier.

An RCPV must have penetrations for filling the interior with contents (and for refuelling rods in the case of reactor vessels). These could be pipes, small windows, doors, etc. Due to the strain and stress concentrations at these points, local cracks may develop. The leakage rate at these points must be determined by a simulated model test, and also during the structural integrity test of the vessel.

In order to assess the leakage through cracks and penetrations in the pressure vessel walls and slabs, a Fluid Mechanics model is required to simulate the air flow under pressure through cracks. Using such a physics model, derivations of 'leakage evaluation equations' (outlined in Appendix 6A), are made possible.

7.2.2 Cracking

Two main types of cracks are encountered in RCPV's. These are:-

- (i) Flexural Cracks
- (ii) Shrinkage Cracks

Flexural cracks are of less importance since they tend to seal up after removal of load, if they are not excessive.

Shrinkage Cracks

The massive nature of the concrete walls of a reactor vessel introduces shrinkage cracks formation.

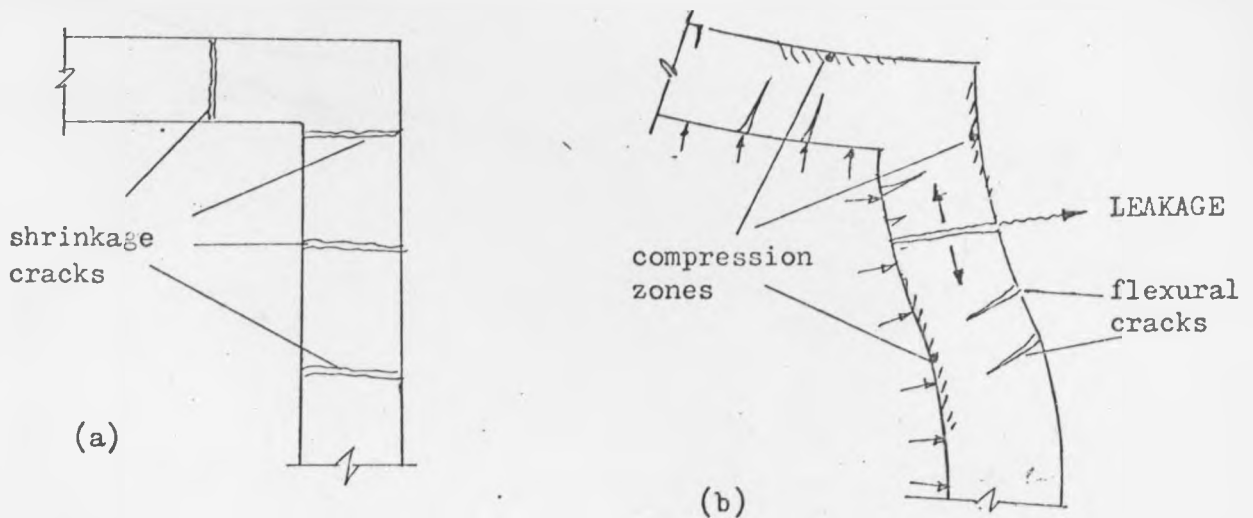


Fig. 7.2 Shrinkage Cracks

Under no (or low) internal load, cracks formed by shrinkage would remain open (Fig. 7.2 (a)). Under load, zones of the slabs in compression would tend to seal up the cracks, while the zones in tension would tend to open them up. Where neither exists, i.e. in zones of contraflexure, leakage paths would be created as 'through'-cracks - Fig. 7.2 (b). (These zones (points) were indicated in Figs. 4.8 (a) and (b).)

Other types of cracks may result from thermal effects. Such effects could be caused by the heat of hydration of cement in the concrete, especially during (and soon after) construction. Other thermal effects are the SBA and DBA temperature transient loadings, discussed in Chapter 4 (Sections 4.4.2 and 4.7.2).

Cracks created by temperature differentials across a concrete wall (except for shrinkage cracks), would be much less serious, with respect to leakage of containments.

7.3 Models

The two types of model that are considered for investigating RCPV's are:-

- (i) Mathematical Model using a Finite Elements Method (FEM) of analysis; and the
- (ii) Direct Model constructed with micro-concrete.

7.3.1 The Mathematical Model (FEM Analysis)

In Chapter 4, I described at length how the FEM analysis was developed and used to analysis two RCPV's, one as a 'thin' shell (two dimensional), and the other as a 'thick' shell (three-dimensional - McGeorge and Swec).

The 'thin' shell model can be used to predict the 'elastic' structural behaviour, as well as the 'elasto-plastic' behaviour. However, because this model does not take into account the wall thickness of the vessel, the results can be incorrect and very misleading, since the wall thickness is among the most important aspects of an RCPV.

Also, cracks due to the anisotropic nature of concrete, the 'doming' action of the vessel under load, creep and shrinkage; are all unaccounted for in the 'thin' shell model.

The results of the analysis of this model, then should only be used as a guide: for preliminary decisions about a micro-concrete model. They can also be used to roughly predict the behaviour of the micro-concrete model, for purposes of choice of scale, instrumentation etc. These results, on their own, are definitely inadequate.

The 'thick' shell model is more representative of the structure. Results obtained by using this three-dimensional model, both by the RCPV Research and Development Group, Kajima Corporation, Japan (Refs. 2.1 and 2.2); and by R. McGeorge and L. F. Swec Jnr (Ref. 4.1), showed very good comparison with results obtained from micro-concrete models.

The plane-strain finite element developed by M. A. Taylor and others, (described in Section 4.5.1), takes into account all the properties of reinforced concrete relevant to cracking analysis. Using this element in the FEM iterative procedure analysis shown in Fig. 4.4, yielded results discussed in Section 4.7, that agreed well with the observed experimental results. This iterative procedure allows for a consideration of several load types in various combination and sequences, the identification of critical cases, and also minimises the amount of computational effort. With this method, relatively accurate predictions of cracking can be made with certainty on the behaviour of an RCPV.

7.3.2 Direct Model (Micro-Concrete)

A direct model of reinforced concrete must be made of micro-concrete. Such a model allows for measurements of deformations, and other prototype quantities of interest, directly from the model. The model scale must therefore be 'large', so that very little 'scaling-down' is performed. Furthermore, in the process of achieving this 'direct' aspect, distortion of similitude laws is quite often inevitable.

In Chapters 1 and 2, I pointed out the difficulties encountered in modelling characteristics that are peculiar to reinforced concrete, namely shrinkage, creep, cracking, bond, and reinforcement. Some of the solutions discussed called for distortion of some quantities. For example, in simulating large deformations δ , the requirement was $\lambda_\delta = \lambda_l \lambda_\epsilon$. In this case with a serious change in geometry occurring, a distorted model was required with λ_ϵ slightly less than unity. Other examples demanded that $\lambda_l = 1$, which necessitates building a full scale model.

The difficulties encountered in modelling leakage rate at

penetrations and construction joints cannot be easily overcome. This aspect is best observed and measured accurately during a model test; using equation 6.1 and 6.2 for leakage assessment.

Other characteristics that require careful observation during testing are properties of cracks such as widths, propagation, orientations; and also formation of through-cracks resulting in further leakage.

When modelling for thermal effects, the most common quantities considered are temperature θ , time t , coefficient of expansion α , specific heat c , thermal conductivity k and the heat transfer coefficient, h . Temperature and time can be modelled individually. The other quantities are normally combined together for model assessment, when similitude laws are applied to quantities like the thermal diffusivity ($D = k/c\rho$) or Nusselt's number ($N = hl/k$), and others. These quantities sometimes cause severe distortions on thermal models. A summary of the distortions and the corresponding corrections (presented by Hovanesian and Kowalski, 1967) are shown in Table 1.2, Section 1.7.3).

7.4 Construction and Testing of Micro-Concrete Models

7.4.1 Construction of Model

The scale chosen for a reinforced micro-concrete model plays a very important part in its construction. This is of particular importance in the size of the reinforcement bars. Steel rods of diameters less than 1mm are impractical. The choice made in this case of using 2mm diameter rods throughout, (Chapter 3), for reinforcement was almost inevitable. This led to changing the spacing and 'number of bars' used in the prototype, for the model. This in turn led to rather incorrect modelling of bond and crack widths characteristics. The inherent distortion was assessed to be in error within 5% - 10%.

RCRV's are heavily reinforced. During construction this creates problems in spacing layout and vibration of the mortar (micro-concrete). The solution that was sought was the use of steel templates for guidance in spacing, have a spacing restriction of not less than 15mm; and then use a miniature poker vibrator for the mortar, 10mm in diameter. Equations 3.1 and 3.2 indicating the scaling factors, ~~that~~ were used to satisfy the reinforcement area similitude only.

The model had its construction planned in 6 stages, as a construction joint was to be made at each stage. (This procedure is similar to that followed in the erection of a typical prototype RCPV).

Strain and other types of gauges that have to be embedded in the mortar require very careful placement. These are therefore kept to a minimum.

7.4.2 Testing of Model

Since the model has not been constructed to completion, I outlined in Chapter 5 how I think testing should be done. This outline of testing depends on the construction procedure followed, which I planned out and presented in Chapter 3. However, in the event of any change in construction and instrumentation, changes in testing procedure may be necessary.

The expected results that I've laid down in Chapter 5 (Section 5.7 and 5.8) have been based on the results obtained from:-

(i) the PCPV Research and Development Group, Kajima Corporation Japan (Refs. 2.1 and 2.2) experiments

(ii) Results of the computer programme 'SLEAP' (Section 4.6.5) that analysed this RCRV as an 'elastic, thin' shell; and

(iii) the results obtained by McGeorge and Swec (Ref. 4.1) in the analysis of a mathematical model of a similar structure, as a 'three-dimensional, non-linear, thick shell'.

I have not attempted to predict the amount of leakage or leakage rates to be expected. The structural integrity and leakage rate of the prototype should be simulated directly by the model test (Chapters 5, 6). Indeed this is one of the main reasons why a decision was made to construct this model at Sydney University.

During the testing of the model, keen and careful observation and record should be made of:-

(i) Flexural and shrinkage cracks

(ii) Widths, penetration and propagation of all cracks

(iii) Location of leakage and its evaluation (using equations 6.1 and 6.2 given in Chapter 6)

(iv) The failure mode as a result of the formation of 'yield line' mechanisms, under excessive pressure.

Conclusions that will be drawn from observations of these phenomena, will advance the 'Study of Cracking in Reinforced Concrete Pressure Vessels Using Micro-Concrete Models', one step forward.

-125-

ACKNOWLEDGEMENTS

I wish to thank Dr R.G. Smith (Senior Lecturer, Department of Civil Engineering, University of Sydney) for his guidance and assistance during the preparation of this thesis.

I also acknowledge with gratitude the permission given to me for use of information and diagrams included in 'Investigation Report No. S 175' of the School of Civil Engineering (June, 1975)

I also thank the laboratory staff of the concrete laboratory at Sydney University, for their assistance, help and patience during the tests and model fabrication.

Plenty of thanks too, to Miss Jeni Beahan for typing this document with dedication.

A.E.W.M.

REFERENCES

Chapter 1

- 1.1: American Concrete Institute Publication No. 24:
'Models for Concrete Structures' - 1970
- 1.2: G.M. Sabins, R.N. White: 'A Gypsum Mortar for
Small Scale Models', ACI Journal, Proceedings
V64, No. 11 - November, 1967
- 1.3: H.J. Cowan, J.S. Cero, G.D. Ding and R.W. Muncey:
'Models in Architecture'. Elsevier Publication,
London - 1968

Chapter 2

- 2.1: Kajima Institute of Construction Technology, Japan.
PCPV Research and Development Group, Kajima Corporation
'Concrete Model Tests on Prestressed Concrete Pressure
Vessels (Part 2)' - September, 1973
- 2.2: Kajima Institute of Construction Technology:
PCPV Research and Development Group, Kajima Corporation
'Concrete Model Tests on Prestressed Concrete Pressure
Vessels (Part 3)' - October, 1973
- 2.3: Kajima Institute of Construction Technology:
PCPV Research and Development Group, Kajima Corporation
'Concrete Model Tests on Prestressed Concrete Pressure
Vessels (Part 1)' - March, 1973

Chapter 4

- 4.1: R. McGeorge and L.F. Swec Jnr: 'Refined Cracked Concrete
Analysis of Concrete Containment Structures Subject to
Operational and Environmental Loadings'. Nuclear
Engineering and Design 29 (1974) 58-70, North Holland
Publishing Company - May, 1974
- 4.2: The Australian Concrete Structures Code of Practice
AS 1480 - 1972
- 4.3: F.A. Taylor, K.J. Romstand, L.R. Herrmann and M.R. Ramey:
'A Finite Element Computer Programme for the Prediction
of the Behaviour of Reinforced and Prestressed Concrete
Structures Subject to Cracking'. Department of Civil
Engineering, University of California - June, 1973
- 4.4: A.S.M.E. 'Standard Code for Concrete Reactor Vessels
and Containments', Section III, Division 2 - 1975







- 4.5: A.O. Currie: 'Elastic Analyses of Orthogonal Slab and Wall Structures Using 'SWEAP''. Technical Report No. U29 School of Civil Engineering, University of Sydney - January, 1976
- 4.6: School of Civil Engineering, University of Sydney: 'Investigation Report No. S 175' - June, 1975
- 4.7: O.C. Zienkiewicz: 'The Finite Element Method in Engineering Science'. McGraw-Hill, London - 1971
- 4.8: P.F. Walsh: 'A Computer Programme for Orthotropic Plane Stress Analysis' - Forest Products Technical Note, No. 12, Division of Building Research, CSIRO - 1973

Chapter 6

- 6.1: A.S.M.E. Boiler and Pressure Vessel Code for 'Concrete Reactor Vessels and Containments'. Section 3, Division 2 - 1973
- 6.2: American National Standards Institute: 'Leakage-Rate Testing of Containment Structures for Nuclear Reactors': N45.4 - 1972
- 6.3: U.S.A Federal Code - 'Part 50 - Licensing of Production and Utilization Facilities', Appendix J (AEC 100 - RF - 10) - 1973.

APPENDIX 3A

Tabulated below are results obtained by testing (100 x 200)mm cylinders of the mortar that was used in the construction of the micro-concrete model. The cylinders were 7 days old (Cast on 12/1/76 and Tested on 19/1/76).

Mark No.	Type of Test	Ultimate Load (kN)	Strength at 7 days (MPa)	Type of Fracture	Strength at 28 days (MPa)
491	COMPRESSION	148	18.25		27.4
492	COMPRESSION	142	17.54		26.1
493	COMPRESSION	140	17.27		26.0
494	TENSION	66	2.04		3.06
495	TENSION	61	1.89		2.84
496	TENSION	65	2.00		3.00

i. Table 3A Results for Test Cylinders

The formula used to convert the strength of the 7 days old sample to that of a 28 days one is empirical:

$$\sigma_{28} = 1.5 \sigma_7$$

The compressive strengths were slightly lower than required; the tensile strengths were as required (31MPa Compression, 3.1MPa Tension).

Overall, the results were satisfactory.

APPENDIX 3B

Alongside with each batch of mortar used for casting of construction Stage 1, strength-checking cylinders were (100 x 200)mm, and 28 days old.

(Cast 20/1/76, tested 17/2/76)











Mark Number	Batch Number	Type of Test	Ultimate Load (kN)	Strength at 28 days (MPa)	Type of Fracture
515	1	COMPRESSION	230	28.4	
516	1	TENSION	96	2.96	
517	2	COMPRESSION	255	31.4	
518	2	COMPRESSION	247	30.5	
519	2	TENSION	99	3.05	
520	2	TENSION	97	2.99	
521	3	COMPRESSION	256.5	31.6	
522	3	COMPRESSION	250.0	30.8	
523	3	TENSION	99	3.05	
524	3	TENSION	101	3.11	

Table 3B Test Results for 'Stage 1' strength check.

The results are in good agreement with the required strengths of the mortar required, i.e. 31MPa in compression and 3.1MPa in tension.

The Determination of Leakage Rate using the Absolute Method.

In this method:

$$P_1 V = W_1 R T_1 \text{ and } P_2 V = W_2 R T_2$$

$$\frac{W_1 T_1}{P_1} = \frac{V}{R} \text{ and } \frac{W_2 T_2}{P_2} = \frac{V}{R}$$

Therefore,

$$\frac{W_1 T_1}{P_1} = \frac{W_2 T_2}{P_2}$$

Whereby,

$$W_1 = \frac{W_2 T_2 P_1}{T_1 P_2} \text{ and } W_2 = \frac{W_1 T_1 P_2}{T_2 P_1}$$

Consequently,

$$\begin{aligned} \text{Leakage} &= \frac{W_1 - W_2}{W_1} = \frac{W_2 \left\{ \frac{T_2 P_1}{T_1 P_2} - 1 \right\}}{W_2 \left\{ \frac{T_2 P_1}{T_1 P_2} \right\}} \\ &= 1 - \frac{T_1 P_2}{T_2 P_1} \end{aligned}$$

and Percentage Leakage,

$$L\% = \left\{ 1 - \frac{T_1 P_2}{T_2 P_1} \right\} * 100 \dots\dots\dots 6.1$$

Corrections for changes in water-vapour-pressure in the contained atmosphere are made by modifying the base equation as follows:-

Percentage Leakage,

$$L\% = 1 - \frac{T_1 (P_2 - P_{v2})}{T_2 (P_1 - P_{v1})} * 100 \dots\dots 6.2$$

Nomenclature

P_1, P_2 = Total absolute pressures in vessel at the start, and end of testing interval.

T_1, T_2 = Mean absolute temperature at the start, and end of testing interval.

W_1, W_2 = Weight of contained air at the start, and end of testing interval.

V = Internal volume of vessel, assumed to remain constant during test.

R = Gas constant for a perfect gas.

P_{v1}, P_{v2} = Water-vapour pressure at the start, and end of the test interval.